Bacterial physiology and enzymology of the membrane-associated methane monooxygenase and ammonia oxidation system from *Methylococcus capsulatus* Bath, 1992 - 1996

by

James Allan Zahn

A Dissertation Submitted to the

Graduate Faculty in Partial Fulfillment of the

Requirements for the Degree of

DOCTOR OF PHILOSOPHY

Department: Microbiology, Immunology and Preventive Medicine
Major: Microbiology (Microbial Physiology)

Approved:

Signature was redacted for privacy.

In Charge of Major Work

Signature was redacted for privacy.

For the Major

Signature was redacted for privacy.

For the Major Department

Signature was redacted for privacy.

For the Graduate College

Iowa State University
Ames, Iowa

1996

TABLE OF CONTENTS

ACKNOWLEDGMENTS

Although nearly four years have passed since my introduction to Iowa State University, I vividly recall my initial visit with Dr. Joel Coats, at that time Chairman of the Interdepartmental Toxicology program. I am grateful for Joel's willingness to support a "homeless" graduate student within his research group. I also thank the Department of Entomology for serving as my major department for the first year and a half at Iowa State University.

I am indebted to Dr. Alan DiSpirito for providing me with the knowledge to design and solve difficult problems in science. I've enjoyed and benefited from the immense level of scientific diversity in the laboratory projects conducted in Alan's laboratory, as well as the "laboratory bench"-training and expertise provided by Alan.

I am grateful to my graduate advisors, Dr. Alan DiSpirito and Dr. Joel Coats, for their efforts towards my professional development and graduate education. I've especially enjoyed the informal level of communication each has offered; I consider each advisor a role model in my development as a scientist. I thank my program of study committee members - Dr. Greg Phillips, Dr. Jim Dickson, and Dr. William Simpkins - for their time and efforts in examining and critiquing my knowledge and research abilities. I thank Dr. David ErkenBrack (Department of Biology, Central College) for his insights into graduate education and encouragement to pursue graduate school. Finally, I thank my family, Jody, Jessica, and Jacob for their willingness to endure the sacrifices imposed by graduate research.

CHAPTER 1. GENERAL INTRODUCTION

Obligate methylotrophic bacteria or methanotrophs are a ubiquitous group of environmental microorganisms which play a pivotal role in the cycling of reduced carbon and nitrogen compounds in the global ecosystem (23, 45, 48). The presence of these organisms throughout the environment, along with their ability to effectively co-metabolize chlorinated hydrocarbon pollutants, such as trichloroethylene has increased the level of scientific interest in these organisms. All methanotrophs utilize methane gas as a sole source of carbon and energy; thus they are categorized within the class of heterotrophic bacteria that utilize organic carbon as a cellular carbon source. Methanotrophs oxidize methane to carbon dioxide in a series of two electron oxidations with methanol, formaldehyde, and formate as intermediates (Fig. 1). Cellular reducing power is generated in the form of $NADH+H^+$ through the oxidation of formate by the cytoplasmic formate dehydrogenase and the hypothesized formaldehyde dehydrogenase reaction (24), although the later has not be conclusively shown for obligate methylotrophic bacteria. Cellular carbon is assimilated at the level of formaldehyde by one of two pathways: 1) Ribulose monophosphate pathway or the 2) serine pathway (19). The identification of the formaldehyde assimilation pathway, as well as the ultrastructural arrangement of the cell membrane has previously served as the basis for grouping methanotrophs into one of three classifications: Type I, Type II, or Type X (Table 1).

Although methanotrophs fall under the bacterial heterotrophic classification, this family of bacteria, in general, exhibits unique metabolic capabilities which rival those found in the chemolithotrophic bacteria. Much of the research presented in

FIG. 1. Mechanism for the oxidation of methane to carbon dioxide. Abbreviations; pMMO, membrane associated methane monooxygenase; sMMO, soluble methane monooxygenaese; MDH methanol dehydrogenase; FalDH, formaldehyde dehydrogenase; FDH, formate dehydrogenase; PQQ, pyroloquinoline quinone; Cyt., cytochrome.

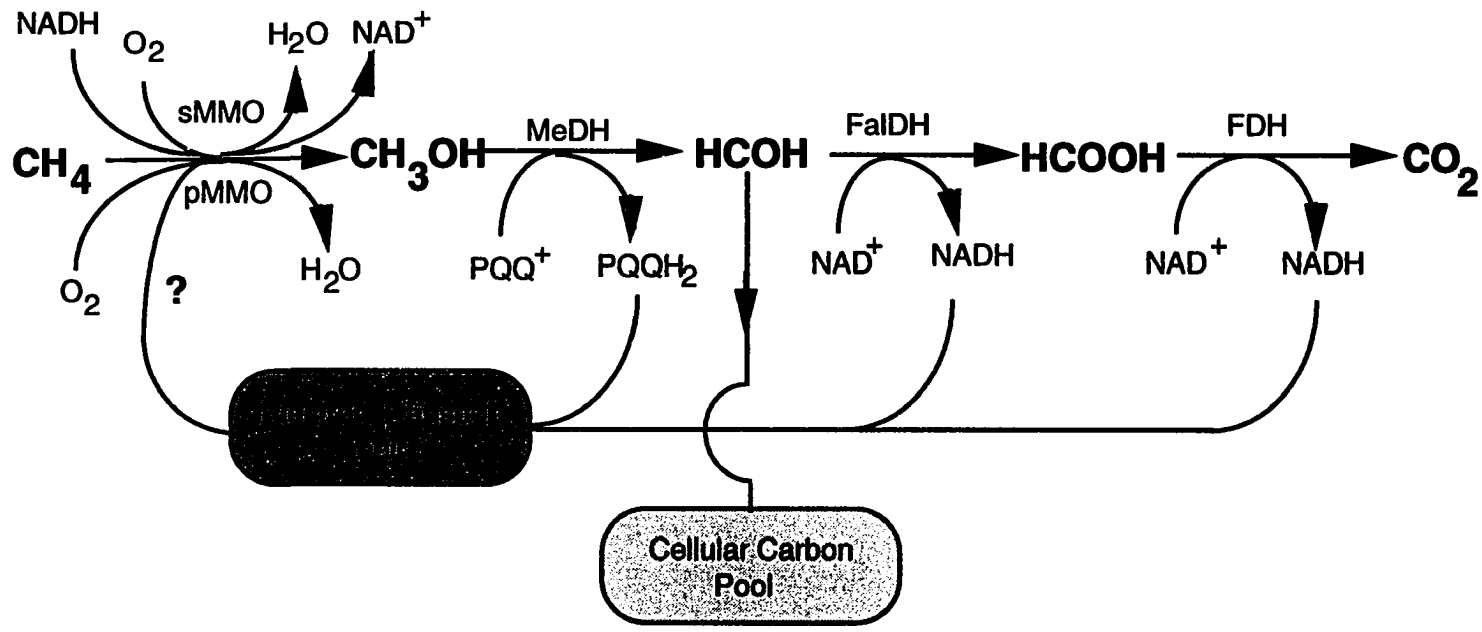
NADH
O_2
H_2O
NAD^+
sMMO
CH_4
CH_3OH
MeDH
HCOH
FalDH
HCOOH
FDH
CO_2
pMMO
O_2
?
H_2O
PQQ^+
$PQQH_2$
NAD^+
NADH
NAD^+
NADH
Cellular Carbon Pool

this work or in representative publications would indicate that the biochemistry and cellular physiology of methanotrophic bacteria most closely resembles that of the chemolithotrophic nitrifying bacteria. The amazingly complicated enzymology, partially unraveled in this work, provides evidence that the environmental role which is currently associated with this group of microorganisms may underestimate their actual environmental significance (48).

Table 1. Categorization of methanotrophic bacteria.

Representative Genus	Type Classification	Membrane Arrangement	Formaldehyde Assimilation Pathway	Carbon Dioxide Fixation
Methylomonas	Type I	Vessicular disc-shaped cellular membrane	Ribulose monophosphate	No
Methylobacter	Type I	Vessicular disc-shaped cellular membrane	Ribulose monophosphate	No
Methylococcus	Type X	Vessicular disc-shaped cellular membrane	Serine/Ribulose monophospate	Yes
Methylosinus	Type II	Paired cellular membrane	Serine	No
Methylocystis	Type II	Paired cellular membrane	Serine	No

Methanotrophs oxidize methane to methanol, via the methane monooxygenase, as a sole carbon and energy source. The enzymology and cellular physiology of at least three representative genera of methanotrophs are complicated by the presence of two distinct methane-oxidizing systems. The two distinct

methane oxidizing systems have been shown to be coordinately regulated by nutritional requirements. This unique regulatory phenomenon associated with some methanotrophic bacteria has been employed in the work presented in this dissertation as a research tool to study the previously uncharacterized membrane-associated methane monooxygenase (pMMO) from the methanotrophic bacterium, *Methylococcus capsulatus* Bath. Environmentally, methane monooxygenase from methanotrophic bacteria is significant since the enzyme will catalyze the degradation of several halogenated aliphatic and aromatic compounds which have been implicated in groundwater pollution (6, 12, 21, 43). In addition, indigenous populations of methanotrophs play a role the reduction of global methane, which is currently the second leading greenhouse gas. A better understanding of the enzyme responsible for methane oxidation in methanotrophs is expected to increase the level of knowledge for these events and allow for their future manipulation in the laboratory and environment. The major objective of research concerning this project was to purify the particulate methane monooxygenase from *M. capsulatus* Bath and secondly, to elucidate the link between the particulate methane monooxygenase and the electron transport chain.

A second objective of research presented in this dissertation was to identify and characterize enzymes associated with the ammonia oxidation pathway in *M. capsulatus* Bath. The relative ecological role of the methanotrophs and nitrifiers in the oxidation of methane and ammonia has yet to be resolved (48). The separation of the relative contributions of ammonia-oxidizing and methane-oxidizing bacteria in the global nitrogen cycle is currently hindered by a lack of information concerning the enzymology of methanotroph nitrification. The information presented here may

provide the needed method of separating the contributions of methanotrophs and nitrifiers in field studies. In addition to the fundamental studies on the initial characterization of the pMMO and enzymes in the ammonia oxidation pathway in *M. capsulatus* Bath, recent research on methane and ammonia oxidation in methanotrophs is reviewed.

Literature Review

Practical applications of methanotrophs

Microorganisms play a crucial role in the maintenance of global ecosystems and have been implicated in the biological transformation of stable, toxic environmental contaminants, which have been released into the environment. Chlorinated hydrocarbon compounds are a well recognized class of environmental pollutants which have historically had many uses including the control and elimination of insects, as industrial solvents for degreasing, as dry cleaning solvents, and as anesthetics (5, 40, 47). The use and disposal of chlorinated hydrocarbon compounds was largely unregulated for approximately fifty decades until the late 1960's and early 1970's when the detrimental environmental and biological impact of this class of chemicals was fully recognized. By the early 1970's, the chlorinated hydrocarbon, trichloroethylene, had become the most prevalent groundwater pollutant in industrial societies throughout Europe and North America (2, 5, 40, 44). Trichloroethylene and chlorinated hydrocarbon compounds in general, exhibit a high level of chemical stability and have been shown to persist under certain environmental conditions for several decades (5, 40). Several genera of prokaryotic

microorganisms have been shown to catalyze the efficient transformation of trichloroethylene by reductive, oxidative, and/or conjugative biotransformation pathways (2, 44). The possibility for the use of indigenous populations of prokaryotic microorganisms for the *in situ* biotransformation of chemically stable organic compounds, including trichloroethylene, has been of special interest to the public and to governmental agencies since the use of indigenous bacterial populations results in minimal environmental impact and eliminates the controversial use of genetically-engineered organisms (1, Fig. 2). Studies concerned with the biodegradation of chlorinated aliphatic hydrocarbons have shown that indigenous populations of methane-oxidizing bacteria or methanotrophs effectively catalyze the biotransformation of trichloroethylene (2, 6, 12, 21, 43, 44). Experiments on the *in situ* bioremediation of trichloroethylene have provided additional evidence that methanotrophs can successfully remediate trichloroethylene-contaminated sites (1, Fig. 2.) In addition to their use in the bioremediation of environmental toxins, methanotrophs have been implicated for their role in the reduction of global methane.

Methanotrophs are a specialized group of bacteria which utilize methane as the sole source of carbon and energy (19). This specialized group of bacteria oxidize methane by a series of two electron steps to carbon dioxide with methanol, formaldehyde and formate as intermediates (Fig. 1). The methane monooxygenase catalyzes the oxidation of methane to methanol and demonstrates a broad substrate specificity which allows for co-oxidation of related alkanes, alkenes, and chlorinated hydrocarbons (Fig. 3). Two distinct forms of the MMO are known to exist within various genera of methanotrophs. The expression of either form has been shown to

FIG. 2. Diagram showing *in situ* methane-enhanced biorestoration of a trichloroethylene-contaminated aquifier. Proposed model adapted from Alexander (1994).

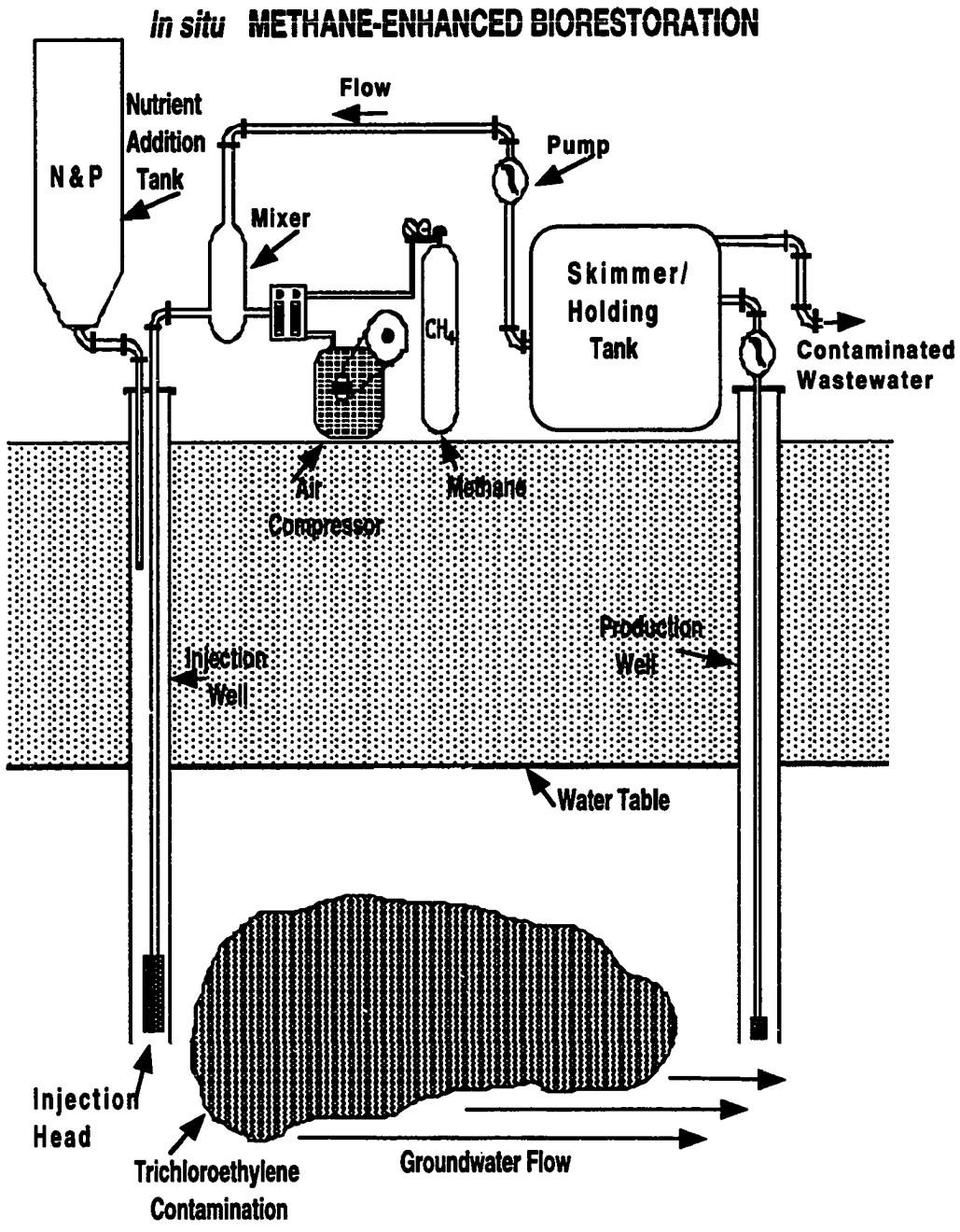
In situ METHANE-ENHANCED BIORESTORATION
N & P
Nutrient Addition Tank
Flow
Pump
Mixer
CH_4
Skimmer/ Holding Tank
Contaminated Wastewater
Air Compressor
Methane
Injection Well
Production Well
Water Table
Injection Head
Trichloroethylene Contamination
Groundwater Flow

FIG. 3. Sample compounds which are co-oxidized by the methane monooxygenase from methanotrophic bacteria. Information taken from DiSpirito, et al., (1990).

Alternate Substrates (co-substrates) Oxidized By The Methane Monooxygenase

- **Alkanes**

- **Alkenes**

- **Halogenated Hydrocarbons**

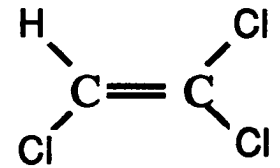

Trichloroethylene

- **Ammonia**

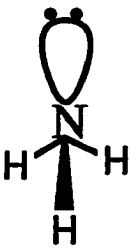

be dependent upon the concentration of copper in the growth medium and on the density of the cells in the culture. At a low copper concentration (< 0.2 μM) and a high biomass ($O.D._{600}$ = >1.5), at least three genera of methanotrophs express a soluble form of the methane monooxygenase (27). The soluble methane monooxygenase (sMMO) is observed in the soluble cellular fraction and the genes for the enzyme have been observed only in three genera of methanotrophs: *Methylosinus* , *Methylococcus*, and *Methylobacterium* (8, 27, 28). The soluble enzyme has been purified from four methanotroph species and is a complex three component enzyme (16, 17, 25, 28, 46). Component A is the hydroxylase, which is composed of three subunits with apparent molecular masses of 54,000, 42,000 and 17,000. Sedimentation experiments of the native hydroxylase from *Methylosinus trichosporium* has suggested that the holo-enzyme exists in an $\alpha_2\beta_2\delta_2$ subunit structure (16). Characterization of the sMMO hydroxylase by electron paramagnetic and Mössbauer spectroscopic methods has indicated that the enzyme active-site contains two binuclear iron centers with the iron atoms of each binuclear iron center arranged in a μ-oxo bridge (15, 16, 20). Electrons for the two electron oxidation of methane are channeled into the hydroxylase component from an iron sulfur (Fe_2S_2) flavoprotein (M_r 44,000) designated component C. Component C obtains reducing equivalents through the oxidation of NADH + H^+. Fully active preparations of the sMMO hydroxylase have been shown to require the presence of an additional regulatory protein (M_r 16,000 Da), component B. Recently, the crystal structure of the sMMO hydroxylase from *M. capsulatus* Bath has been resolved at 2.2 Å (31). The crystal structure of the hydroxylase has confirmed the presence of two μ-oxo

bridged iron centers in the catalytic active-site of the active enzyme (31, 32). A comprehensive review covering the most recent structural and functional developments of the sMMO enzyme has recently been published (24).

Regulation of the cellular MMO distribution

When copper concentrations in the growth media are increased above 0.2 μM, methanotrophs express a membrane-associated or particulate methane monooxygenase (pMMO) (Fig. 4). Unlike the narrow spectrum of methanotrophs which are able to express a sMMO enzyme, the pMMO has been observed in all known isolates of methane-oxidizing bacteria (19, 23). In addition to the change in the cellular location of the methane oxidation enzymes, the copper sufficient condition has been shown to greatly influence the physiological state of the cell by inducing major changes in cellular ultrastructure and biochemistry (4, 10, 11, 12, 13, 22, 23, 29, 30 33, 37). This major physiological change in methane oxidation enzymes, cell ultrastructure, and biochemistry between expression of the sMMO and pMMO has been referred to as "switch-over" and was first proposed by Higgins and co-workers in 1980 (4, 33) and later was defined by Dalton and co-workers in 1984 (11). The initial report of a switch-over phenomena in methanotrophic bacteria suggested that the distribution of methane monooxygenase (MMO) activities between the membrane and soluble cellular fractions in *Methylosinus trichosporium* OB3b was dependent upon growth conditions (33). The growth conditions that produced optimal membrane-associated MMO activity were also correlated to an increase in the cell membrane content or intracytoplasmic membrane as determined by electron microscopy (4). Effector studies showed differences in the sensitivity of

FIG. 4. Diagram showing the biochemical changes in the SDS-PAGE profile of subcellular fractions of the methanotroph, *M. capsulatus* Bath (Zahn and DiSpirito, unpublished results) expressing the pMMO (5 μM copper sulfate concentration in the growth media) or sMMO (< 0.1 μM copper sulfate concentration in the growth media). The figure shows the polypeptide components that are associated with the switch-over event in *M. capsulatus* Bath (Dalton, et al., 1984).

Soluble Methane Monooxygenase

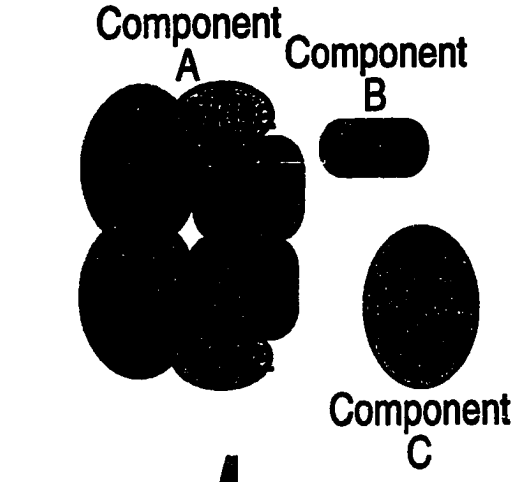

Particulate Methane Monooxygenase-Associated Polypeptides

47kDa
? 35kDa ?
27kDa
25kDa

the MMO derived from either the soluble or membrane fraction and suggested that the localized forms of MMO represented two, distinct methane oxidation systems in *M. trichosporium* (7). Although oxygen tension, methanol, and nitrogen content in the media were found to alter the MMO distribution in *M. trichosporium* OB3b, the specific factors controlling the regulation of the switch-over event in methanotrophic bacteria were largely unresolved in the initial reports of switch-over. During this time, several studies showed that high concentrations of methanotroph cells in culture correlated with a high distribution of soluble MMO activity (11). Based on these observations, Dalton and co-workers (11) proposed that the MMO distribution was regulated by the nutritional status of the organism since this factor, along with oxygen tension, was dramatically altered by the cell density of the culture. Studies by this group also showed, for the first time, the effect of copper ions on regulation of the MMO distribution in *M. capsulatus* Bath (11, 29, 30, 37).

The membrane-associated methane monooxygenase

A problem in the study of methanotrophs as a global methane sink or in bioremediation processes is the lack of knowledge concerning the enzymology of the membrane-associated methane monooxygenase and the basic bioenergetics associated with methane oxidation. Historically, the study of the methane-oxidizing enzymes from methanotrophs has been associated with intense controversy over subcellular location (41, 42), prosthetic groups (3, 9, 11, 26, 41) polypeptide components (3, 11, 14, 41), and reproducibility of purification procedures (3, 14, 36, 41). A retrospective view of early reports concerned with the MMO purification and/or characterization indicates that the controversy was fueled primarily by the

individual differences in the laboratory growth conditions of methanotrophs. Early reports of the purification of pMMO from *M. trichosporium* OB3b (42) and *M. capsulatus* (3) served to greatly hinder the progress on understanding the enzymology of pMMO, since these reports were un-reproducible in other laboratories or in subsequent attempts by the authors (3). Furthermore, the reports caused general confusion within the field of methylotrophy over the actual enzymology of pMMO and resulted in the decline of the number of laboratories committed to studying the system.

Studies in the early 1980's that investigated changes in the profile of membrane polypeptides associated with the switch-over event in *M. capsulatus* Bath implicated four, copper-inducible membrane polypeptides (Mr 47000, 35000, 27000, and 25000 Da) as putative subunits of the pMMO (11, 29, Fig. 4). During the mid-1980's, several laboratories attempted, with little success, the purification of the pMMO from various methanotrophic bacteria. These attempts focused on the isolation of methane- or propylene-oxidizing activity from the membrane fraction and did not proceed beyond the detergent solublization of the membrane fraction. Finally near the end of the decade, Drummond, et al., (14) reported a reproducible procedure for the solublization of the pMMO from *M. capsulatus* Bath using the non-ionic detergent dodecyl maltoside. When reconstituted into artificial phospholipid vesicles, this system exhibited partial propylene-oxidizing activity. Unfortunately, further attempts to purify the complex resulted in the complete loss of pMMO activity.

In light of the problems of maintaining *in vitro* pMMO activity, there has been a recent trend by several research groups to diverge from an emphasis on the purification of the pMMO towards an emphasis on the analysis of active, crude

membrane fractions in order to study the basis for pMMO instability and to identity co-factors which may be present in the pMMO. Work by Prior and Dalton (29, 30) in the mid-1980's established that copper, when added to growth media or to *in vitro* assays of pMMO, could dramatically increase the activity of the enzyme. These studies suggested that copper was present in the active site of the pMMO, and that the enzyme could be stabilized by exogenous copper. Using crude membrane fractions, Chan, et al., (9) and Nguyen, et al., (26) have shown that membrane suspensions prepared from cells of *M. capsulatus* Bath expressing the soluble MMO exhibit low copper concentrations and a minor copper EPR signal while the membrane fraction from cells expressing the pMMO had a high copper content and showed the presence of two distinct copper EPR resonances. One signal was attributed to a type 2 copper center on the basis of the EPR spectral characteristics ($A_{||} \sim 18 \times 10^{-3} cm^{-1}$) ($g_{||} = 2.25$; $g_{\perp} \sim 2.058$). The other copper signal, occurring near $g \sim 2.06$, was broad and nearly isotropic. Unlike the type 2 copper signal, the isotropic signal was difficult to saturate at low temperatures (< 10 K) and hence was isolated by recording the spectrum at high microwave powers. Theoretical analysis of electron paramagnetic resonance spectroscopic and magnetic susceptibility data suggested that the isotropic signal originated from a novel multinuclear copper cluster. The authors suggested that the trinuclear copper cluster may be associated with the active site(s) of the pMMO since the concentration of the isotropic copper signal increased proportionally to pMMO specific activity. Calculations based on copper concentration in the membrane fraction and the concentration of copper-inducible polypeptides indicated that approximately 5 to 8 trinuclear copper clusters

were present per enzyme (S. Chan, personal communication). Consistent with Chan and co-workers prior work, which suggested the presence of copper in the active site of the pMMO, Semrau, et al., (34, 35) have concluded that copper plays a primary role in the active site rather than a structural role, such as in the stabilization of the enzyme. An unfortunate circumstance of this data, generated on crude membrane preparations that contained other uncharacterized copper-containing species, is the fact that the observations may not accurately represent the true properties of the pMMO. Therefore, until the pMMO can be purified in an active state, the results of these studies are of limited significance.

Electron Donor Specificity of the pMMO

Recently there has been a concerted effort to address the problem of *in vitro* pMMO instability through *in vivo* studies of the enzyme's electron donor specificity (10, 36). Both the sMMO and cell-free extracts of pMMO have been shown to utilize reduced pyridine nucleotides (NAD(P)H + H^+) as electron donors (11). Although both enzymes appear to be similar in electron donor specificity, studies by Dalton et al., (11) indicated that there were distinct differences in the electron donor pathway from the hypothetical NADH:ubiquinone oxidoreductase to the site of methane oxidation in the respective enzymes. When *M. capsulatus* Bath was grown under conditions of pMMO expression, methanol served as a suitable electron donor to the enzyme. However, when the organism was grown under conditions favoring the expression of the sMMO, methanol could no longer support the enzymatic turn-over of methane. These studies suggested that NAD(P)H + H^+ was not the direct electron donor for the membrane-associated form of the enzyme and that the reductant for

the pMMO from methanol was generated via an electron transfer protein without the involvement of NAD(P)H + H^+. Electron transport inhibitor studies on cell-free fractions of the pMMO using NADH + H^+ as the reductant confirmed that the pMMO was coupled to the electron transport chain (38, 39). Unfortunately, the pMMO was sensitive to all inhibitors tested, except amytal, which inhibits NADH:ubiquinone oxidoreductase at the ubiquinone binding site. Therefore, these studies provided no useful information on the energy coupling system associated with the pMMO. In an effort to determine the probable electron donor to the pMMO, DiSpirito et al., (unpublished results) designed an elaborate respiratory inhibitor study using whole cells of *M. capsulatus* Bath, a number of common respiratory inhibitors, and acetylene gas, which acts as a suicide substrate of the pMMO. By testing a wide range of inhibitor concentrations in the presence and absence of acetylene, the study showed that low concentrations of rotenone, *o*-phenantroline and HOQNO were inhibitory specifically towards methane oxidation activity. All three inhibitors were previously shown to inhibit the quinone/cytochrome bc_1 complex, therefore these results indicated that a *b*-type cytochrome was the initial electron donor to the pMMO. Using the results of DiSpirito et al., which indicated the pMMO from *M. capsulatus* Bath was coupled to the electron transport at the cytochrome *b* level, Shiemke, et al., (36) proposed and successfully showed that plastoquinol analogs could serve as direct electron donors to the detergent-solublized pMMO. The study further suggested that detergent-induced disruption of the electron transport chain, between the hypothetical NADH:ubiquinone oxidoreductase and the methane-

oxidation site of pMMO, was probably responsible for the loss of NADH + H^+-driven pMMO activity in detergent-solubilized membrane extracts.

Dissertation Organization

This dissertation is organized into a paper-style format and contains original research papers that are published or have been submitted for publication in the respective journals. As indicated by the title of the dissertation, the research emphasis is focused on the enzymology and microbial physiology of *M. capsulatus* Bath in two separate research areas. Chapters 2 and 3 are devoted to research conducted on the membrane-associated methane monooxygenase. These chapters describe for the first time, a reproducible procedure for the isolation of the pMMO from *M. capsulatus* Bath and describe a series of experiments on whole cell, cell free, and purified fractions of pMMO that were used in the characterization of the enzyme. Chapters 4 and 5 focus on the identification of enzymes which are involved in the ammonia oxidation pathway in *M. capsulatus* Bath, namely cytochrome P-460 and cytochrome *c'*. These enzymes probably function in a general maintenance or in a "housekeeping" role to reduce the cellular concentration of the ammonia oxidation products that are adventitiously generated by the non-specific oxidation of ammonia by the pMMO. Following the last paper is a General Conclusions chapter.

Literature Cited

1. **Alexander, M.** 1994. Biodegradation and bioremediation. Academic Press, Inc. San Diego, CA. pp. 248-271.
2. **Anderson, T.A., and B.T. Walton.** 1992. Comparative plant uptake and microbial degradation of trichlorethylene in the rhizospheres of five plant species-Implications for bioremediation of contaminated surface soils. Oak Ridge National Lab, Oak Ridge, Tennessee.

3. **Ankent'eva, N.F., and R.I. Govozdev.** 1988. Purification and physiochemical properties of methane monooxygenase from membrane structures of *Methylococcus capsulatus.* Biokhimiya. **53:** 91-96.
4. **Best, D.J., and I.J. Higgins.** 1981. Methane-oxidizing activity and membrane morphology in a methanologrown obligate methanotroph, *Methylosinus trichosporium* OB3b. J. Gen. Microbiol. **125:** 73-84.
5. **Browning, Ethel.** 1965. Toxicity and metabolism of industrial solvents. Elsevier Publishing Company, Amsterdam, Netherlands. pp. 189-212.
6. **Brusseau G.A., H.-C. Tsien , R.S. Hanson, and L.P. Wackett.** 1990. Optimization of trichloroethylene oxidation by methanotrophs and the use of colorimetric assay to detect soluble methane monooxygenase activity. Biodegradation **1:** 19-29.
7. **Burrows, K.J., A. Cornish, D. Scott, and I.J. Higgins.** 1984. Substrate specificities of the soluble and particulate methane mono-oxygenases of *Methylosinus trichosporium* OB3b. J. Gen. Microbiol. **130:** 3327-3333.
8. **Cardy, D.J.N., V. Laidler, G.P.C. Salmond, and J.C. Murrell.** 1991. Molecular analysis of the membrane monooxygenase (MMO) gene cluster of *Methylosinus trichosporium* OB3b. Mol. Microbiol. **5:** 335-342.
9. **Chan, S.I., H.T. Nguyen, A.K. Shiemke, and M.E. Lidstrom.** 1993 Biochemical and biophysical studies toward characterization of the membrane-associated methane monooxygenase. *In.* Microbial Growth on C_1 Compounds (J.C. Murrell and D.P. Kelly, eds) pp. 93-107.Intercept Ltd., Hampshire, UK.
10. **Cook, S.A., and A.K. Shiemke.** *In Press.* Evidence that copper is a required cofactor for the membrane-bound form of methane monooxygenase. J. Inorg. Biochem.
11. **Dalton H., S.D. Prior, and S.H. Stanley.** 1984. Regulation and control of methane monooxygenase.*In*: Microbial Growth on C_1 Compounds (R.L. Crawford and R.S. Hanson, eds), pp. 75-82. American Society for Microbiology Press, Washington, DC.
12. **DiSpirito, A.A., J. Gulledge, A.K. Shiemke, J.C. Murrell, M.E. Lidstrom, and C.L. Krema.** 1992. Trichloroethylene oxidation by the membrane-associated methane monooxygenase in type I, type II and type X methanotrophs. Biodegradation **2:** 151-164.
13. **DiSpirito, A.A., A.K. Shiemke, S.W. Jordan, J.A. Zahn, and C.L. Krema.** 1994. Cytochrome *aa*$_3$ from *Methylococcus capsulatus* Bath. Arch. Microbiol. **161:** 258-265.
14. **Drummond, D., S. Smith, and H. Dalton.** 1989. Solubilisation of methane monooxygenase from *Methylococcus capsulatus* (Bath). Eur. J. Biochem. **182:**667-671.
15. **Fox, B.G., K.K. Surerus, E. Münck, and J.D. Lipscomb.** 1988. Evidence for a μ-oxo-bridged binuclear iron cluster in the hydroxylase component of methane monooxygenase. J. Biol. Chem. **263:** 10553 - 10556.
16. **Fox, B.G., W.A. Froland, J.E. Dege, and J.D. Lipscomb.** 1989. Methane monooxygenase from *Methylosinus trichosporium* OB3b. J. Biol. Chem. **264:** 10023-10033.

17. **Green, J., and H. Dalton.** 1985. Protein B of soluble methane monooxygenase from *Methylococcus capsulatus* (Bath). A novel regulatory protein of enzyme activity. J. Biol. Chem. **260:** 15795-15802.
18. **Green, J., and H. Dalton.** 1989. Substrate specificity of soluble methane monooxygenase: mechanistic implication. J. Biol. Chem. **264**: 17698-17703.
19. **Green, P.** 1992. Taxonomy of methylotrophic bacteria. *In.* Methane and Methanol Utilizers (J.C. Murrell and H. Dalton,eds). pp. 23-57. Plenum Press, New York, New York.
20. **Hendrich, M.P., E. Münck, B.G. Fox, and J.D. Lipscomb.** 1990. Inter-spin EPR studies of the fully reduced methane monooxygenase hydroxylase component. J. Am. Chem. Soc. **112:** 5861 - 5865.
21. **Koh, S.-C., J.P. Bowman, G.S. Sayler.** 1993. Soluble Methane Monooxygenase Production and Trichloroethylene Degradation by a Type I Methanotroph, *Methylomonas methanica* 68-1. App. and Environ. Microbiol. **59**:960-967.
22. **Leak, D.J., S.H. Stanley, H. Dalton.** 1985. Implications of the nature of methane monooxygenase on carbon assimilation in methanotrophs. *In.* Microbial Gas Metabolism: Mechanistic, Metabolic, and Biotechnological Aspects. pp. 201-208. Society for General Microbiology, London, United Kingdom.
23. **Lidstrom, M.E., J.D. Semrau.** 1995. Metals and Microbiology: The Influence of Copper on methane Oxidation. *In* Aquatic Chemistry. pp. 195-201. American Chemical Society.
24. **Lipscomb, J.D.** 1994. Biochemistry of the soluble methane monooxygenase. Ann. Rev. Biochem. **48:** 371-399.
25. **Lund, J., and H. Dalton.** 1985. Further characterization of the FAD and Fe_2S_2 redox centers of component C, the NADH: acceptor reductase of the soluble methane monooxygenase of *Methylococcus capsulatus* (Bath). Eur. J. Biochem. **147**: 291-296.
26. **Nguyen ,H.-H.T., A.K. Shiemke, S.J. Jacobs, B.J. Hales, M.E. Lidstrom, and S.I. Chan.** 1994. The nature of the copper ions in the membranes containing the particulate methane monooxygenase from *Methylococcus capsulatus* (Bath). J. Biol. Chem. **269**: 14995-15005.
27. **Patel, R.N., and J.C. Savas.** 1987. Purification and properties of the hydroxylase component of methane monooxygenase. J.Bacteriol. **169**: 2313-2317.
28. **Pilkington, S.J., and H. Dalton.** 1991. Purification and characterization of the soluble methane monooxygenase from *Methylosinus sporium* demonstrates the highly conserved nature of the enzyme in methanotrophs. FEMS Microbiol. Lett. **78:** 103-108.
29. **Prior, S.D., and H. Dalton.** 1985. The effect of copper ions on membrane content and methane monooxygenase activity in methanol-grown cells of *Methylococcus capsulatus* (Bath). J. Gen. Microbiol. **131:** 155-163.
30. **Prior, S.D., and H. Dalton.** 1985. Acetylene as a suicide substrate and active site probe for membrane monooxygenase from *Methylococcus capsulatus* (Bath). FEMS Microbiol. Lett. **29:** 105-109.

31. **Rosenzweig, A.C., C.A. Frederick. S.J. Lippard, and P. Nordlund.** 1993. Crystal structure of a bacterial non-haem iron hydroxylase that catalyses the biological oxidation of methane. Nature. **366**: 537-543.
32. **Rosenzweig, A.C., P. Nordlund, and P.M. Takahara.** 1995. Geometry of the soluble methane monooxygenase catalytic diiron center in two oxidation states. Chem. Biol. **2**: 409-418.
33. **Scott, D., J. Brannan, and I.J. Higgins.** 1981. The effect of growth conditions on intracytoplasmic membranes and methane monooxygenase activities in *Methylosinus trichosporium* OB3b. J. Gen. Microbiol. **125:** 63-72.
34. **Semrau, J.D., D. Zolandz, M.E. Lidstrom, and S.I. Chan.** 1995. The role of copper in the pMMO *Methylococcyus capsulatus* Bath: a structural *vs.* catalytic function. J. Inorg. Chem. **58**: 235-244.
35. **Semrau, J.D., A. Chistoserdov, J. Lebron, A. Costello, J. Davagnino, E. Kenna, A.J. Holmes, R. Finch, J.C. Murrell, and M.E. Lidstrom.** 1995. Particulate methane monooxygenase genes in methanotrophs. J. Bacteriol. **177**: 3071-3079.
36. **Shiemke, A.K., S.A. Cook, T. Mily, and P. Singleton.** 1995 Detergent solubilization of membrane-bound methane monooxygenase requires plastoquinol analogs as electron donors. Arch. Biochem. Biophys. **321:** 421-428.
37. **Stanley, S.H., S.D. Prior, D.J. Leak, and H. Dalton.** 1983. Copper stress underlines the fundamental change in intracellular location of methane mono-oxygenase in methane utilizing organisms: studies in batch and continuous cultures. Biotechnol. Lett. **5**: 487-492.
38. **Stirling, DI, and H. Dalton** (1977) Effect of metal-binding agents and other compounds on methane oxidation by two strains of *Methylococcus capsulatus.* Arch. Microbiol. 114: 71 - 76
39. **Stirling D.I., J. Colby and H. Dalton** (1979) A comparison of the substrate and electron-donor specificity of the methane mono-oxygenase from three strains of methane-oxidizing bacteria. Biochem.J. 177: 362-364
40. **Thomas, J.M., and C.H. Ward.** 1989. *In Situ* biorestoration of organic contaminants in the subsurface. Environ. Sci. Technol. **23:** 760-766.
41. **Tonge, G.M., D.E.F. Harrison, and I.J. Higgins.** 1977. Purification and properties of the methane mono-oxygenase enzyme system from *Methylosinus trichosporium* OB3b. Biochem. J. **161**: 333-334.
42. **Tonge, G.M., D.E.F. Harrison, D.J. Knowles, I.J. Higgins.** 1975. Properties and partial purification of the methane-oxidising enzyme system from *Methylosinus trichosporium.* FEBS Letters. **58**: 293-299.
43. **Tsien, H.-C., G.A. Brusseau, R.S. Hanson, and L.P. Wackett.** 1989. Biodegradation of Trichloroethylene by *Methylosinus trichosporium* OB3b. App. and Environ. Microbiol. **55**: 3155-3161.
44. **Walton, B.T., and T.A. Anderson.** 1992. Plant-microbe treatment systems for toxic waste. Current Opinion in Biotechnology. **3**:267-270.
45. **Whittenbury R., and H. Dalton.** 1981. The methylotrophic bacteria. pp 894-902. *In* M.P.Starr (H.G. Truper, A. Balows, and H.G. Schlegel ,eds) The Prokaryotes, Vol.I Springer-Verlag, New York.

46. **Woodland, M.P., and H. Dalton.** 1984. Purification and characterization of component A of the methane monooxygenase from *Methylococcus capsulatus* (Bath). J. Biol. Chem. **259**: 53-60.
47. **Wright, P.F.A., W.D. Thomas, and N.H. Stacey.** 1991. Effects of trichloroethylene on hepatic and splenic lymphocytotoxic activities in rodents. Toxicology. **70**: 231-242.
48. **Zahn, J.A., C. Duncan, and A.A. DiSpirito.** 1994. Oxidation of hydroxylamine by cytochrome P-460 of the obligate methylotroph *Methylococcus capsulatus* Bath. J. Bacteriol. **176:** 5879-5887.

CHAPTER 2. MEMBRANE-ASSOCIATED METHANE MONOOXYGENASE FROM *Methylococcus capsulatus* Bath

A paper published in the Journal of Bacteriology[1]

James A. Zahn and Alan A.DiSpirito

Abstract

An active preparation of the membrane-associated methane monooxygenase (pMMO) from *Methylococcus capsulatus* Bath was isolated by ion exchange and hydrophobic interaction chromatography using dodecyl-β-D-maltoside as the detergent. Duroquinol was the reductant. The active preparation consisted of three major polypeptides with molecular masses of 47,000 and 27,000, and 25,000 Da. Two of the three polypeptides, the 47,000 and 27,000 Da, were identified as the polypeptides induced when cells expressing the soluble MMO are switched to culture medium in which the pMMO is expressed. The 27,000 Da polypeptide was identified as the acetylene binding protein. The active enzyme complex contained 2.5 iron and 14.5 copper atoms per 99,000 Da. The electron paramagnetic resonance spectrum of the enzyme showed evidence for a type 2 copper center ($g_{\perp}$ = 2.057, $g_{||}$ = 2.24, and $|A_{||}|$ = 172 G), a weak high spin iron signal (g= 6.0) and a broad low field (g = 12.7) signal. Treatment of the pMMO with nitric oxide, produced the ferrous-nitric oxide derivative observed in the membrane fraction of cells expressing the pMMO. Using duroquinol as a reductant, the specific activity of purified enzyme was 6.6 ± 2.4 nmol propylene oxidized • min^{-1} • mg $protein^{-1}$. The

---

[1] Reprinted with permission from the Journal of Bacteriology, **178**, 1018-1029.

activity was stimulated by ferric and cupric metal ions in addition to the cytochrome *b* specific inhibitors, myxothiazol and 2-heptyl-4-hydroxyquinoline-*N*-oxide.

The copper-binding cofactor (cbc) is a siderphore-like molecule, which binds 2 to 3 copper ions per subunit. CBC accounted for approximately 75% of the membrane-associated copper in cells grown in high (>5 μM) copper medium. The EPR of the purified sample was complex. The majority of the copper was EPR silent, but both type 1 ($g_{\perp}$ = 2.02, $g_{||}$= 2.415, and $|A_{||}|$= 83 [G]), and type 2 ($g_{\perp}$ = 2.035, $g_{||}$= 2.373, and $|A_{||}|$= 123 [G]) copper signals are observed.

Key words: Methanotroph, *Methylococcus capsulatus* Bath, membrane-associated methane monooxygenase, particulate methane monooxygenase, methane oxidation, cytochrome *b*-559/569.

Abbreviations: MMO, methane monooxygenase; pMMO, membrane-associated methane monooxygenase; sMMO, soluble methane monooxygenase; EPR, electron paramagnetic resonance; MOPS 3-[N-morpholino]propanesulfonic acid; MES 2-[morpholino]ethanesulfonic acid; PIPES, piperazine-N-N'-bis-[2-ethanesulfonic acid]; CHAPS, 3-[(3-cholamidopropyl)dimethylammonio]-1-propanesulfonate; NMS, nitrate mineral salts; EDTA, ethylaminediamine-tetraacetic acid; ICP-AES, inductively coupled plasma atomic emission spectroscopy; MALDI, matrix-assisted linear desorption laser ionization; 2-heptyl-4-hydroxyquinoline-*N*-oxide, HOQNO.

INTRODUCTION

In methanotrophs, the oxidation of methane to methanol is catalyzed by the methane monooxygenase (MMO) (31). In some genera, either a soluble or a membrane-associated MMO is present depending on the copper concentration during growth (12, 41, 51). At low copper to biomass ratios, the enzyme activity is observed in the soluble fraction and is referred to as the soluble MMO (sMMO). At higher copper to biomass ratios, methane oxidation activity is catalyzed in the membrane fraction by a different enzyme referred to as the membrane-associated or particulate MMO (pMMO). The polypeptides and genes for the sMMO have been characterized in several different methanotrophs (17, 18, 21, 22, 39, 56). The pMMO has proven more elusive. Tonge *et al.* (52) reported the solublization of methane-oxidizing activity from *Methylosinus trichosporium* OB3b with phospholipase C or sonification. A three subunit enzyme was isolated from this solubilized fraction with molecular masses of 47,000, 13,000 and 9,400 Da. The 13,000 Da polypeptide was a CO-binding *c*-type cytochrome. The 47,000 Da polypeptide contained approximately one copper atom per molecule and the 9,400 Da polypeptide was reported to be a regulatory protein. The purified enzyme could use ascorbate, but not NADH as a reductant. Akent'eva and Gvozdev(1) also reported the isolation of a membrane-associated, methane-oxidizing enzyme from *M. capsulatus* which utilized NADH as a reductant. This enzyme was composed of two subunits, molecular masses 45,000 and 35,000 Da, in a $\alpha_4\beta_4$ subunit structure, with 4 moles of non-heme iron and 1 mole copper per mole enzyme complex.

However, attempts to reproduce these results in this and other laboratories have not been successful.

Three observations aided in the stabilization of cell-free, membrane-associated methane oxidation activity and in the isolation of the pMMO from *M. capsulatus* Bath. First, the pMMO was shown to contain at least one iron atom center. Second, the addition of high concentrations of iron as well as copper to the growth medium were required for optimal cell free pMMO activity. Third, maintaining anaerobic conditions during solublization from the membrane fraction stabilized cell free pMMO activity. This report describes a reproducible procedure for the solubilization and isolation of a membrane-associated methane oxidation complex from *M. capsulatus* Bath.

MATERIALS AND METHODS

Organism and cultivation. *M. capsulatus* Bath was grown in nitrate mineral salts media (NMS) (54) plus 0 μM, 0.2 μM, 0.5 μM, 1.0 μM, 2.5 μM, 5.0 μM, 10.0 μM or 20.0 μM $CuSO_4$, and a vitamin mixture (29) at 37°C under an atmosphere of 40% methane, 20% oxygen, and 40% (vol/vol/vol) air. Cells grown under low (i.e. no copper addition) copper conditions were cultured by a semi-continuous method using NMS plus a vitamin mixture under copper limitation at 37°C in a 12-liter fermentor sparged at flow rates between 80 and 150 ml/minute methane and 2000 to 2500 ml/minute air. Cell batches exhibiting less than 100% soluble methane monooxygenase activity associated were discarded (typically the first and second batches were discarded).

Cells cultured for the isolation of the pMMO were grown in NMS plus 5μM $CuSO_4$. The copper concentration in the growth medium was increased as the cell

density increased. When the cell density reached an optical density of 0.3 - 0.4 at 600 nm, the copper and iron concentrations were increased incrementally, with the addition of 10 μM $CuSO_4$, 5 μM ferric ethylaminediamine-tetraacetic acid (FeEDTA), and 5 μM ferrous sulfate every 6 to 8 hours to a final concentration of 60 μM copper and 60 μM iron at late log phase (OD_{600nm} = 1.4 - 1.7). Cells were harvested by centrifugation at 13,000 x g for 15 minutes at 4°C, and resuspended (1:5 w/v) in 30 mM 3-[N-morpholino]propane-sulfonic acid (MOPS), pH 7.3 (buffer A).

Isolation of Washed Bacterial Membranes. All purification procedures were performed at 4°C under anaerobic conditions unless otherwise stated. Cells (29.2 grams wet weight) were lysed in a French pressure cell at 18,000 lb/in^2. The homogenate was centrifuged at 12,000 x g for 20 minutes to remove unlysed cells and debris. The supernate was collected and centrifuged at 140,000 x g for 2 hours to sediment membranes. The supernate was discarded and the membranes resuspended using a Dounce homogenizer in buffer A containing 1 M KCl, and centrifuged for 2 hours at 140,000 x g. The supernatant was discarded and the salt-washed membrane pellet (12.7 grams wet weight) was resuspended in 50 ml of buffer A using a Dounce homogenizer and stored under reduced argon.

Isolation of the pMMO. The membrane suspension (36 mg protein/ml) was transferred into a 125 ml serum vial sealed with a teflon/silicone septum and deoxygenated for several cycles of vacuum followed by reduced (i.e. deoxygenated though a heated copper column) argon. The anaerobic membrane fraction was transferred into an anaerobic chamber at room temperature, and the solution was stirred for 15 minutes under an atmosphere of 5% hydrogen and 95% nitrogen.

Following equilibration of the sample, a 10 % (w/v) solution of dodecyl-β-D-maltoside was added to a final concentration of 1.4 mg detergent per mg protein while stirring. The solution was stirred for 45 minutes at room temperature and then centrifuged at 140,000 x g for 2 hours at 4°C. The detergent-solubilized membrane fraction was diluted to a detergent/solvent ratio of 6 mg dodecyl maltoside/ ml of deoxygenated buffer A and loaded onto a DEAE-cellulose (2.5 x 28 cm) column, fitted with flow adapters and equilibrated with deoxygenated buffer A. The pMMO did not bind to the column and eluted in the flow-through fractions using deoxygenated buffer A. The flow-through fractions were combined and loaded on a 2.5 x 24 cm Phenyl-Sepharose column equilibrated with deoxygenated buffer A. The column was washed at a flow rate of 4 cm/hr with 1 column volume of buffer A plus 0.01% dodecyl-β-D-maltoside (buffer B). The pMMO fraction remained bound to the column and appeared as a diffuse, light gray band which migrated slowly through the column during the washing step with buffer B. The pMMO fraction was eluted from the column with 300 ml of a buffer containing 30 mM MOPS (pH 7.3) and 0.9% dodecyl maltoside (buffer C). The sample was concentrated under reduced nitrogen at 4°C on a stirred cell (PM-30 filter) to a final protein concentration of 85.5 mg/ml. The isolated preparations of pMMO could be stored for more than one week under reduced argon or nitrogen at 0 - 4°C with no appreciable loss of enzyme activity.

Labeling of the pMMO with [U-^{14}C] Acetylene . [U-^{14}C] acetylene was synthesized from $Ba^{14}CO_3$ (specific activity of 50 mCi/mmol) (Amersham, Corp. IL) and barium metal as previously described by Hyman and Arp (26). Exactly 200 µl isolated enzyme (12.1 mg protein)was transferred to a 6 ml serum vial. Reduced

duroquinone or ascorbate/phenazine methosulfate was added to the vial to a final concentration of 35 μM or 10 mg/ml and 6 μM, respectively. The vial was sealed with a teflon/silicone septum and 12 μl of [U-^{14}C] acetylene (9.0 x 10^5 dpm/μl) and 1 ml of oxygen were added to the vial with a syringe. The vials were incubated on a reciprocal shaker (200 rpm) at 37°C for 1 hour. The reaction was terminated by freezing the samples at -20° C for 1 hour.

Whole cell samples of *M. capsulatus* Bath were labeled with [U-^{14}C] acetylene as described previously by DiSpirito, et al. (14). A 2 ml suspension of cells (0.1 g wet weight/ ml buffer A) was placed in a 6 ml vial with 2.5 mM formate. The vial was sealed and 40 μl of [U-^{14}C] acetylene (9.0 x 10^5 dpm/μl) and 1 ml of oxygen were added through the septum with a syringe. Labeled cells were lysed in a French pressure cell at 18,000 lb/in^2. The homogenate was centrifuged at 12,000 x g for 20 minutes to remove unlysed cells and debris. Purified pMMO, cell-free, or washed membrane polypeptides of *M. capsulatus* Bath were separated by SDS-polyacrylamide gel electrophoresis and the dried gels were incubated in a phospor cassette for 3 - 4 days and were analyzed on a Molecular Dynamics model 400A PhosphoImager for [U-^{14}C] acetylene-labeled polypeptides.

Isolation of the 47,000-27,000 Da switchover polypeptides. The term "47,000-27,000 Da switchover polypeptides" is used for the polypeptides induced when cells expressing the sMMO convert to expression of pMMO under altered growth conditions (51). The salt-washed membrane pellet was resuspended in 10 mM Tris-HCl, pH 8.0 (buffer D) plus 1.5 % Triton X-100 (w/v) (Surfact Amps, Perice Chem. Co., IL) to a final protein concentration of 16 mg/ml using a Dounce homogenizer. The suspension was incubated for 1 h with stirring and centrifuged at

140,000 x g for 2 h. The supernate was dialyzed against 6 changes of buffer D plus, 0.01% Triton X-100 (buffer E) and loaded on a 2.5 x 15 cm DEAE-cellulose column equilibrated with buffer E. The flow-through fractions were collected and loaded on a DEAE-Sepharose CL-6B column (2.5 x 28 cm) equilibrated with buffer E. The column was developed with a linear gradient of 0 to 1 M KCl in buffer D followed by a linear gradient of 0.01% to 1.4% Triton X-100 plus 1 M KCl in buffer D. Fractions which eluted at approximately 0.8% (w/v) Triton X-100 were collected and dialyzed against 3 changes of buffer D. Following dialysis, the sample was loaded on a DEAE-Sepharose CL-6B column (1.25 x 10) equilibrated with buffer D. The column was washed with 200 ml of 1 mM 3-[(3-cholamidopropyl) dimethylammonio]-1-propanesulfonate (CHAPS) in buffer D and eluted with buffer D plus 1% CHAPS, 1% octyl-glycoside and 1 M KCl. The samples were dialyzed against 3 changes of buffer B plus 1 mM CHAPS, and concentrated with a stirred cell (PM-30 filter). The sample was loaded on to a 5-20% sucrose density gradient containing 500 mM potassium phosphate (pH 7.0) with 2 mM CHAPS and centrifuged for 12 hours at 130,000 x g. The major, gray/tan-colored band at the bottom of the tube (47,000-27000 Da switchover polypeptides) and a brown-red band at the top of the tube (cytochrome *b*-559/569) were collected and dialyzed for 12 h against 3 changes of buffer D plus 1 mM CHAPS.

Isolation of the copper-binding cofactor (cbc). Salt-washed membranes were resuspended in 5 mM CHAPS with a Dounce homogenizer (final concentration of 30 mg protein/ml). The solution was centrifuged at 140,000 x g for 2 hours and the supernate discarded. The pellet was resuspended in 20 - 30 times the pellet volume of 50% N,N-dimethyl formamide (DMF), and centrifuged at 13,000 x g for 25

minutes. The supernate was saved and the pellet resuspended in 20 - 30 times the pellet volume of 100% DMF and centrifuged at 13,000 x g for 25 minutes. The supernate was combined with the 50% DMF fraction and dried under vacuum on a rotary evaporator at 60°C. The sample was resuspended in a minimal volume of 50 mM phosphate buffer, pH 7.0 and loaded on a 2.5 x 20 cm silica gel (40-140 mesh) column. The column was washed with one column volume of H_2O, one column volume of 50% methanol and eluted with 50% methanol plus 20 mM HCl. The sample was freeze-dried and resuspended in buffer B.

Protein, metal and heme determinations. The concentrations of heme *a*, heme *b*, and heme *c* were measured by the pyridine hemochromogen method (13) using the $\Delta\varepsilon_{587nm}$ of 21.7 $cm^{-1}mM^{-1}$ for heme *a* (55), the $\Delta\varepsilon_{557nm}$ of 34.4$cm^{-1}mM^{-1}$ for heme *b* (55) and the $\Delta\varepsilon_{550nm}$ of 29.1$cm^{-1}mM^{-1}$ for heme *c* (19). The simultaneous determination of heme A, heme B and heme C in washed membrane fractions were also estimated by the Berry and Trumpower method (7).

The separation of extractable hemes was performed by reverse-phase high-performance liquid chromatography. Salt-washed membrane fractions (43.4 mg protein) were extracted twice with an acetone/HCl (99:1 v/v) solution at -20°C. The combined extracts were partitioned into diethyl ether, washed twice with H_2O, and dried in a stream of nitrogen. The hemes were solublized with 2 ml of an acetonitrile-water-trifluroacetic acid (50:49.92:0.08) solution and filtered through a 0.45 μm filter. The filtered heme-containing solutions were separated by gradient reverse-phase high performance liquid chromatography (HPLC) using a VyDac semi-preparative C_{18} column (10 x 250 mm) at a flow rate of 4.0 ml/minute using

water-trifluroacetic acid (99.9:0.1) (buffer B) and acetonitrile-trifluroacetic acid (99.92:0.08) (buffer C) as the mobile phase. The linear gradient consisted of 40% buffer C at 10 minutes following injection to 100% buffer C at 40 minutes. Heme standards were composed of bovine hemoglobin (protoheme) and *M. capsulatus* (Bath) cytochrome aa_3 (15). Fractions exhibiting an absorbance at 400 nm were collected and lyophilized to dryness for analysis of molecular mass by matrix assisted laser desorption ionization (MALDI) time of flight mass spectroscopy on a Finnigan LASERMAT 2000 mass spectrometer using synapinic acid as a matrix (4).

Inorganic sulfide content of samples was determined by the method of Beinert (5). Solutions of sodium sulfide were used as reference standards.

For metal analysis, samples were dialyzed for 18 hours against five changes of 5 mM PIPES, 5 mM NaEDTA, pH 7.0 buffer. Following dialysis, samples were diluted (50:50 v/v) in concentrated nitric acid and digested 24 hours at 110° C. After cooling, samples were brought to a volume of 25 ml with H_2O and were analyzed for sulfur, copper, iron, molybdenum, manganese, and zinc by inductively coupled plasma atomic emission spectroscopy with a model 3410 ICP AES (Applied Research Laboratories).

Protein was assayed by the method of Lowry et al. (32) using bovine serum albumin as a standard.

Enzyme Activity. Methane monooxygenase activity was determined by the epoxidation of propylene as previously described (14) using duroquinol, 35 mM, (for pMMO containing extracts) or 7 mM NADH (for sMMO containing extracts) for the reductant in cell free fractions or 2.5 mM formate in whole cell samples. The

reaction was initiated by the injection of propylene (2 ml) and oxygen (1 ml) through the septum of a sealed vial. Reaction mixtures were incubated at 37° C on a rotary shaker at 250 rpm.

Trichloroethylene oxidation was monitored as described by DiSpirito et al. (14). Soluble methane monooxygenase activity was monitored by the formation of naphthol from naphthalene by the method of Brusseau et al. (8).

The method for reduction of duroquinone to duroquinol was performed by a modification of the method described by Shiemke et al. (50) except, the quinol was added as a solid and was present at higher concentrations (25-35 mM). Duroquinone (Sigma Chemical, St. Louis, MO) (0.2 g) was dissolved in approximately 20 ml of HCl-acidified (3 mM HCl in solvent) ethanol. Sodium hydrosulfite (0.28 g) was added to the solution with continuous stirring. After 3 minutes, sodium borohydride (0.07 g) was added and the solution became colorless within 1 minute. Stirring was discontinued and the solution was allowed to stand for 15 minutes to promote full reduction of the quinone. After 15 minutes, the solution was diluted with 150 ml of distilled H_2O and suction-filtered through a Whatman #1 filter paper. The water-insoluble quinol remained colorless and did not pass through the filter. Finally, the quinol was washed with approximately 200 ml of H_2O to remove excess sodium hydrosulfite and sodium borohydride and dried by suction filtration. The quinol (3-6 mg) was placed in empty serum vials and stored at -20° C for no longer than 2 days before use.

The absence of sMMO activity was confirmed by lack of methane oxidation activity in the soluble fraction, by monitoring for the formation of naphthol from naphthalene (8) and by the SDS-polyacrylamide gel profile of polypeptides.

In inhibitor studies, the enzyme was pre-incubated for 5 minutes at 37°C with the inhibitor before the reaction was started by the addition of propylene. Stock solutions of 2-heptyl-4-hydroxyquinoline-*N*-oxide (HOQNO) were prepared in dimethyl sulfoxide (DMSO). At the concentrations used (1 µl/ml), DMSO showed no effect on the rate of propylene oxidation by the purified enzyme. Myxothiazol stock solutions were prepared in ethanol, added to empty reactions vials and the ethanol evaporated under a stream of reduced nitrogen. Reaction mixtures consisted of the enzyme, 35 mM duroquinol, and either 190 µM HOQNO or 164 µM myxothiazol in a 7 ml serum vial. Protein concentrations were 1.0 mg/ml in whole cell assays and 2 mg/ml in pMMO assays. The reactions were initiated by injection of propylene (2 ml) and oxygen (1 ml). Reaction mixtures were incubated at 37°C on a rotary shaker at 250 rpm.

Cytochrome oxidase activity was assayed by recording oxygen uptake at 37°C in the presence of ascorbate-N,N,N',N'-tetramethyl-*p*-phenylenediamine dihydrochloride (TMPD) as described by Ferguson-Miller et al. (16). The oxygen electrode was calibrated as previously described (44).

Spectroscopy. Optical absorption spectroscopy and X-band electron paramagnetic resonance (EPR) spectra were obtained as previously described (57) Operating parameters are outlined in the figure legends.

Anaerobic Reduction and Formation of Nitrosyl Derivatives of the Washed Membrane Fraction. Anaerobic reduction of samples was performed in a Coy anaerobic chamber at 20°C in an atmosphere of 5% hydrogen and 95% nitrogen. Oxygen concentrations were maintained at levels below 1 ppm during all anaerobic procedures. Samples were deoxygenated on a vacuum line with

repeated cycling with argon and vacuum then transferred into the anaerobic chamber and stirred for 30 minutes in 3 ml reaction vials (Pierce, Rockford, IL) which were fitted with magnetic stirring bars. Following displacement of the oxygen, samples were reduced by the addition of sodium ascorbate to a final concentration of 10 mg/ml and phenazine methosulfate (PMS) to a final concentration of 6 μM and incubated with stirring for 45 minutes (10). For ascorbate/PMS-reduced EPR spectra, samples were transferred from the vial to quartz EPR tubes. The tubes were capped within the anaerobic chamber and immediately frozen under liquid nitrogen following transfer from the chamber.

The nitric oxide derivative of ascorbate/PMS-reduced samples were prepared using the *in situ* reduction of the nitrite ion as the source of the nitric oxide (10). The protein-NO complex was formed anaerobically with reduced samples by adding solid $H^{14}NO_2$ or $H^{15}NO_2$ (ICL, Andover, MA) to a final concentration of 5 mg/ml. The samples were incubated with stirring for approximately 4 minutes following the addition of nitrite and then transferred into quartz EPR tubes. The tubes were capped within the anaerobic chamber and immediately frozen under liquid nitrogen.

Preparation of antibodies against the pMMO and cytochrome *caa*$_3$ - cytochrome-*c*-557 complex. Cytochrome *caa*$_3$-cytochrome *c*-557 complex and the pMMO were purified as described by DiSpirito et al. (15), and Zahn and DiSpirito (this paper), respectively. Antiserum against these polypeptides were raised in two 10-week-old female, New Zealand White Rabbits. Each enzyme [0.6 mg per rabbit] was diluted in Ribi adjuvant according to the manufacturers recommendations and injected intradermally. Immunogloblin G was purified from serum using immobilized

Protein A (Pierce, Rockford, IL, USA) and concentrated using a Centriprep 30 concentrator (Amicon, Inc., Beverly, MA).

Electrophoresis and Immunoblot Analysis. Sodium dodecyl sulfate (SDS)-polyacrylamide slab gel electrophoresis was carried out by the method of Laemmli (28) on 12 to 15% gels. Unless indicated, reductants were not added to the buffers and the samples were incubated at room temperature for 10 to 30 minutes prior to loading. Gels were stained for total protein with Coomassie brilliant blue R, by the diaminobenzidine method (35) for *c*-type cytochromes, or blotted for immunoassays. Densitometry was performed on dried gels stained with Coomassie R-250 using a Bioimaging Technologies Biovideo MP1000 gel documentation system.

Proteins were blotted onto nitrocellulose using a Mini Trans-Blot electrophoretic transfer cell (Bio-Rad Laboratories, Richmond, CA) per manufacturer's directions. Following treatment with serum raised against purified protein, filter bound antibodies were detected with the alkaline phosphatase assay following manufacturer's directions (Bio-Rad Laboratories).

Amino Acid Analysis and Sequence. Amino acid analyses were performed with an Applied Biosystems 420A Derivitizer coupled to an Applied Biosystems 130A separation system. Samples were hydrolyzed under vacuum in 6 M HCl plus 1.5% phenol at 150° C for 1 hour. Quantitation of cysteine was performed by conversion of cysteine residues to pyridylethyl cysteine by reaction of free protein sulfhydryls with 4-vinyl pyridine(34).

Amino acid sequence analyses were performed by Edman degradation with an Applied Biosystems 477A Protein Sequencer coupled to a 120A Analyzer. Sequence analyses of the 47,000, 27,000, and 25,000 Da pMMO polypeptides were performed samples electroblotted to PVDF membranes using a transfer buffer composed of 10mM 3-[cyclohexylamino]-1-propanesulfonic acid (pH 11) and 10% methanol.

RESULTS

Optimization of membrane-associated methane oxidation activity. Consistent with previous studies (38), the concentration of copper in the growth medium stabilized methane oxidation activity in the membrane fraction (Fig. 1A). Whole cell propylene oxidation rates from cells cultered in copper concentrations between 0.5 and 20 μM remained essentially constant (approximately 125 nmol•min^{-1}•mg protein^{-1}). However, the activity in the washed membrane fraction increased proportionally with the copper concentration in the growth medium. Unfortunately, using a 10% inoculum (optical density at 600 nm of 1 - 1.5) copper concentrations above 10 μM were toxic, and no growth was observed at concentrations greater than 20 μM. The copper concentration in the growth medium could be increased above 20 μM if added as the cell density increased (see Materials and Methods). The propylene oxidation activity in the whole cell or washed membrane fractions from cells cultured in media containing a final concentration of 60 μM $CuSO_4$ was lower than the rate observed from cell cultures in 20 μM copper. The pMMO activity in the detergent solublized fraction was 2 to 2.5 fold higher than the rate observed from cell cultures in grown in fixed copper (5 μM)

FIG. 1. The effect of copper ion concentration on the rate of membrane-associated methane oxidation (A) and on the iron-uptake*versus* methane oxidation (B) in *M. capsulatus* Bath. Points represent cells grown in media containing 1.0 (1), 2.5 (2) , 5.0 (3), 10.0 (4), and 20.0 (5) μM $CuSO_4$.

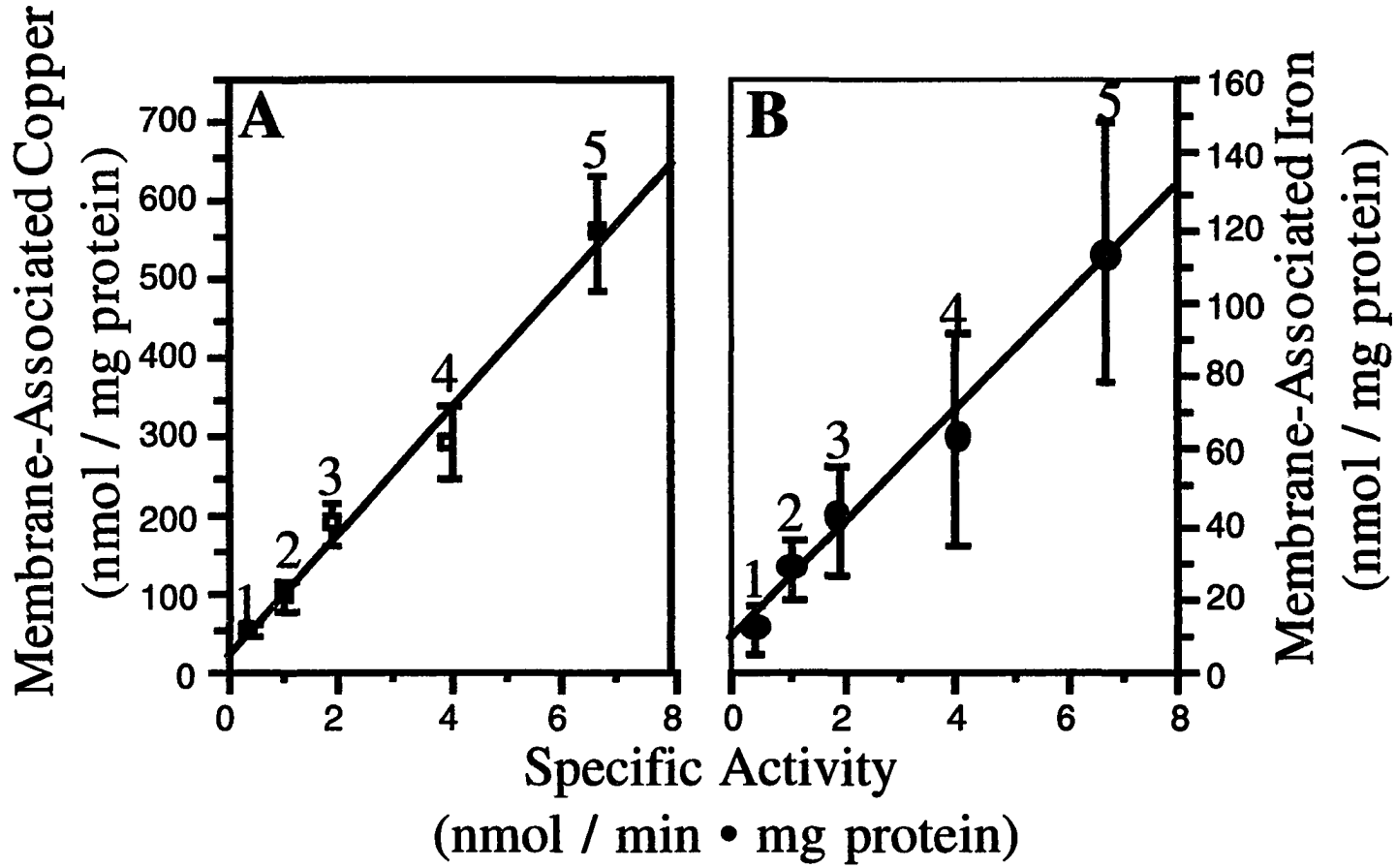
A
B
Membrane-Associated Copper
(nmol / mg protein)
Membrane-Associated Iron
(nmol / mg protein)
Specific Activity
(nmol / min • mg protein)
0
100
200
300
400
500
600
700
0
20
40
60
80
100
120
140
160
0
2
4
6
8
1
2
3
4
5

and iron (0.9 μM) concentrations. Propylene oxidation activity in the 10% dodecyl β-D-maltoside detergent extract was also stimulated 1.5 fold with the addition of *equimolar concentrations of iron with copper.*

Copper induced iron uptake. Nguyen et al. (38) observed a non-proportional increased iron uptake in the washed membrane fraction with increased copper in the growth medium. The increased iron was observed without added iron to the growth medium. We observe a similar trend in cells cultured in media containing 0.5 to 20 μM Cu and 0.9 μM iron. However, in contrast to the study by Nguyen et al. (38) the results from this study showed a proportional increase in iron uptake by the membrane fraction with increased copper in the growth medium (Fig. 1B). Individual data points shown in figure 1 were the calculated means of 14 separate experiments. The stochiometry of iron to copper in the washed membrane fraction was 3.5 to 4.9 copper atoms per iron in cells expressing the pMMO. The increased iron uptake in cells grown in 0.5 to 20 μM Cu^{2+} occurred in culture media containing a constant (0.9 μM) iron concentration. We will refer to this increase of iron as "copper-induced iron uptake".

Localization of copper-induced iron uptake. To identify the polypeptide(s) responsible for iron uptake, the total soluble and membrane-associated heme, the extractable hemes, the concentration of the major membrane-associated respiratory polypeptides, and spectral properties (absorption and electron paramagnetic resonance spectroscopy) were compared. As determined by the pyridine ferrohemochromagen assay (13), there was less than a 25% difference in the concentration of *c*-heme in the soluble fraction and less than an 8% difference in

total heme A, heme B, or heme C in the membrane fraction of cells in expressing the different MMO's (Table 1).

Heme extraction, HPLC purification, and characterization by mass spectrometry were found to be an efficient means by which to remove spectral interferences of cytochrome *c* in the analysis of membrane samples. The elution profile recorded at 400 nm for extractable heme from the membranes of *M. capsulatus* (Bath) grown in the absence of copper and expressing 100% of the MMO activity in the soluble fraction and in the presence of 5 μM $CuSO_4$ and expressing 100% of the MMO activity in the membrane fraction were simular. The elution profiles for the extracted heme were compared to standards composed of protoheme extracted from bovine hemoglobin and *M. capsulatus* Bath cytochrome *aa*3. Peaks eluting at 20.9 minutes (61.8% solvent B) have been assigned to protoheme due to similarities in elution profile and molecular mass of extracted protoheme from bovine hemoglobin. Comparisons of the mass spectra of the collected peaks at 20.9 minutes show that both samples have a molecular mass of 620 Da. This molecular mass value is in good agreement with the molecular mass of protoheme at 617 Da. Peaks which elute 29.6 minutes (79.2% solvent B) have been assigned to heme A based on the comparison of elution time to heme A extracted from *M. capsulatus* (Bath) cytochrome *aa*3, on the molecular mass (856 Da) and by the ferrohemochromagen spectral similarities to extracted heme A from *M. capsulatus* (Bath) cytochrome *aa*3. Concentrations of heme A and B were 21% and 18% higher in the membrane fraction of cells expressing the sMMO. These results are similar to the results calculated by the pyridine ferrohemochromagen

assay and provide a method to quantify extractable heme from membrane samples (Table 1).

Nguyen et al.(38) suggested the increased iron in the membrane fraction was associated with cytochrome *c*-557. To determine if this cytochrome was the source of the copper induced iron uptake, immunoblot analysis of membrane fractions isolated from cells expressing the sMMO and from cells expressing the pMMO with antibodies against cytochrome *aa*3-cytochrome *c*-557 were determined. The results demonstrated that the expression level of the polypeptides in this complex were unchanged with respect to copper availability in the growth medium (data not shown). Ascorbate-TMPD oxidase activity per mg protein was also unchanged when the membrane fractions from cells expressing the soluble MMO were compared to the membrane fractions of cells expressing the membrane-associated MMO.

EPR spectra of the washed-membrane fraction. In agreement with Nguyen et al. (38), under low microwave power settings we observe a very intense copper signal with a $g_{\perp} = 2.057$ and hyperfine splitting constants of $g_{||} = 2.27$ and $|A_{||}| = 174$ [G] in the membranes isolated from cells grown in the presence of 5μM CuSO4. These copper signals are similar to the type 2 copper associated with the pMMO (Table 3). No observable copper resonances were detectable in the membranes of cells expressing the sMMO (results not shown).

Analysis of subtracted EPR spectra for membrane samples shows a minor increase for the g = 4.05 and g = 4.61 from the membranes of cells expressing the sMMO and an increase in the population of a and g = 6.00 signal from the

membranes expressing the pMMO (results not shown). Studies of *b*-type cytochromes from *M. capsulatus* (Bath) have indicated that the signals ($g = 4.05$ and $g = 4.61$) arise from cytochrome bb_3 (Zahn and DiSpirito, unpublished results). The signal at g = 6.00 appears to be associated with a non-heme iron species associated with pMMO, since the concentrations of membrane-associated heme A, B, or C were not altered with the expression of the different methane monooxygenases. Quantitation of the iron concentration by EPR integration of the $g = 6.0$ signal shows the signal accounted for less than 15 % of the increased iron associated with the membrane fraction of cells expressing the membrane-associated MMO.

The nitric oxide derivative EPR spectrum of the membrane fraction from cells expressing the pMMO identified the source of the additional iron (Fig. 2 trace C). The spectrum illustrates the majority of the iron is EPR-silent and is either a single ferrous iron center or a component in an iron-iron or iron-copper center (2, 3, 23, 24, 25). This ferrous iron atom has been identified as the iron center associated with the pMMO (see Figs. 6 and 7).

Purification of the pMMO. Table 2 summarizes the isolation of pMMO from *M. capsulatus* Bath. Several features of the purification procedure described in the Materials and Methods must be stringently followed to avoid enzyme inactivation. First, supplementation of the growth media with copper and iron increased the specific activity 4-fold in the detergent solublized fraction over membrane preparations grown in NMS media containing 5μM $CuSO_4$. Second, the loss of methane oxidation activity was minimized by maintaining anaerobic conditions during solublization. Lastly, once solublized, the enzyme is stabilized by

FIG. 2. EPR spectra for NO-treated-KCl-washed membrane cell extracts *M. capsulatus* Bath expressing the (A) pMMO, the (B) sMMO, and (C) spectrum A minus spectrum B. Protein concentration was 55 mg/ml in 10 mM Tris, pH 8.0 at 7.7° K. Operating parameters were: Modulation frequency, 100 kHz; Modulation amplitude, 12.5 G; Time constant 100 ms. The microwave frequency was 9.421 GHz and the microwave power was 2.2 mW.

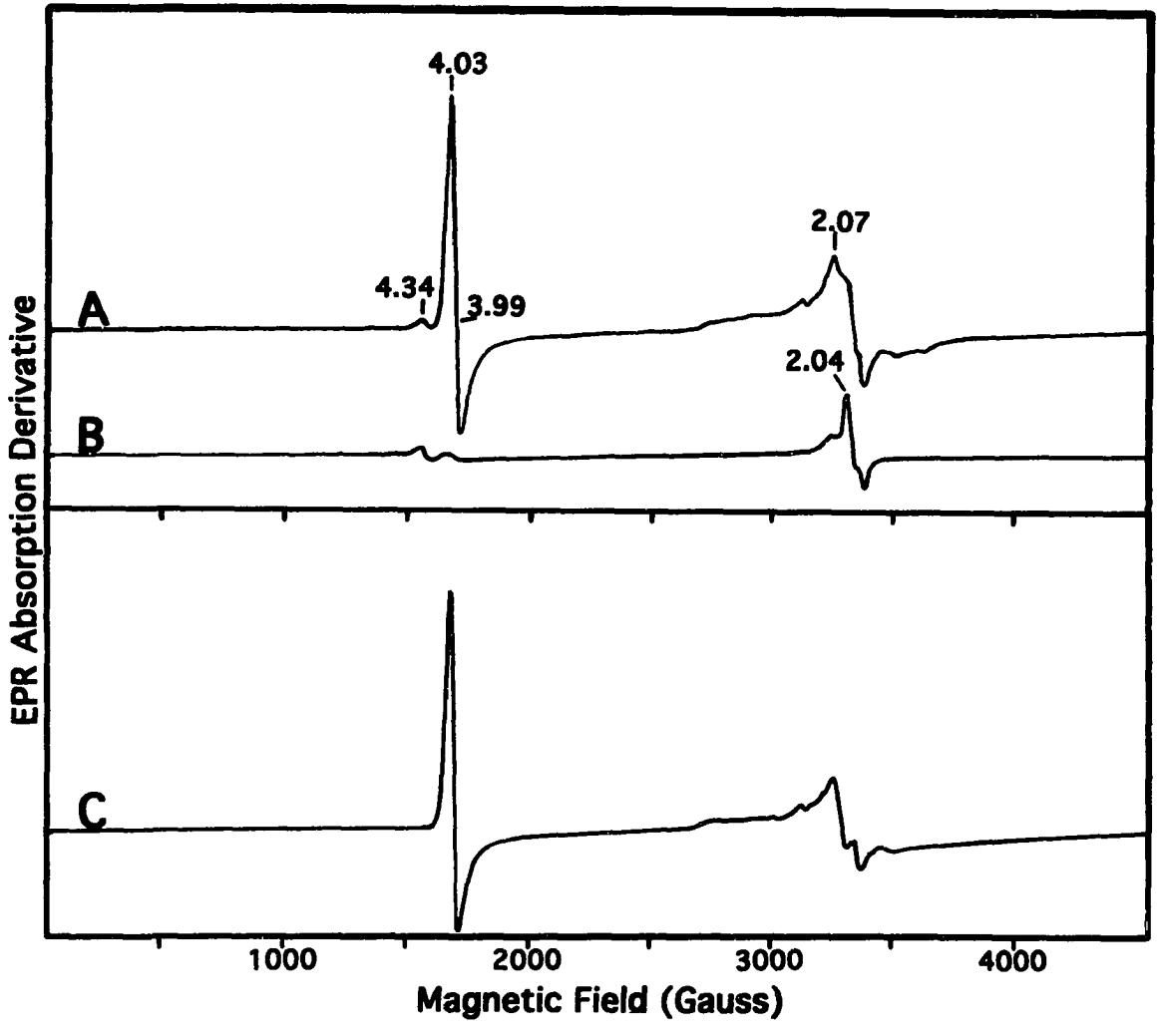
4.03
2.07
4.34
3.99
2.04
A
B
C
EPR Absorption Derivative
1000
2000
3000
4000
Magnetic Field (Gauss)

Table 1. Heme composition in *M. capsulatus* Bath expressing the pMMO or sMMO. Cells expressing the pMMO were grown in NMS media supplemented with 5 μM copper sulfate. Concentrations are given in nmol/mg protein.

	sMMO		pMMO		pMMO vs. sMMO[1]	
	Soluble fraction	Membrane fraction	Soluble fraction	Membrane fraction	Increase (%)	Decrease (%)
Copper	0.7	17	0.4	189	1112	
Iron	2.4	3.1	1.8	42	1355	
Heme A	0	0.07	0	0.09		7.7
Heme B	0	0.39	0	0.36		7.9
Heme C	-	0.38	-	0.35		4.8
Heme C	1.63	-	1.12	-	22	
Total	1.63	0.84	1.12	0.8		20.4
Percent Heme[2]	68	26	62	1.9		

[1]Percent difference between the metal or heme content in the membrane fractions of cells expressing the membrane-associated MMO from cells expressing the soluble MMO.

[2]Percent of total iron in the heme fraction.

Table 2. Purification of pMMO from *M. capsulatus* Bath using 35 mM duroquinol as the *invitro* pMMO reductant.

Step	*Protein (mg)*	*Total Activity (nmol min.$^{-1}$)*	*Specific Activity (nmol min.$^{-1}$ mg^{-1})*	*Yield*
Whole cell (20 mM formate)	4520	-	60.50	-
Cell-Free S-13K	4382	36896	8.42	100
Membrane P-140K	2705	28132	10.40	76
1M KCl Salt-Washed Membrane P-140K	2312	21663	9.37	59
Dodecyl Maltoside Extract	1920	18931	9.86	51
DEAE-Cellulose	1296	13297	10.26	36
Phenyl Sepharose CL4B	983	10892	11.08	30

maintaining protein concentrations above 15 mg/ml with maximum activities at 85 mg/ml. The pMMO activity also showed nearly an exponential relationship to protein concentration.

Properties of the pMMO. The properties of pMMO are summarized in Table 4 and Figs. 4 - 8.

Subunit structure and metal components. On SDS-polyacrylamide gels the membrane-associated methane oxidation complex consists of polypeptides with molecular masses of 47,000, 27,000, and 25,000 Da, as well as a trace contaminating polypeptides with molecular massed of 37,000, 32,000 and 20,000 Da (Fig. 3A lane B). The 37,000 and 20,000 Da polypeptides were identified as cytochrome *b*-559/569 and co-purified with the pMMO. All attempts to remove these polypeptides resulted in enzyme inactivation.

Acetylene has been shown to be an irreversible inhibitor of both methane monooxygenases (42). Previous studies have shown that when cells from different methanotrophs were grown under conditions in which they express the pMMO and exposed to ^{14}C-acetylene, a major labeled polypeptide was located in the membrane and with one exception, had a molecular weight of 25,500 to 26,000 Da (14, 42). The phosphoimage of the washed membrane fraction or purified pMMO treated with ^{14}C-acetylene is shown in Fig. 3A lanes D and E. The increased sensitivity of the phosphorescence image over fluorograms showed the labeling of the 47,000 Da polypeptide as well as the 27,000 Da polypeptide. The labeling of the 47,000 Da polypeptide was reproducible, although the level of labeling was always lower than observed for the 27,000 Da polypeptide (Fig. 3B). The labeling of the 47,000 Da polypeptide may result from an activated acetylene intermediate such as ketene (42)

Fig. 3A. SDS-polyacylamide gel electrophoresis of the cell-free fraction isolated from *M. capsulatus* Bath whole cells treated with [U-^{14}C] acetylene using formate as the reductant (lanes B and D) and of purified pMMO treated with [U-^{14}C] acetylene using duroquinol as the reductant (lanes C and E). Lanes A through C were stained for total protein with Coomassie brilliant blue R-250 and lanes D and E are a phosphorescence image of [U-^{14}C] acetylene-labeled polypeptides exposed for 3.5 days on a storage phosphorescence imaging screen. BioRad low-range molecular mass standards are shown in lane A.

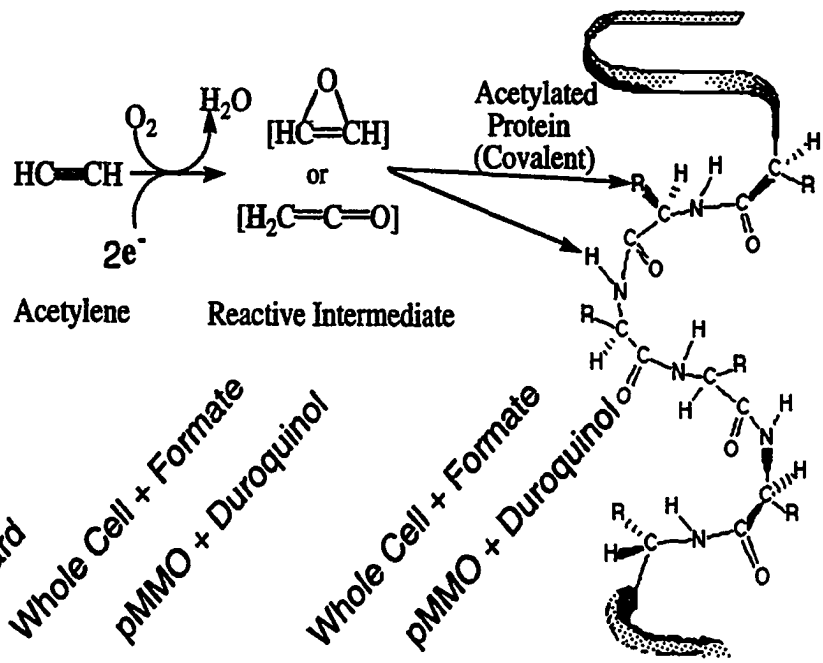
HC≡CH
O2
H2O
2e-
[HC=CH]
or
[H2C=C=O]
Acetylene
Reactive Intermediate
Acetylated Protein (Covalent)

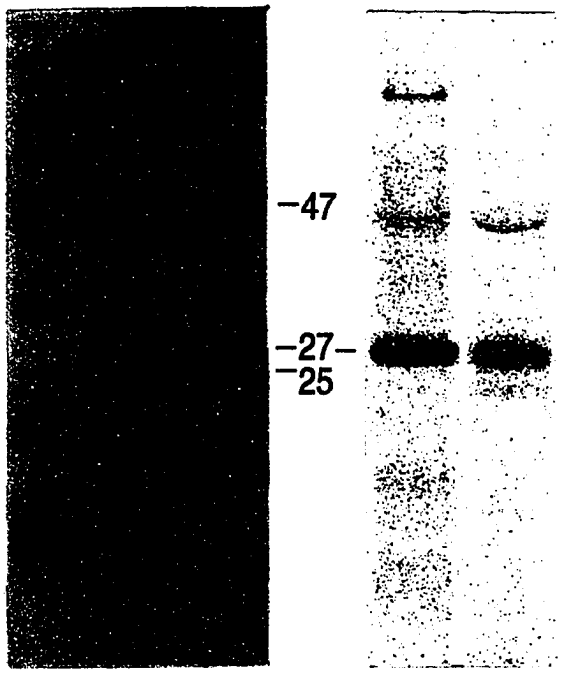
Standard
Whole Cell + Formate
pMMO + Duroquinol
Whole Cell + Formate
pMMO + Duroquinol
47
27
25

Fig. 3B. SDS-polyacrylamide gel electrophoresis of purified pMMO from *M. capsulatus* Bath treated with [U-^{14}C] acetylene using duroquinol as the reductant (lanes B and C) and ascorbate as the reductant (lane A). Lanes D through G were stained for total protein with Coomassie brilliant blue R-250 and lanes A through C are a phosphorescence image of [U-^{14}C] acetylene-labeled polypeptides exposed for 3.5 days on a storage phosphorescence imaging screen. BioRad low-range molecular mass standards are shown in lane G.

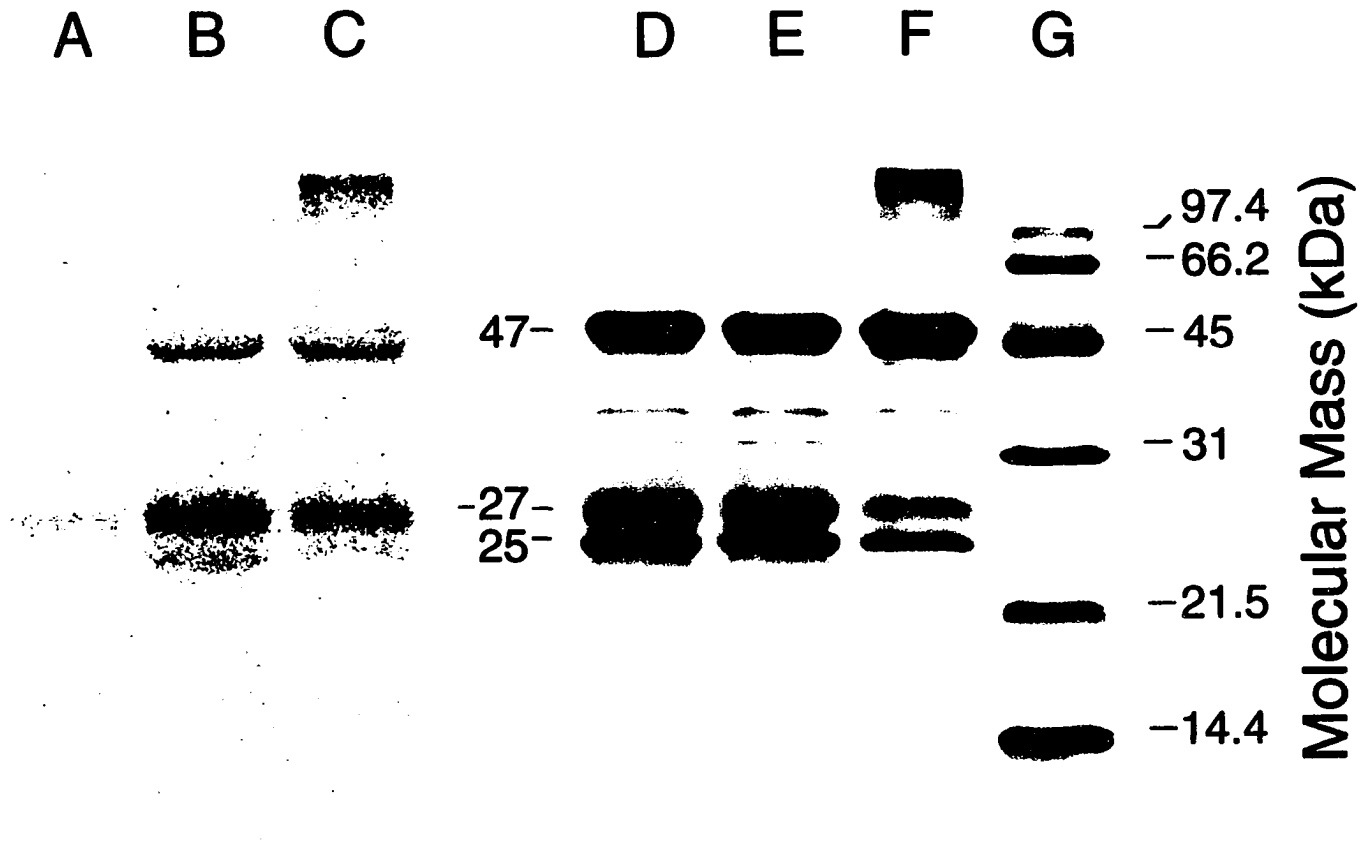
A
B
C
D
E
F
G
97.4
66.2
47
45
31
27
25
21.5
14.4
Molecular Mass (kDa)

which diffuses from the active site and forms a covalent attachment to amino acid residues in the active site or with neighboring polypeptides. A similar phenomena has been observed with the ammonia monooxygenase (27).

The N-terminal sequence of the 47,000, 27,000 and 25,000 Da polypeptides presented in Fig. 5 were identical to the translated amino acid sequence from *M. capsulatus* Bath *pmmo* B, *pmmo* A, and *pmmo* C, respectively (11, 48).

The active enzyme complex contained 2.5 iron and 14.5 copper atoms based on the molecular mass determined by SDS-polyacrylamide gel electrophoresis (99,000 Da). The enzyme preparation contained less than 11 molar % Mo, Mn and Zn.

Spectral Properties. The EPR spectra of the pMMO were similar to the washed membrane fraction from cells expressing the pMMO (38, 48) with a type 2 copper center ($g_{\perp} = 2.057$, $g_{||} = 2.24$, and $|A_{||}| = 172$ G) and a weak high spin iron signal (Fig. 6 trace A). Under higher microwave powers, there was a proportional increase in the intensity of a high spin ferric signal (g= 6.0) and a broad low field (g = 12.5) signal (Fig. 6). This low field signal has been observed in several mononuclear and binuclear oxygen binding metal centers such as those found in cytochrome *c* oxidases, μ-oxo-bridged enzymes and in oxygen transporting proteins (2, 3, 20, 23, 24, 25, 31, 38). In the sMMO, the g = 15 signal is only observed with the fully reduced Fe(II)-Fe(II) hydroxylase component (24, 31). In the pMMO from *M. capsulatus* Bath, this signal was observed in the resting sample, suggesting the signal does not originate from a μ-oxo-bridged iron center. Reduction of the pMMO with ascorbate and PMS results in the loss of the g = 12.7 signal in all preparations.

Fig. 4. Immunoblot analysis of *M. capsulatus* Bath cell fractions exhibiting soluble or particulate MMO activity with antibodies against pMMO. Results for KCl-washed membrane franctions from cells expressing the sMMO (lanes A [12 μg protein] and E [36 μg protein]) and the pMMO (lanes B [12 μg protein] and F [36 μg protein]) and for soluble fractions from cells expressing the sMMO (lanes C [16 μg protein] and G [48 μg protein]) and the pMMO (lanes D [16 μg protein] and H [48 μg protein]) are shown. Lanes A through D were stained with Coomassie brilliant blue R-250. Lanes E through H were probed with antibodies to pMMO.

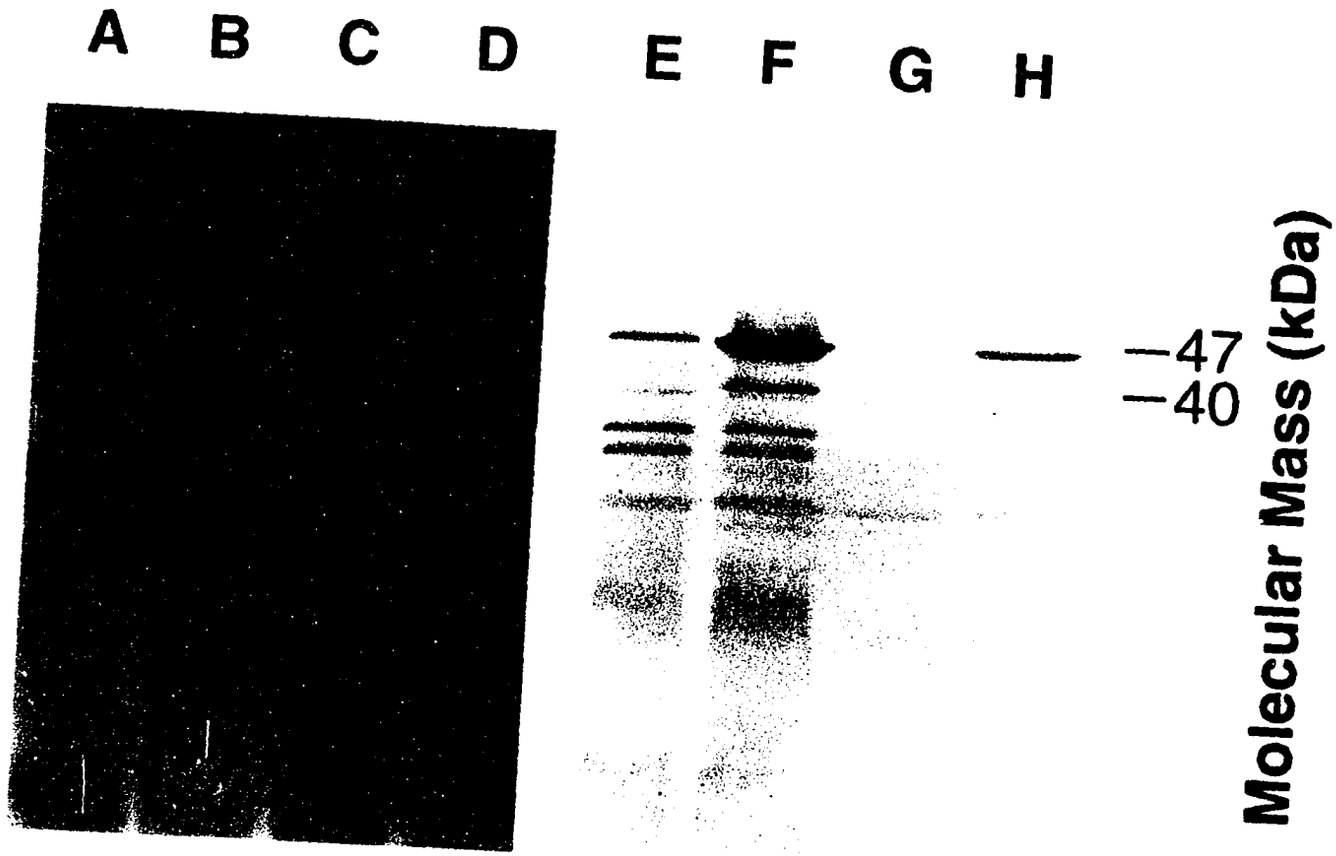
A
B
C
D
E
F
G
H
47
40
Molecular Mass (kDa)

FIG. 5. Sequence alignments showing sequence homology of the individual subunits of the pMMO translated amino acid sequence from the pMMO gene sequence. (A) Sequence alignment of the 47,000 Da (a) polypeptide. (B) Sequence alignment of the 27,000 Da acetylene-binding (b) polypeptide. (C) Sequence alignment of the 25,000 Da (g) polypeptide. Circles indicate identical amino acid matches; "N" indicates the N-terminus of the polypeptide. Question marks indicate unidentifed amino acids.

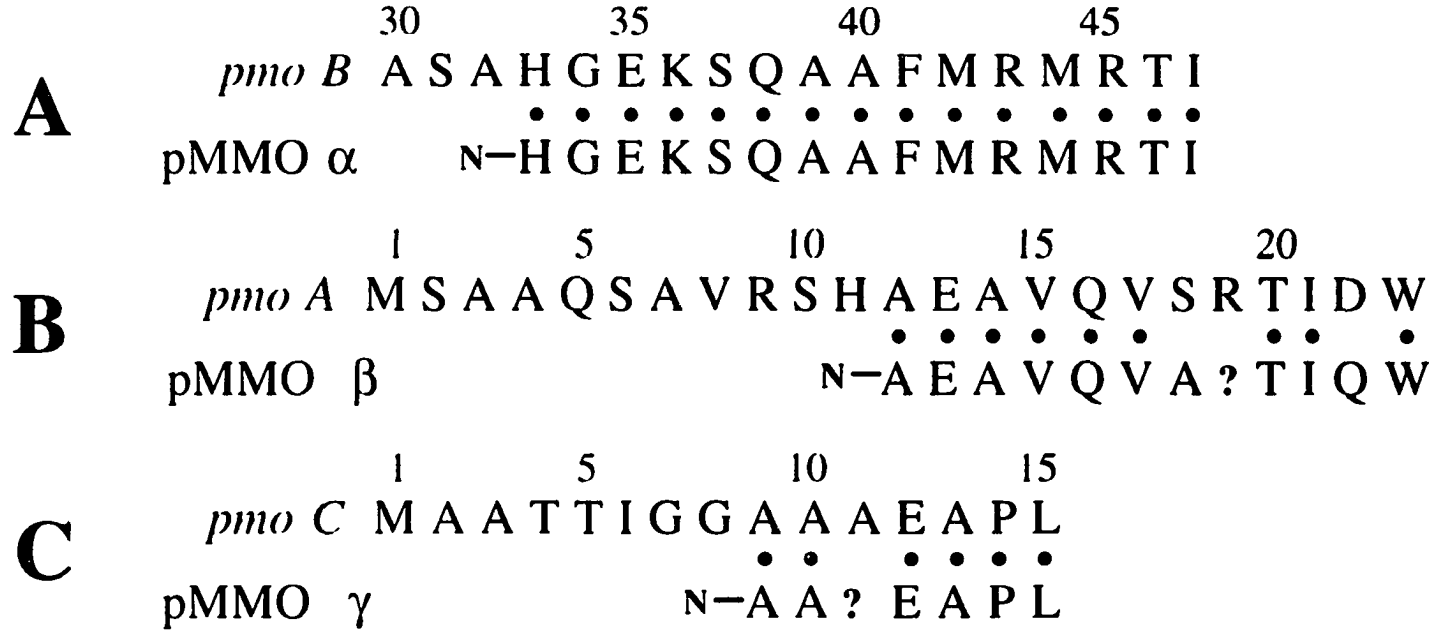
A
30 35 40 45
pmo B A S A H G E K S Q A A F M R M R T I
pMMO α N–H G E K S Q A A F M R M R T I
B
1 5 10 15 20
pmo A M S A A Q S A V R S H A E A V Q V S R T I D W
pMMO β N–A E A V Q V A ? T I Q W
C
1 5 10 15
pmo C M A A T T I G G A A A E A P L
pMMO γ N–A A ? E A P L

The presence of an integer spin signal in pMMO has not been confirmed by parallel mode cavity EPR experiments.

In contrast to previous studies on membrane samples (38, 48), the "broad isotropic" signal believed to be associated with a novel trinuclear copper cluster described under high microwave powers was not observed in the isolated enzyme.

Treatment of reduced pMMO with nitric oxide, produced a ferrous-nitric oxide derivative with an electronic spin of $S = 3/2$ (Fig 6 trace D). Nitric oxide has been used as an active site probe to detect ferrous iron in several mononuclear non-heme proteins to produce an S = 3/2 EPR-detectable species with g-values near 4 and 2. The EPR signals near g = 4 and g = 2 have been ascribed to high-spin ferric iron.

Enzyme activity. The purified enzyme oxidized propylene to propylene oxide at rates of 6.6 ± 2.4 nmol.•min^{-1}•mg $protein^{-1}$. The pMMO showed a pH optimum at pH 7.5 with duroquinol as the reductant (Fig. 7). In preparations of pMMO isolated from cells containing suboptimal concentration of iron, propylene oxidation activity was stimulated by the addition of ferric iron (Table 3). The stimulation of propylene oxidation by iron was not observed in preparations of pMMO isolated from cells grown in media containing a final concentration of 60 μM Cu and 60 μM iron. Propylene oxidation activity of the enzyme isolated from cells cultured in high copper and iron media was more stable and did not require the addition of iron or copper to the reaction mixture for optimal activity.

Using an enzyme preparation with a propylene oxidation rate of 6.2 nmol•min^{-1}•mg protein, the rate methane and tricholoethylene oxidation was 7.8 nmol•min^{-1}•mg protein, and 1.3 nmol•min^{-1}•mg protein, respectively.

FIG. 6. Electron paramagnetic resonance spectra for pMMO from *M. capsulatus* Bath at microwave powers of 0.2 mW (A), 2 mW (B) 20 mW (C) and the nitric oxide derivative of the fully reduced enzyme (D) at a microwave power of 2 mW. The protein concentration was 37 mg/ml in 10 mM PIPES (pH 7.0) and 0.3% dodecyl maltoside at 8° K. The specific activity for the preparation was 4.8 nmol. propylene oxide • min-1 • mg protein-1. Operating parameters were: Modulation frequency, 100 kHz; modulation amplitude, 10 G; time constant 100 ms. The microwave frequency was 9.429 GHz.

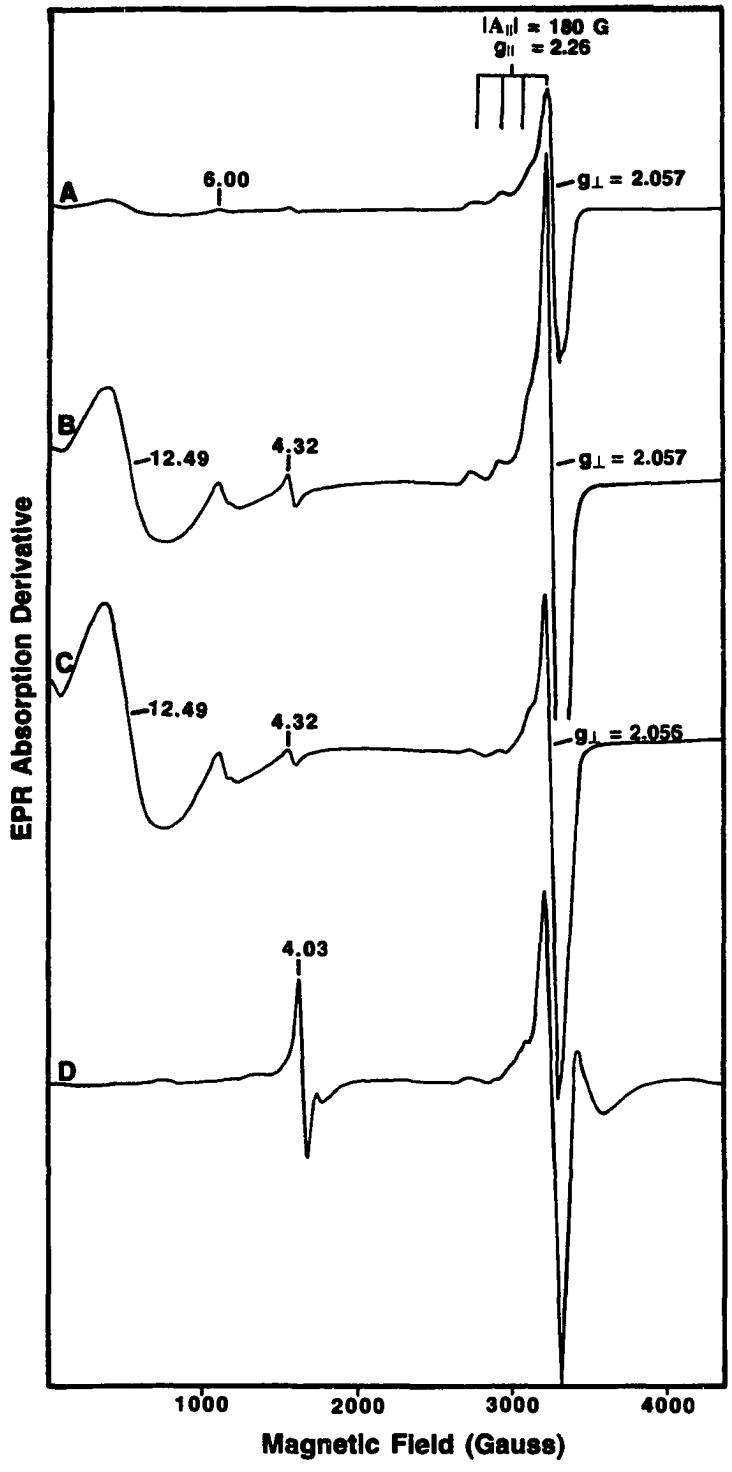
$|A_{\parallel}| \approx 180$ G
$g_{\parallel} = 2.26$
A
6.00
$g_{\perp} = 2.057$
B
12.49
4.32
$g_{\perp} = 2.057$
C
12.49
4.32
$g_{\perp} = 2.056$
4.03
D
EPR Absorption Derivative
1000
2000
3000
4000
Magnetic Field (Gauss)

The purified enzyme from *M. capsulatus* Bath was inhibited by freeze thaw treatment, heat (1 minute 100°C), proteases, by acetylene, carbon monoxide, cyanide and azide. Propylene oxidation activity by the purified enzyme was stimulated 1.4 fold by HOQNO and 1.5 fold by myxothiazol (Table 4).

TABLE 3. Effect of added metal ions on propylene oxidation by the purified pMMO from *M. capsulatus* Bath.

Effector	*Concentration (mM)*	*Specific Activity (nmol• min-1 • mg protein-1)*	*Relative Activity (% of Control)*
Control	-	4.44 ± 0.04	100
Cu(I)Cl	1.0	3.00	68
	5.0	2.78	63
$Cu(II)Cl_2$	0.3	5.52	124
	1.0	4.88	110
	5.0	1.08	24
$Fe(II)SO_4$	1.0	3.54	80
	5.0	2.82	64
$Fe(II)SO_4$+Cys	2.0	<0.60	14
$Fe(III)Cl_3$	0.3	6.72	151
	1.0	7.74	174
	5.0	6.20	140
	10.0	<0.60	14

Nature of the pMMO prosthetic groups, isolation of the 47,000-27,000 Da switchover polypeptides. Solublization of pMMO polypeptides in Triton X-100 or CHAPS followed by separation on a sucrose gradient resulted in the loss of enzyme activity. However, this treatment removed the "loosely-associated" copper (*i.e.* copper associated with the 618 Da copper-binding cofactor) and cytochrome *b*-559/569. This treatment also allowed for the selective isolation of the 47,000-27,000 Da pMMO polypeptides.

The selective isolation of the switchover polypeptides has provided increased insight into the nature of the prosthetic groups associated with the pMMO. SDS-denaturing gels of the Triton X-100 purified fraction of pMMO demonstrated the presence of 2 polypeptides with molecular masses of 47,000 and 27,000 Da. The stochiometry of the 47,000 and 27,000 Da polypeptides stained with Coomassie brilliant blue were 1 : 0.9, respectively. For discussion purposes, this fraction is referred to as the "47,000-27,000 Da switchover polypeptides". Since propylene oxidation activity was absent in Triton X-100 or CHAPS, the identity of these polypeptides as pMMO components were confirmed by N-terminal sequence and purification of $^{14}C_2H_2$-labeled polypeptides from active membrane fractions.

As isolated, the fraction contained approximately one non-heme iron, one copper and one acid labile sulfur based on a molecular mass of 74,000 Da. The remaining cytochrome *b*-559/569 and the majority of the copper associated with the pMMO were separated from the 47,000-27,000 Da switchover polypeptides by this treatment. The copper removed from the complex was associated with a 618 Da molecule (Table 5).

The 47,000-27,000 Da switchover complex showed no optical spectra. The electron paramagnetic resonance spectra contained a weak high spin signal (g = 6.0) and the type 2 copper signal observed in the membrane fraction (Fig. 8). The intensity of the type 2 copper signal was highly dependent upon the preparation and on the detergent utilized for solublization of the complex (Fig. 8). The low field signal observed in the holoenzyme was also preparation dependent. in active pMMO preparations lacking the broad g = 12.7 signal, the signal can be generated by the addition of duroquinol and acetylene to the resting sample.

FIG. 7. Effect of pH on propylene oxidation by the isolated membrane-associated methane monooxygenase from *M. capsulatus* Bath. Reaction mixtures consisted of 600 µl of pMMO extract (39.8 mg protein), and 35 mM duroquinol in a 7 ml serum vial. Buffer (50µL additions) were added to a final concentration of 50 mM to samples purified in a buffer containing 10 mM PIPES, pH 7.0 (Specific Activity = 5.9 nmol. • min.-1 • mg protein-1).

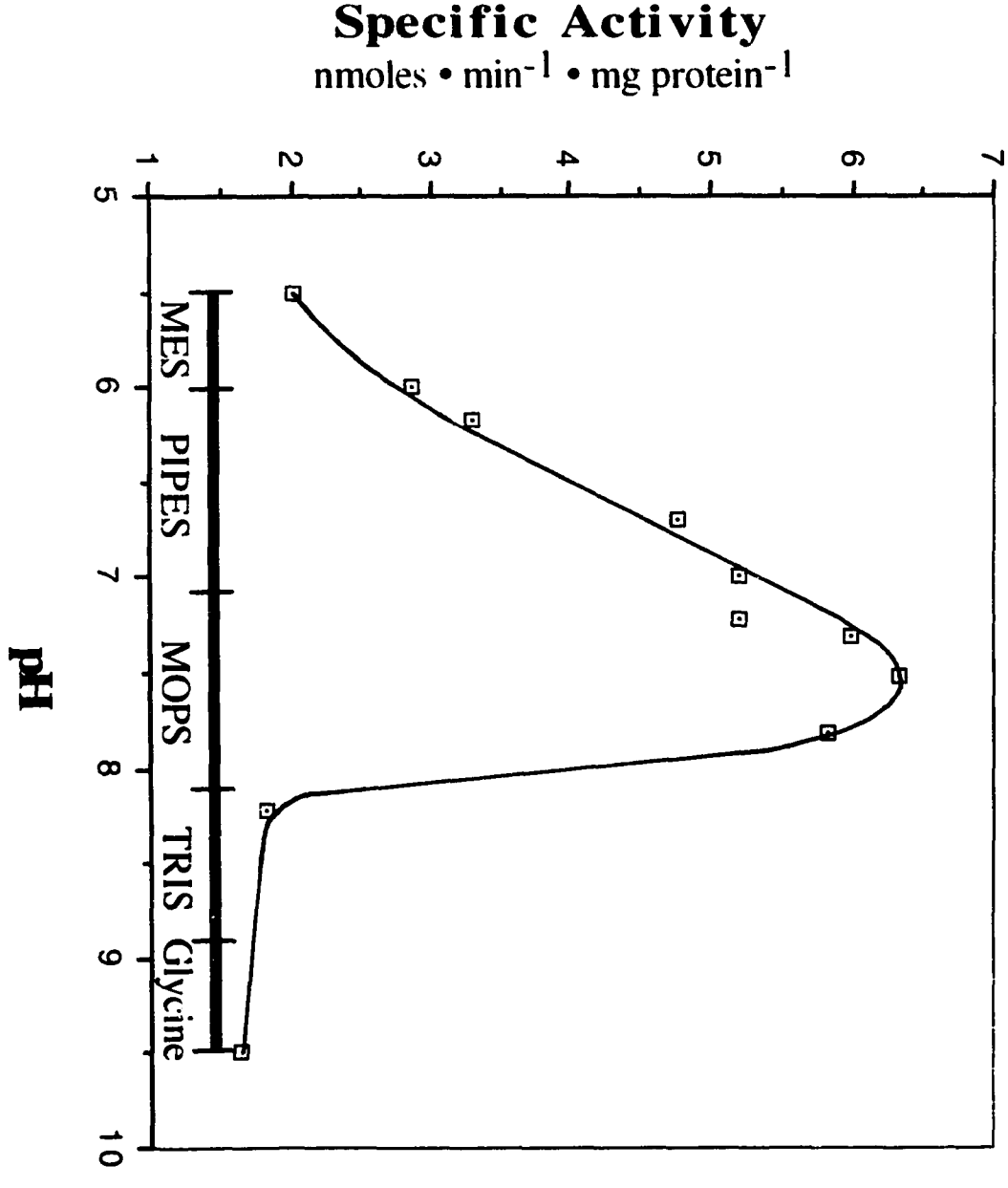
Specific Activity
nmoles • min-1 • mg protein-1
1
2
3
4
5
6
7
pH
5
6
7
8
9
10
MES
PIPES
MOPS
TRIS
Glycine

TABLE 4. Effect of inhibitors on propylene oxidation by whole cell and by the purified pMMO from *M. capsulatus* Bath. Reaction mixtures consisted of 600 ul of purified pMMO (30.2 mg/ml) and 35 mM duroquinol or 1 ml of whole cells (1mg/ml) and 20 mM formate as the reductant.

Effector	*Concentration (μM)*	*Propylene Oxidation Percent Inhibition or Stimulation*[1]	
		Whole cell	*pMMO*
KCN	10	96	nd[2]
	50	19	71
	100	0	59
	250	0	27
	500	0	19
	750	0	0
NaN_3	10	69	nd
	50	0	44
	250	0	8
	500	0	0
HOQNO[3]	20	178	106
	50	0	0
Myxothiazol[4]	4	nd	78
	33	nd	85
	164	nd	152
	328	nd	138

[1]100% propylene oxidation rate: whole cell: 78 nmol/min•mg protein; pMMO 6.2 nmol/min•mg protein

[2]not determined

[3]Solublized in dimethyl sulfoxide.

[4]Solvent (methanol) removed by evaporation under vacuum.

Figure 8 trace D shows the EPR spectrum for the anaerobically reduced sample of 47,000-27,000 switchover polypeptides solublized in 1 mM CHAPS. As with active pMMO preparations, treatment of the reduced 47,000-27,000 Da switchover polypeptides with nitric oxide produced a ferrous-nitric oxide derivative with an electronic spin of $S = 3/2$ (Fig. 8 trace E). Two different techniques have

FIG. 8. Electron paramagnetic resonance spectra for the 47,000-27,000 Da switchover polypeptides from *M. capsulatus* Bath. The 47,000-27,000 Da switchover polypeptides (A) in 10 mM Tris-HCl, 0.1% CHAPS, pH 8.0 protein concentration 31 mg/ml; of (B) 47,000-27,000 Da switchover polypeptides in 10 mM Tris-HCl, 0.1% Triton X-100, pH 8.0, protein concentration 48 mg/ml; of (C) acetylene derivative of the 47,000-27,000 Da switchover polypeptides purified from $^{14}C_2H_2$-labeled membranes in 10 mM Tris-HCl, 0.1% CHAPS, pH 8.0, protein concentration 34 mg/ml; the fully ascorbate-reduced enzyme (D), protein concentration 31 mg/ml; and (E) the nitric oxide derivative of the fully reduced enzyme in 10 mM Tris-HCl, 0.1% CHAPS, pH 8.0., protein concentration 31 mg/ml. Operating parameters were: modulation frequency, 100 kHz; modulation amplitude, 20 G; microwave power 2.02 mW; time constant 100 ms. The microwave frequency was 9.421 GHz.

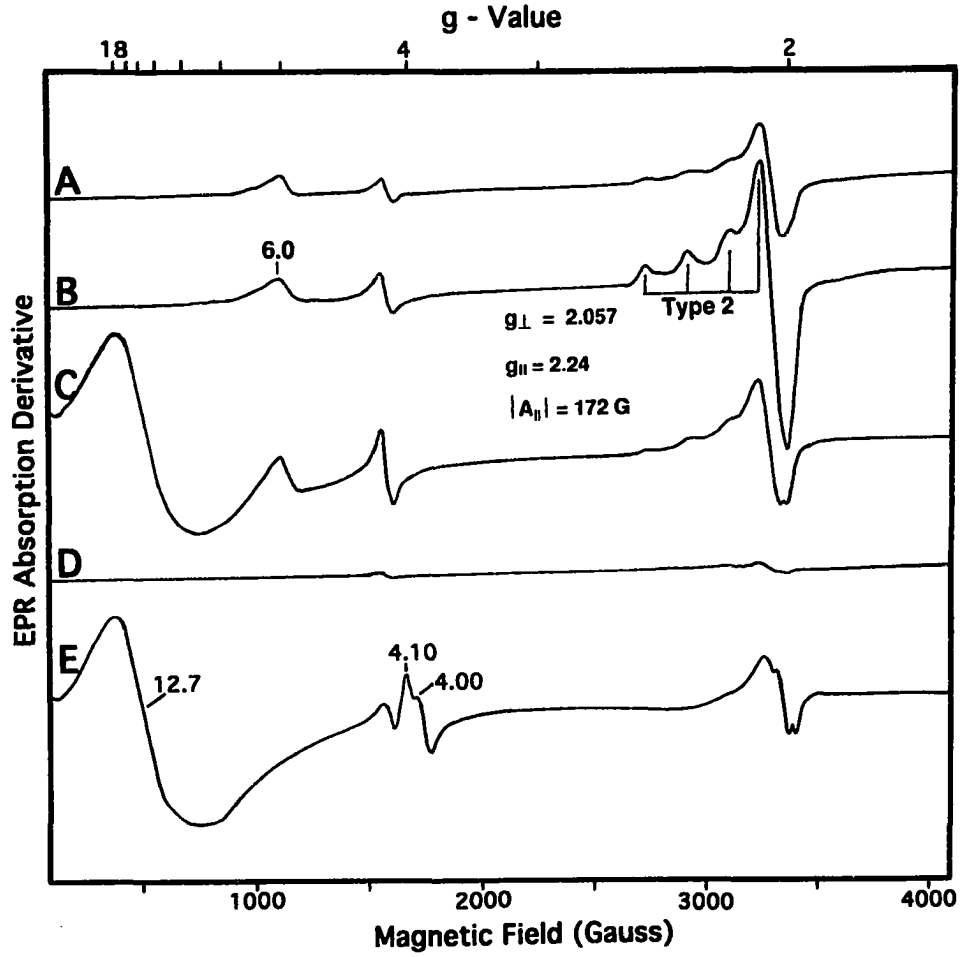
g - Value
18
4
2
A
B
C
D
E
6.0
Type 2
$g_\perp$ = 2.057
$g_\parallel$ = 2.24
$|A_\parallel|$ = 172 G
12.7
4.10
4.00
EPR Absorption Derivative
1000
2000
3000
4000
Magnetic Field (Gauss)

commonly been employed to produce the iron-NO complex for cytochrome *c* oxidase. The first technique is the addition of nitric oxide gas to the reduced enzyme (3, 36). The second technique is the formation of the nitrosyl derivative by the *in situ* reduction of the nitrite ion (36, 37). Figure 8 trace E shows the ^{15}N-nitrosyl derivative for the 47,000-27,000 Da switchover polypeptides which was similar to spectra in Fig. 3 trace C and Fig. 6 trace D. The spectrum shows the presence of an intense low-field signal at g = 12.7, presumed to be due to an integer spin, and the EPR signals arising from the S = 3/2 non-heme iron species at g = 4.10, g = 4.00, and g ≈ 2.0. Although the spectrum of the S = 3/2 species of the 47,000-27,000 switchover polypeptides showed a striking resemblance to the EPR spectrum for the nitrosyl derivative of protocatechuate 4,5-dioxygenase from *Pseudomonas testosteroni* (30), the S = 2 feature at g = 12.7 has previously not been observed for dioxygenase enzymes. The lack of nuclear hyperfine structure associated with the resonances near g = 4 and g = 2 were confirmed by comparison of the ^{15}N-nitrosyl derivative spectra to EPR spectra generated for the ^{14}N-nitrosyl derivative. No detectable changes were observed for subtracted EPR spectra of the ^{14}N *minus* ^{15}N-nitrosyl derivatives.

Properties of copper-binding cofactor (cbc). The cellular location of the cbc varied, depending on the copper concentration in the growth medium. In cells cultured in low, i.e. no added copper, copper medium the cbc was observed extracellular faction. In *M. capsulatus* Bath the cbc is reponsible for the yellow color associated with spent medium from cell cultured in low copper media, concentration. No copper was associated with the cbc isolated from spent culture media. The concentratrion of the cbc decreased in cells cultured in high copper media.

FIG. 9. Reverse-phase high performance liquid chromatographic separation of pMMO polypeptides solublized in 0.5% Triton X-100. HPLC instrument conditions were as follows: Flow rate, 4 mL/min; Detector wavelength, 225 nm; Column, VyDac semi-preparative C_{18} column (10 x 250 mm); Solvent A, DH2O + 0.1% trifluroacetic acid; Solvent B, Acetonitrile + 0.1% trifluroacetic acid. Three major peaks (B', ≈40 min., and A') were collected, lyophilized to dryness, and analyzed by SDS-PAGE (inset) to identify apparent molecular masses. The major peak at ≈40 min. was identified as Triton X-100. SDS-PAGE separation of Peak A' is shown in lane A (inset); this peak contains both 27,000 Da and 25,000 Da bands. The SDS-PAGE profile of Peak B' shows that this peak contains the 47,000 Da polypeptide.

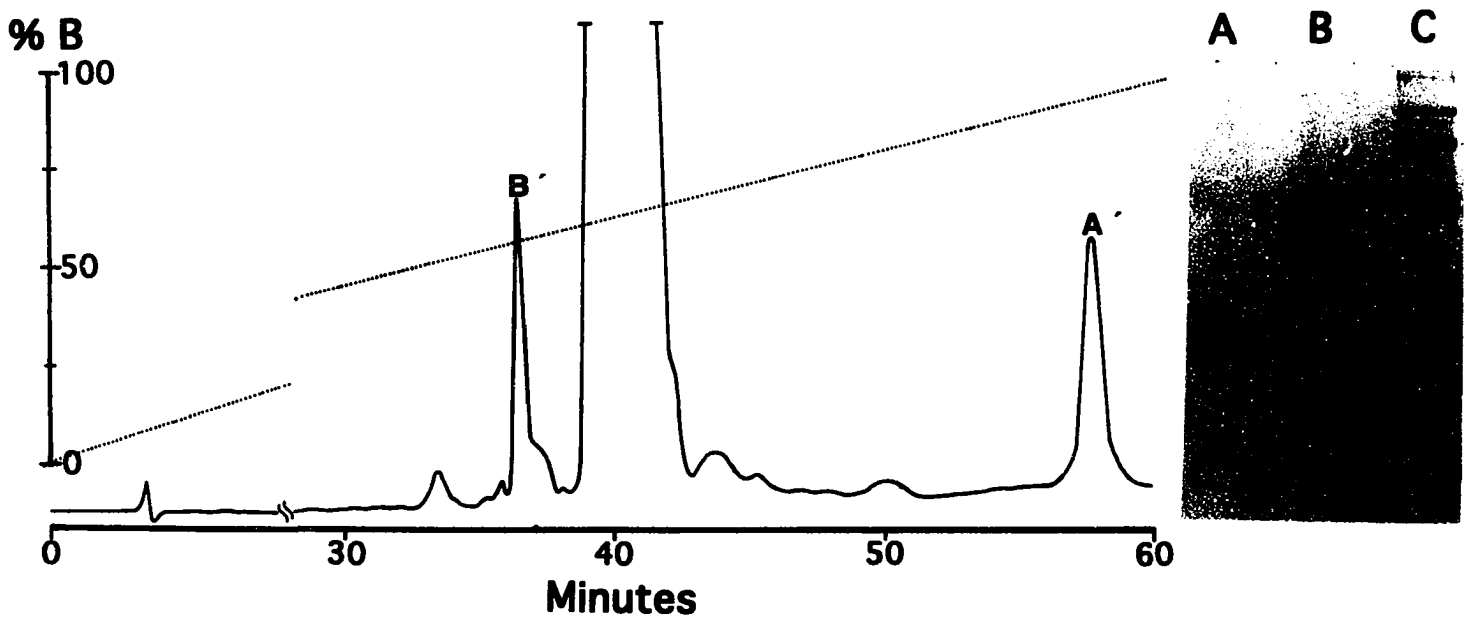
% B
100
50
0
B´
A´
0
30
40
50
60
Minutes
A
B
C

FIG. 10. Matrix-assisted laser desorption/ionization mass spectrum of copper-binding cofactor from *M. capsulatus* Bath.

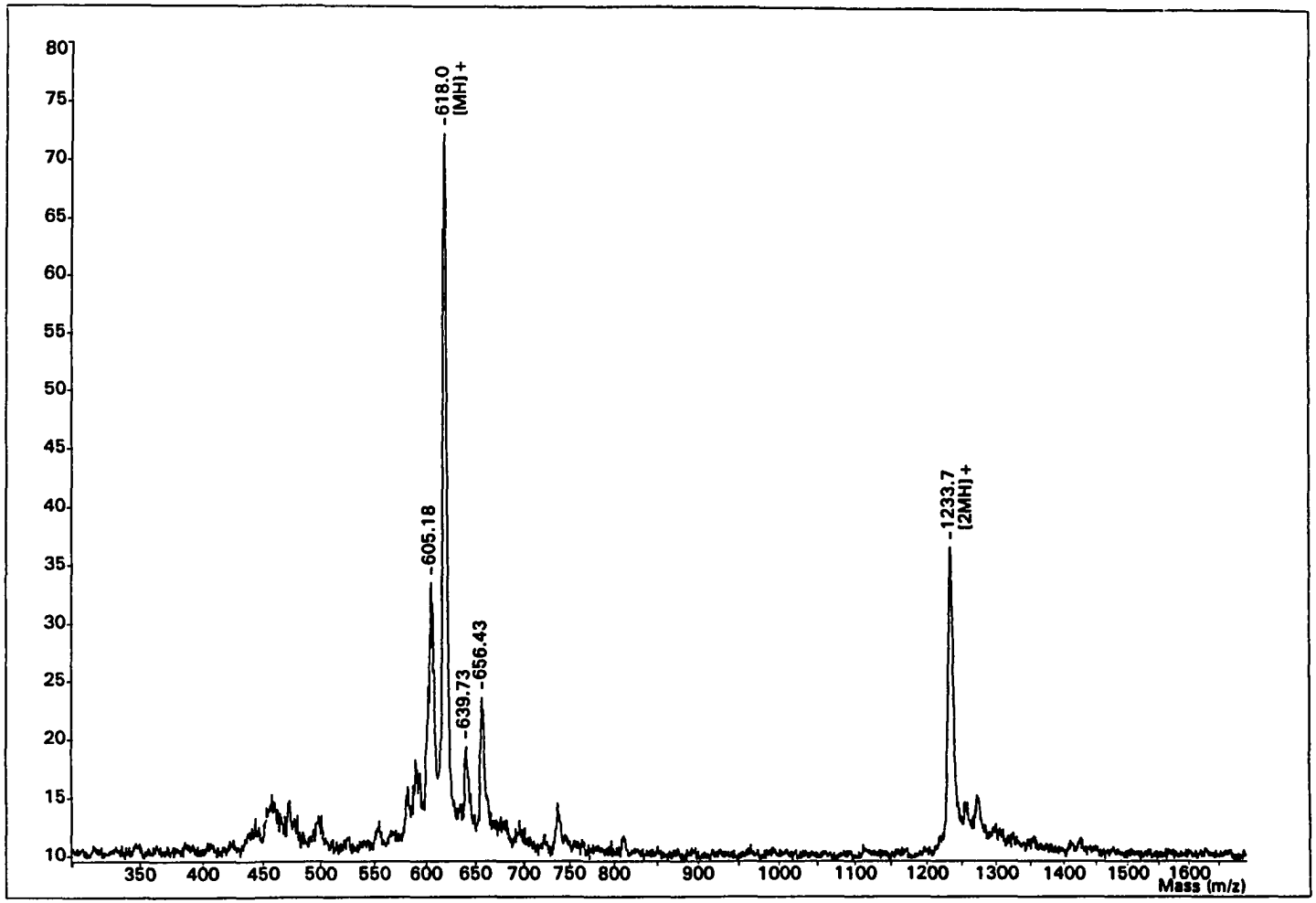
80
75
70
65
60
55
50
45
40
35
30
25
20
15
10
618.0
[MH]+
605.18
639.73
656.43
1233.7
[2MH]+
350
400
450
500
550
600
650
700
750
800
900
1000
1100
1200
1300
1400
1500
1600
Mass (m/z)

TABLE 5. Properties of pMMO from *M.capsulatus* Bath.

Property	*pMMO*	*47,000-26,000 Da Switchover Complex*
Specific Activity (nmol propylene • min^{-1} • mg^{-1})	4.2 - 11.08	0
Subunit Molecular Mass (Da)	47,000, 27,000, and 25,000	47,000 and 27,000
Metal Concentration (nmol/nmol enzyme)		
Fe	2.5±0.7[a]	0.9±0.3[b]
Cu	14.6±1.9[a]	0.6±0.1[b]
Cu/Fe	5.8	0.7
EPR Signals		
Resting	12.5 [c], 6.0, 4.3, $\|A_{\|\|}\|$ = 180 G, $g_{\|\|}$ = 2.26, $g_{\perp}$ = 2.057	12.7 [c], 6.0, 4.3, $\|A_{\|\|}\|$ = 172 G, $g_{\|\|}$ = 2.24, $g_{\perp}$ = 2.057
Nitric Oxide Derivative	4.03	4.10, 4.00, 3.95

[a] Mole enzyme calculations based on the molecular weight of 99,000 Da as determined on SDS-denaturing gels and assuming a 1:1:1 ratio subunit ratio. Protein concentration determined by the Lowry method (32)

[b] The holoenzyme molecular mass was estimated to be 74,000 Da based on a 1:1 stochiometry of pMMO subunits.

[c] Observation was preparation dependent.

The decreased cbc in the spent culture media was associated with and increased concentration of cbc assciated with the membrane fraction. The cbc isolated from the membrane fraction was associated 2 to 3 copper atoms. In cells cultured in media containing 5 μM Cu^{2+}, over 75% of the membrane-associated copper is associated with the cbc. The cbc is a small molecule (M_r 1,200) composed of two identical subunits (618 Da) (Fig. 10). Each subunit binds 2 to 3 copper atoms. The EPR of the purified sample was complex, having both type 1 ($g_{\perp}$

FIG. 11. Electron paramagnetic resonance spectra for the copper-binding cofactor (42.4 mmoles) containing (A) 0 mmoles copper; (B) 1.75 mmoles copper; (C) 4.24 mmoles copper; and (D) 5.0 mmoles copper). Operating parameters were: modulation frequency, 100 kHz; modulation amplitude, 0.25 G; time constant 100 ms. The microwave frequency was 9.42 GHz, gain 3.3 and microwave power 2.02 mW.

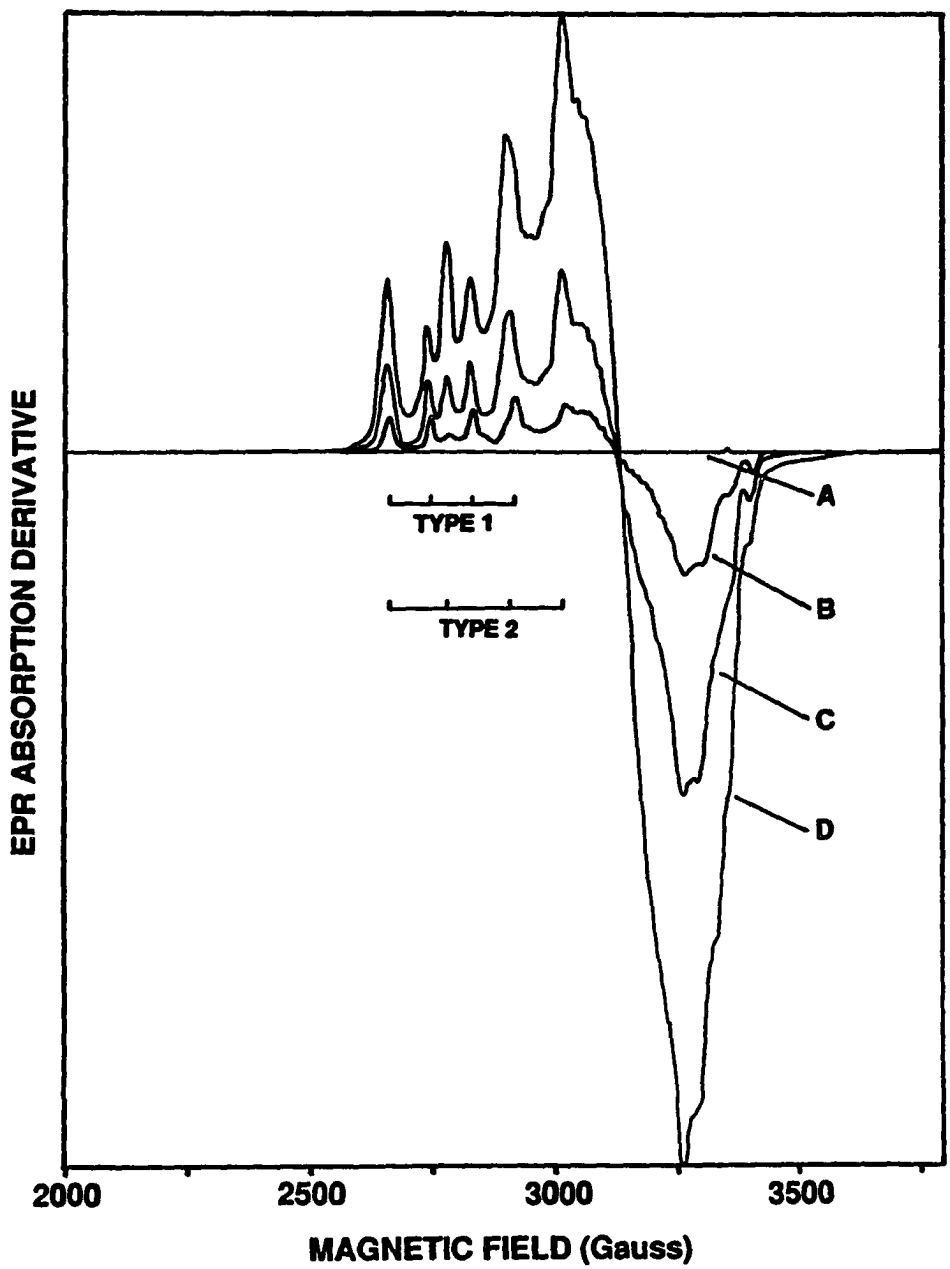
EPR ABSORPTION DERIVATIVE
TYPE 1
TYPE 2
A
B
C
D
2000
2500
3000
3500
MAGNETIC FIELD (Gauss)

FIG. 12. Absorption spectra of 54 mM copper-free copper-binding cofactor from *M. capsulatus* Bath titrated with $CuCl_2$. The inset shows the relationship of the change in A_{245} to copper addition. For absorbance, the full scale equals 1.2.

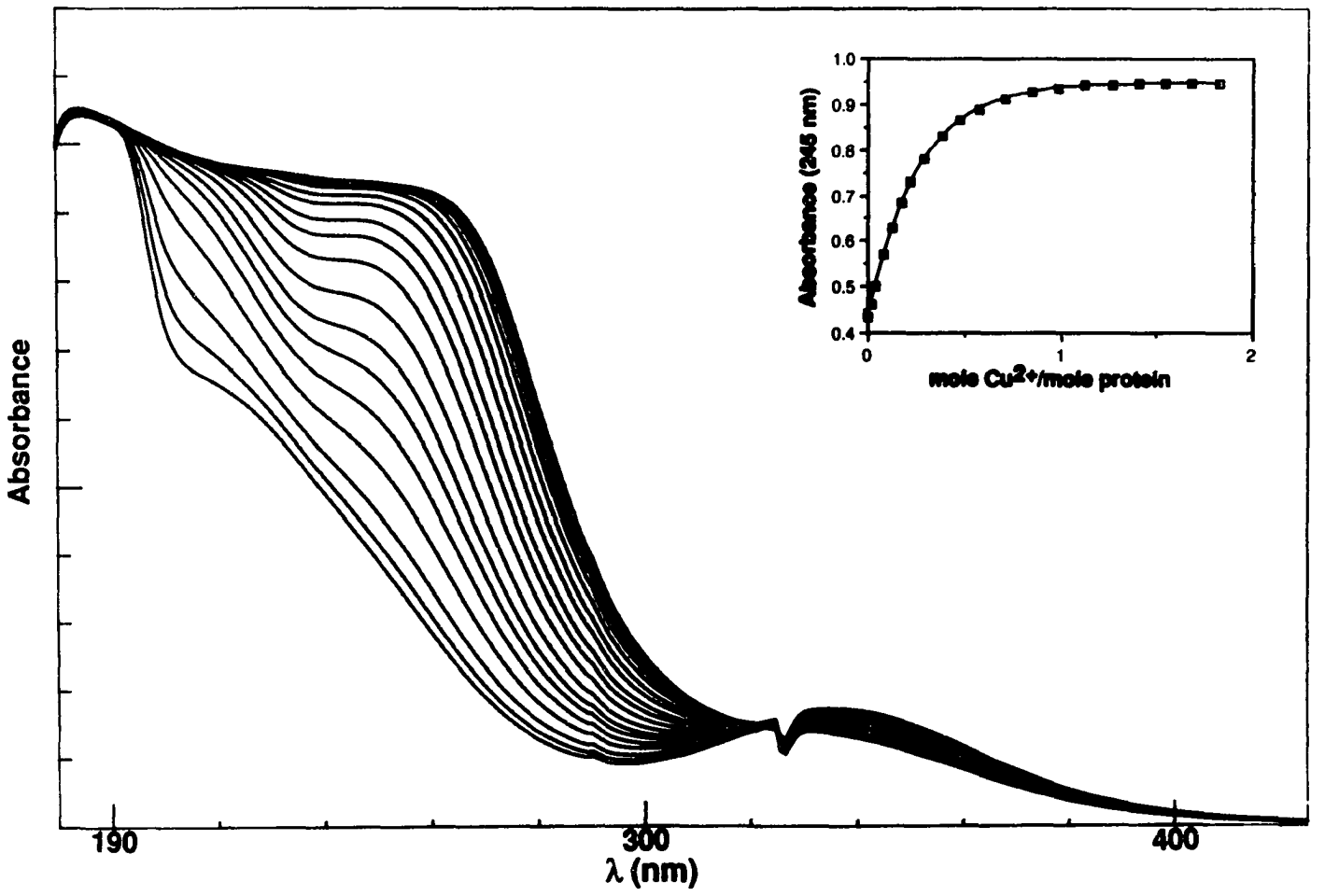
Absorbance
190
300
400
λ (nm)
Absorbance (245 nm)
1.0
0.9
0.8
0.7
0.6
0.5
0.4
0
1
2
mole Cu2+/mole protein

= 2.02, $g_{||}$= 2.415, and $|A_{||}|$= 83 [G]), and type 2 copper signals ($g_{\perp}$ = 2.035, $g_{||}$= 2.373, and $|A_{||}|$= 123 [G]) (Fig. 10). EPR spectra from sub-saturating levels of copper is shown to emphasize the copper signals. Although we use the terms type 1 and 2 to describe the two copper centers in the cbc, neither falls directly into this classification. The type 1 center shows similar EPR spectral properties to other type 1 copper centers, but the absorption spectrum is quite different from previously described type I copper-containing enzymes (Fig. 12). The type 1 center shows absorption maxima at 245 and 340 nm and no absorbance at 600 nm (Fig. 12). The absorption spectrum of the cbc is similar to metallothioneins (42). The EPR splitting constant of the type 2 center falls between the type 1 and type 2 (40).

Copper titration experiments indicate the type 1 site is loaded preferentially to the type 2 site (Figs. 11 and 12). The addition of *p*-hydroxymercuribenzoate (43) causes the release of copper from the cbc and reveals that less than 30% of the copper is EPR detectable (results not shown). In the report by Nguyen et al. (30) only 30 to 35% of the membrane-associated copper in *M. capsulatus* Bath is detectable by EPR. This difference may reflect the percentage of the cbc that is EPR silent.

DISCUSSION

In contrast to the sMMO, little is known concerning the bioenergetics of methane oxidation by the pMMO. This report describes the initial isolation and characterization of the pMMO as well as some of the biochemical changes related to the expression of the pMMO in *M. capsulatus* Bath. Nguyen et al. (38) reported the switchover event from sMMO to pMMO in *M. capsulatus* Bath was accompanied

by an increase in the concentration of membrane-associated copper and iron. Although copper resonances were detected and presumed to be associated with the pMMO, no EPR signals were detected to support the observed increase in iron. The results reported in this study show that the majority of the iron associated with the membrane fraction is EPR silent. The EPR spectra of the membrane fraction shows an increase in a high spin ($g = 6$) signal in the membrane fraction of cells expressing the membrane-associated MMO. However, the majority of the copper-inducible iron in the membrane fraction is only EPR detectable with the addition of nitric oxide. The nitric oxide experiments indicate that the non-heme iron in the pMMO is either a single ferrous iron, a iron-iron, or iron-copper center (2, 3, 23 - 25). Nitric oxide has been shown to bind to the Fe^{2+}-containing enzymes to yield an EPR spectrum with a characteristic $S = 3/2$ spin system due to the formation of a ferrous-nitrosyl complex (2). The 47,000-27,000 Da switchover complex contains a nitric oxide-binding ferrous iron center and was the only membrane-associated NO-binding ferrous iron center in high concentration in the membrane fraction from *M.capsulatus* Bath.

The pMMO appears to be a three polypeptide enzyme with molecular masses of 47,000, 27,000 and 25,000 Da (Fig. 13). The active enzyme contains 2.5 iron and 14.6 copper atoms per 99,000 Da. The majority of the copper associated with the enzyme appears to be associated with a small (618 Da) co-factor which can separated from the pMMO polypeptides by detergent replacement with CHAPS followed by separation on a sucrose gradient. Once separated, the 47,000-27,000 Da switchover polypeptides contain approximately one non-heme iron, one copper and one acid-labile sulfur. Using the *N*-terminal amino acid sequence of the 47,000 and 25,000 Da polypeptides purified on SDS-denaturing gels, Semrau et al. (48) and

Costello et al. (11) have recently isolated the structural genes for the pMMO. The results reported in this paper verify the identity of *pmo* A, *pmo* B and *pmmo* C as structural genes for the pMMO.

Although not apparent on SDS-denaturing gels stained with Coomassie brilliant blue, active preparations of the pMMO contained non-stoichiometric concentrations of cytochrome *b*-559/569. The ratio was estimated by the concentration of protoheme to be approximately 3 to 7 mole % cytochrome *b*-559/569 depending on the preparation. The role, if any, for cytochrome *b*-559/569 in methane oxidation has not been determined. Methane dependent re-oxidation of ferrous cytochrome *b*-559/569 by pMMO provides some evidence for a role for this cytochrome as the initial electron donor to the pMMO. In addition, the cytochrome was reduced by duroquinol. Furthermore, methane oxidation activity was lost with the separation of cytochrome *b*-559/569, and once separated, activity cannot be restored by recombining the fractions. The reason for the loss of activity at this step has not been determined. It may be the result of the loss of the 618 Da copper-binding cofactor which is also separated from the 3 pMMO polypeptides in any purification that resulted in the removal of the remaining cytochrome *b*-559/569. However, the majority of the available evidence indicates the cytochrome *b*-559/569 is not directly involved in methane catalysis. First, the concentration of cytochrome *b*-559/569 was unaffected by the expression of pMMO. Second, traditional inhibitors of *b*-type cytochromes (53), HOQNO and myxothiazol, stimulated propylene oxidation at mole ratios commonly observed to completely inhibit *b*-type cytochromes. Third, there was no relation between the level of contaminating cytochrome *b*-559/569 and propylene oxidation rates in the purified samples. Lastly,

the kinetic parameters for quinol oxidation suggested that cytochrome *b* was not the electron acceptor of duroquinol. Duroquinol rapidly reduced cytochrome *b*-559/569 at equimolar concentrations. However, propylene oxidation rates by isolated enzyme increased proportionally with duroquinol concentration up to 35 mM. Duroquinol precipitated out of solution at higher concentrations. This observation suggested a direct electron transfer to pMMO from the quinol and the K_M for the reaction is above 35 mM.

The results presented in this paper allow for the development of a working model of the pMMO. All available evidence indicates the catalytic site involves both iron and copper, although we have not excluded the possibility of a single ferrous iron center or an iron-iron center. The majority of the copper associated with the pMMO appears to be loosely associated with the enzyme and may provide a secondary functions such as enzyme stabilization, maintaining a particular redox state, or as a copper scavenger. This model is based on the following observations. First, the stoichiometry of copper to iron is one to one in the 47,000-27,000 Da switchover polypeptides. Second, the addition of acetylene, an irreversible inhibitor of the pMMO, to the 47,000-27,000 Da switchover complex results in the generation of a broad low field integer spin-like (g = 12.7) signal. This integer spin signal has been observed in all known μ-oxo-bridged enzymes, as well as for the copper/heme enzyme, cytochrome *c* oxidase (23, 25, 45). Although these two groups of enzymes demonstrate a great diversity in structure and function, all enzymes which exhibit the $S = 2$ signal possess either a mononuclear or a binuclear metal center composed of iron or iron and copper atoms. As with cytochrome oxidase, all enzymes exhibiting an integer spin signal share the ability to bind or interact with oxygen (45).

Fig. 13. Proposed mechanisms of methane oxidation by the pMMO using duroquinol (DQ) as a reductant. Models of methane oxidation with cytochrome *b*559/569 as the initial electron donor (A) and with duroquinol oxidized directly by the pMMO (B) are shown.

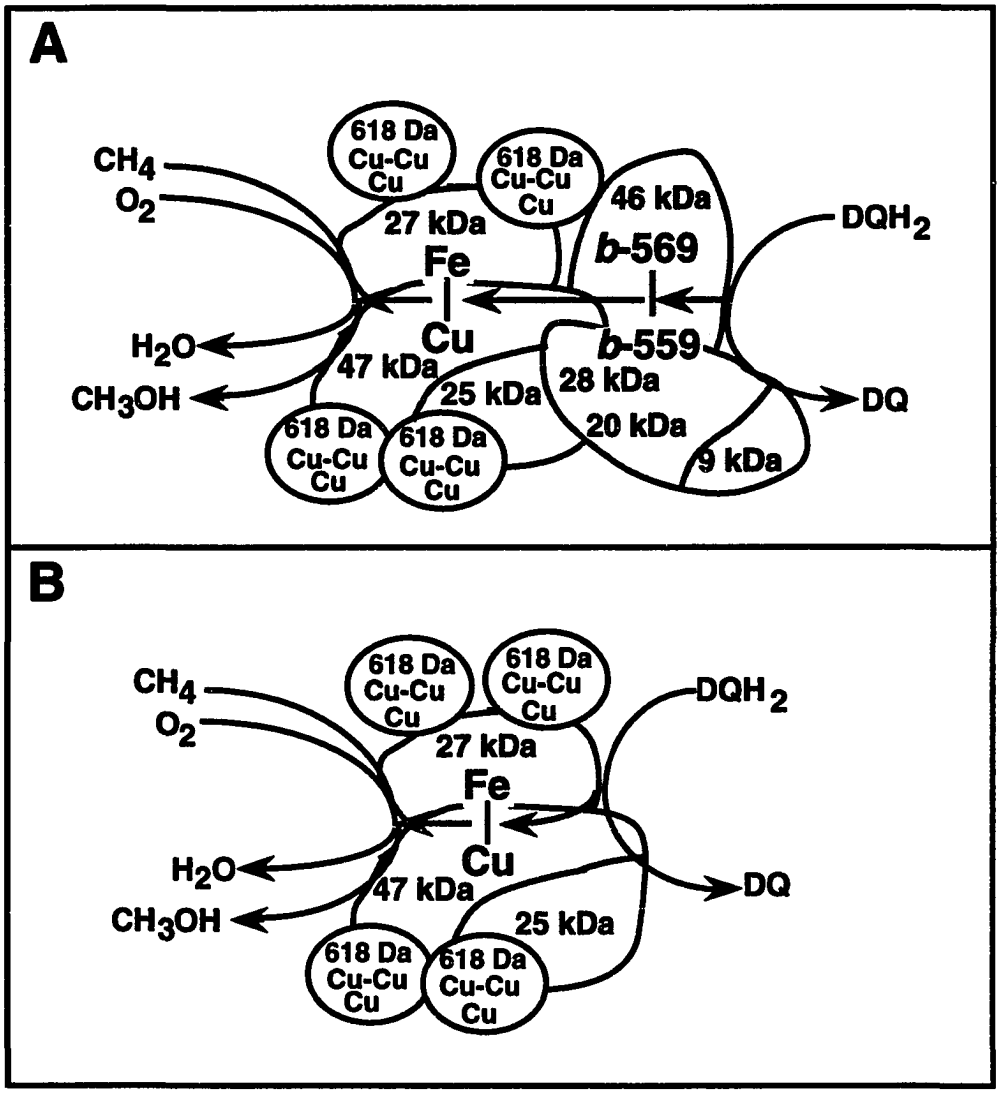
A
618 Da Cu-Cu Cu
618 Da Cu-Cu Cu
CH4
O2
27 kDa
46 kDa
b-569
DQH2
Fe
Cu
H2O
47 kDa
b-559
28 kDa
CH3OH
25 kDa
DQ
618 Da Cu-Cu Cu
618 Da Cu-Cu Cu
20 kDa
9 kDa
B
618 Da Cu-Cu Cu
618 Da Cu-Cu Cu
CH4
O2
DQH2
27 kDa
Fe
Cu
H2O
47 kDa
DQ
CH3OH
25 kDa
618 Da Cu-Cu Cu
618 Da Cu-Cu Cu

Nitric oxide derivative EPR spectra of the membrane fractions from cells expressing the pMMO, or of purified pMMO also indicates the active site contains a ferrous iron center. The identity of a ferrous iron center as a switchover copper-induced center is shown by nitric oxide treatment of the membrane fraction from cells expressing the pMMO. The presence of iron in the enzyme was also supported by the observation that Fe^{3+} could serve to activate pMMO activity in purified preparations of *M. capsulatus* Bath pMMO.

The model proposed in this paper (Fig. 13) differs from the trinuclear copper cluster proposed by Nguyen et al. (38) and Semrau et al. (48). The trinuclear copper cluster model was based on correlating spectral (EPR) changes in the membrane fraction to membrane-associated methane oxidation activity and changes in elemental (copper and iron) composition of the membrane fraction. The "broad isotropic copper signal" previously observed by Nguyen, et. al. (38), was not detected in purified preparations of pMMO. However, this signal may originate from a small membrane-associated, copper-binding cofactor. This cofactor binds 2 to 3 copper atoms per mole polypeptide and exhibits a complex EPR spectrum which can account for the previously observed signal (Zahn and DiSpirito, unpublished results). Future studies will address the role, if any, of this copper-binding cofactor as well as cytochrome*b*-559/569 in methane oxidation.

ACKNOWLEDGMENTS

We thank A.B. Hooper (University of Minnesota), D.M. Arciero (UM), D.J. Bergman (UM) and C.L. Krema (ISU) for their evaluation of this manuscript and useful suggestions and F.C. Minion for the assistance and use of the gel

documentation system. This work was supported by the Iowa State University Office of Biotechnology (ADS) and Iowa State University Professional Advancement Grant (JAZ).

LITERATURE CITED

1. **Ankent'eva, N.F., and R.I. Govozdev.**1988. Purification and physiochemical properties of methane monooxygenase from membrane structures of *Methylococcus capsulatus*. Microbiology **53**: 93-96.
2. **Arciero, D.M., J.D. Lipscomb, B.H. Huynh, T.A. Kent, and E. Münck.** 1983. Evidence for direct substrate binding to the active site Fe^{2+} of extradiol dioxygenases. J. Biol. Chem. **258:** 14981 - 14991.
3. **Arciero, D.M., and J.D. Lipscomb.** 1986. Binding of ^{17}O-labeled substrate and inhibitors to protocatechuate 4,5-dioxygenase-nitrosyl complex. J. Biol. Chem. **261:** 2170 - 2178.
4. **Baldwin, M.A., R. Wang, K.-M. Pan, R. Hecker, N. Stahl, B.T. Chait and S.B. Prusiner.** 1993. Matrix-assisted laser desorption/ionization mass spectrometry of membrane proteins: the scrapie prion protein. Tech. Protein Chem. **9:** 41 - 45.
5. **Beinert H.** 1983. Semi-micro methods for analysis of labile sulfide and of labile sulfide plus sulfane sulfur in usually stable iron-sulfur proteins. Anal. Biochem. **131**: 373 - 378.
6. **Bergmann, D.D., and A.B. Hooper.** 1994. Sequence of the gene, *amo*B, for the 43-kDa polypeptide of ammonia monooxygenase of *Nitrosomonas europaea*. Biochem. Biophys. Res. Commun. **204**: 759 - 762.
7. **Berry, E.A., and B.L. Trumpower.** 1987. Simultaneous determination of hemes *a, b,* and *c* from pyridine hemochrome spectra. Anal. Biochem. **161:** 1 - 15.
8. **Brusseau G.A., H.-C. Tsien , R.S. Hanson, and L.P. Wackett.** 1990. Optimization of trichloroethylene oxidation by methanotrophs and the use of colorimetric assay to detect soluble methane monooxygenase activity. Biodegradation **1:** 19-29.
9. **Cardy, D.J.N., V. Laidler, G.P.C. Salmond, and J.C. Murrell.** 1991. Molecular analysis of the membrane monooxygenase (MMO) gene cluster of *Methylosinus trichosporium* OB3b. Mol. Microbiol. **5**: 335 - 342.
10. **Cheesman, M.R., N.L. Watmough, C.A. Pires, R. Tuner, T. Brittain, R.B. Gennis, C. Greenwood, and A.J. Thomson.** 1993. Cytochrome *bo* from*Escherichia coli*: identification of haem ligands and reaction of the reduced enzyme with carbon monoxide. Biochem. J. **289:** 709 - 718.
11. **Costello, A.M., T.L. Peeples, and M.E. Lidstrom.** personal communications.
12. **Dalton H., S.D. Prior, and S.H. Stanley.** 1984. Regulation and control of methane monooxygenase.*In*: R.L. Crawford and R.S. Hanson (eds) Microbial Growth on C_1 Compounds, pp. 75-82. American Society for Microbiology Press, Washington, DC.

13. **DiSpirito, A.A.** 1990. Soluble cytochromes from *Methylomonas* A4. Meth. Enzymol. **188:** 289 - 297.
14. **DiSpirito, A.A., J. Gulledge, A.K. Shiemke, J.C. Murrell, M.E. Lidstrom, and C.L. Krema.** 1992. Trichloroethylene oxidation by the membrane-associated methane monooxygenase in type I, type II and type X methanotrophs. Biodegradation **2:** 151 - 164.
15. **DiSpirito, A.A., A.K. Shiemke, S.W. Jordan, J.A. Zahn, and C.L. Krema.** 1994. Cytochrome *aa*$_3$ from *Methylococcus capsulatus* Bath. Arch. Microbiol. **161:** 258 - 265.
16. **Ferguson-Miller, S., D.L. Brautigan, and E. Margollash.** 1976. Correlation of the kinetics of electron transfer activity of various eukaryotic cytochromes *c* with binding to mitochondrial cytochrome *c* oxidase. J. Biol. Chem. **251:** 1104 - 1115.
17. **Fox, B.G., K.K. Surerus, E. Münck, and J.D. Lipscomb.** 1988. Evidence for a μ-oxo-bridged binuclear iron cluster in the hydroxylase component of methane monooxygenase. J. Biol. Chem. **263:** 10553 - 10556.
18. **Fox, B.G., W.A. Froland, J.E. Dege, and J.D. Lipscomb.** 1989. Methane monooxygenase from *Methylosinus trichosporium* OB3b. J. Biol. Chem. **264:** 10023-10033.
19. **Fuhrhop, J.-H.** 1975. Laboratory methods in porphyrin and metalloporphyrin research. Elsevier Scientific Publishers, New York.
20. **Galpin, J.R., G.A. Veldink, J.F.G. Vliegenthart, and J. Boldingh.** 1978. The interaction of nitric oxide with soybean lipoxygenase-1. Biochim. Biophys. Acta **536**, 356 - 362.
21. **Green, J., and H. Dalton.** 1985. Protein B of soluble methane monooxygenase from *Methylococcus capsulatus* (Bath). A novel regulatory protein of enzyme activity. J. Biol. Chem. **260**, 15795-15802.
22. **Green, J., and H. Dalton.** 1989. Substrate specificity of soluble methane monooxygenase: mechanistic implication. J. Biol. Chem. **264**: 17698-17703.
23. **Hagen, W. R.** 1982. EPR of non-kramers doublet in biological systems, characterization of an $S = 2$ system in oxidized cytochrome *c* oxidiase. Biochim. Biophys. Acta **708:** 82 - 98.
24. **Hendrich, W.P., and P.G. Debrunner.** 1989. Integer-spin electron paramagnetic resonance of iron proteins. Biophys. J. **56:** 489 - 506.
25. **Hendrich, M.P., E. Münck, B.G. Fox, and J.D. Lipscomb.** 1990. Inter-spin EPR studies of the fully reduced methane monooxygenase hydroxylase component. J. Am. Chem. Soc. **112:** 5861 - 5865.
26. **Hyman, M. R., and D.J. Arp.** 1990. The small-scale production of [U-14C] acetylene from $Ba^{14}CO_3$: Application to labeling of ammonia monooxygenase in autotrophic nitrifying bacteria. Annal. Biochem. **190**: 348 - 353.
27. **Hyman, M.R., and D.J. Arp.** 1992. $^{14}C_2H_2$- and $^{14}CO_2$-labeling studies of the *de novo* synthesis of polypeptides by *Nitrosomonas europaea* during recovery from acetylene and light inactivation of ammonia monooxygenase. J. Biol. Chem. **267:** 1534 - 1445.

28. **Laemmli U.K.** 1970 Cleavage of structural proteins during the assembly of the head of bacteriophage T4. Nature (London) **227:** 680 - 685.
29. **Lidstrom, M.E.** 1988. Isolation and characterization of marine methanotrophs. Antonie van Leewenhoek J. Microbiol. Serol. **54:** 189 - 199.
30. **Lipscomb, J.D., J.W. Whittaker, and D.M. Arciero.** 1982.*In* Oxygenases and Oxygen Metabolism. ed. M. Nizaju, S. Yamamoto, Y. Ishimura, M.J. Coon, L. Ernster, and R.W. Estabrook. Academic Press, New York.
31. **Lipscomb, J.D.** 1994. Biochemistry of the soluble methane monooxygenase. Ann. Rev. Biochem. **48:** 371 - 399.
32. **Lowry, O.H., N.J. Rosebrough, A.L. Farr, and R.J. Randall.** 1951. Protein measurement with the Folin phenol reagent. J. Biol. Chem. **193:** 265 - 275.
33. **Lund, J., and H. Dalton.** 1985. Further characterization of the FAD and Fe_2S_2 redox centers of component C, the NADH: acceptor reductase of the soluble methane monooxygenase of *Methylococcus capsulatus* (Bath). Eur. J. Biochem. **147**: 291-296.
34. **Mak, A.S., and B.L. Jones** .1978. Application of S-pyridylethylation of cysteine to sequence analysis of proteins. Anal. Biochem. **83**: 432 - 440.
35. **McDonnel A., and L.A. Staehelin.** 1981. Detection of cytochrome *f.* a *c*-class cytochrome, with diaminobenzidine in polyacrylamide gels. Anal.Biochem. **117**: 40 - 44.
36. **Moss, R.H., and S.I. Chan** 1980. Electron paramagnetic resonance studies of nitrosyl ferrous heme complexes. Determination of an equilibrium between two conformations. J. Biol. Chem. **255:** 7876 - 7882.
37. **Nelson, M.J.** 1987. The nitric oxide complex of ferrous soybean lipoxygenase-1. J. Biol. Chem. **262**: 12137 - 12142.
38. **Nguyen ,H.-N., A.K. Shiemke, S.J. Jacobs, B.J. Hales, M.E. Lidstrom, and S.I. Chan.** 1994. The nature of the copper ions in the membranes containing the particulate methane monooxygenase from *Methylococcus capsulatus* (Bath) J. Biol. Chem. **269**: 14995 - 15005.
39. **Patel, R.N., and J.C. Savas.** 1987. Purification and properties of the hydroxylase component of methane monooxygenase. J.Bacteriol. **169**: 2313-2317.
40. **Pilkington, S.J., and H. Dalton.** 1991. Purification and characterization of the soluble methane monooxygenase from *Methylosinus sporium* demonstrates the highly conserved nature of the enzyme in methanotrophs. FEMS Microbiol. Lett. **78:** 103-108.
41. **Prior, S.D., and H. Dalton.** 1985. The effect of copper ions on membrane content and methane monooxygenase activity in methanol-grown cells of *Methylococcus capsulatus* (Bath). J. Gen. Microbiol. **131:** 155 - 163.
42. **Prior, S.D., and H. Dalton.** 1985. Acetylene as a suicide substrate and active site probe for membrane monooxygenase from *Methylococcus capsulatus* (Bath). FEMS Microbiol. Lett. **29:** 105 - 109.
43. **Rupp, H., and U. Weser.** 1974. Conversion of methallothionein into Cu-thionein, the possible low molecular weight form of neonatal hepatic mitochondrocuprein. FEBS Lett. **44**: 293 -297.

44. **Robinson J. and J.M. Cooper.** 1970. Method of determining oxygen concentrations in biological media, suitable for calibration of oxygen electrode. Anal. Biochem. **33**: 390 - 399.
45 **Rich, P.R., J.C.Salerno, J.S. Leigh, and W.D. Bonner Jr.** 1978. A sin 3/2 ferrous-nitric oxide derivative of an iron-containing moiety associated with *Neurospora crassa* and higher plant mitochondria. FEBS Lett. **93**: 323 - 325.
46. **Saierno, J.C., and J.N. Seidow.** 1979. The nature of the nitric oxide complexes of lipoxygenase. Biochim. Biophys. Acta **579**: 246 - 251.
47. **Scott, D., J. Brannan, and I.J. Higgins.** 1981. The effect of growth conditions on intracytoplasmic membranes and methane monooxygenase activities in *Methylosinus trichosporium* OB3b. J. Gen. Microbiol. **125:** 63 - 72.
48. **Semrau, J.D., D. Zolandz, M.E. Lidstrom, and S.I. Chan.** 1995. The role of copper in the pMMO *Methylococcyus capsulatus* Bath: a structural *vs.* catalytic function. J. Inorg. Chem. **58**: 235 - 244.
49. **Semrau, J.D., A. Chistoserdov, J. Lebron, A. Costello, J. Davagnino, E. Kenna, A.J. Holmes, R. Finch, J.C. Murrell, and M.E. Lidstrom.** 1995. Particulate methane monooxygenase genes in methanotrophs. J. Bacteriol. **177**: 3071 - 3079.
50. **Shiemke, A.K., Cook, S.A., Mily, T., and Singleton, P.** (1995) Detergent solubilization of membrane-bound methane monooxygenase requires plastoquinol analogs as electron donors. Arch. Biochem. Biophys. **321:** 521 - 528.
51. **Stanley, S.H., S.D. Prior, D.J. Leak, and H. Dalton.** 1983. Copper stress underlines the fundamental change in intracellular location of methane mono-oxygenase in methane utilizing organisms: studies in batch and continuous cultures. Biotechnol. Lett. **5**: 487 - 492.
52. **Tonge, G.M., D.E.F. Harrison, and I.J. Higgins.** 1977. Purification and properties of the soluble methane mono-oxygenase from *Methylosinus trichosporium* OB3b. Biochem. J. **161**: 333-334.
53. **von Jagow, G., and Th.A. Link.** 1986. Use of specific inhibitors on the mitochondrial bc_1 complex. Meth. Enzymol. **126:** 253 - 271.
54. **Whittenbury R., and H. Dalton.** 1981. The methylotrophic bacteria. pp 894-902. *In* M.P.Starr, H.G. Truper, A. Balows, and H.G. Schlegel (eds) The Prokaryotes, Vol.I Springer-Verlag, New York.
55. **Williams, J.N.** 1964. A method for the simultaneous quantitative estimation of cytochrome *a*, *b*, c_1 and *c* in mitochondria. Arch. Biochem. Biophys. **107**: 537 - 543.
56. **Woodland, M.P., and H. Dalton.** 1984. Purification and characterization of component A of the methane monooxygenase from *Methylococcus capsulatus* (Bath). J. Biol. Chem. **259**: 53-60.
57. **Zahn, J.A., C. Duncan, and A.A. DiSpirito.** 1994. Oxidation of hydroxylamine by cytochrome P-460 of the obligate methylotroph *Methylococcus capsulatus* Bath. J. Bacteriol. **176:** 5879 - 5887.

CHAPTER 3. CHARACTERIZATION OF COPPER-INDUCED IRON UPTAKE IN THE MEMBRANE FRACTION OF *Methylococcus capsulatus* Bath: FURTHER EVIDENCE FOR A NON-HEME IRON CENTER IN THE METHANE-ASSOCIATED METHANE MONOOXYGENASE

A paper to be submitted to Archives of Microbiology

[2]James A. Zahn[A,B], Joel R. Coats[B,C], and Alan A.DiSpirito[A,B]

Abstract

Biochemical changes associated with the expression of the soluble (sMMO) or particulate (pMMO) methane monooxygenase in *Methylococcus capsulatus* Bath have been characterized using SDS-PAGE, immunoblot analysis, electron paramagnetic resonance (EPR) spectroscopy, and analysis of heme by pyridine ferrohemochromagen spectra and coupled high performance liquid chromatography/mass spectroscopy in order to identify the source of copper-induced iron uptake in the membrane fraction.

Immunoblot analysis of *Methylococcus capsulatus* (Bath) cell extracts grown to express either the sMMO or pMMO with antibodies against *M. capsulatus* Bath cytochrome aa_3/c-557 complex show that the expression level of cytochrome aa_3/c-557 is unaffected by copper availibility and therefore, cannot be responsible for the copper-induced increase in membrane-associated iron as previously suggested by Nuygen et al., 1994.

---

[2] [A] Department of Microbiology, Immunology, and Preventive Medicine and [B] Graduate Program in Toxicology Iowa State University Ames, IA 50011, USA. [C]Department of Entomology, Iowa State University, Ames, IA 50011.

Analysis of the membrane fraction from cells expressing the pMMO by electron paramagnetic resonance spectroscopy shows the presence of a very intense copper signal with a $g_{\perp} = 2.057$ and hyperfine splitting constants of $g_{||} = 2.27$ and $|A_{||}| = 174$ [G] . Analysis of subtracted EPR spectra for membrane samples grown to express either the sMMO or pMMO shows an minor increase in the g = 4.05 and g = 4.61 signals from the membranes of cells expressing the sMMO and an increase in the population of a g = 6.00 (S = 5/2) signal from cell membranes expressing the pMMO. The signal at g = 6.00 appears to be associated with a non-heme species since the concentration of membrane-associated heme A, B, or C is not altered by copper supplementation.

Immunoblot analysis of the membrane fraction from Type I and Type II methanotrophs and of the nitrifying bacterium, *Nitrosomonas europeae*, with antibodies against the pMMO from *M. capsulatus* Bath has confirmed the highly conserved nature of the pMMO and ammonia monooxygenase polypeptides.

Key Words: Methanotrophs, *Methylococcus capsulatus* Bath, Cytochrome *b*, Cytochrome *a*, Soluble Methane Monooxygenase, Particulate Methane Monooxygenase, Electron Paramagnetic Resonance.

Abbreviations: MMO, methane monooxygenase; pMMO, membrane-associated methane monooxygenase, sMMO, soluble methane monooxygenase, EPR, Electron paramagnetic resonance; RP-HPLC, Reverse-phase high performance liquid chromatography.

Introduction

Methanotrophs are an environmentally ubiquitous group of gram negative bacteria which derive cellular energy and carbon from the oxidation of methane (Whittenbury and Dalton, 1981; Anthony, 1982). The methane monooxygenase (MMO) catalyzes the initial step in the oxidation of methane to methanol and demonstrates a broad substrate specificity which allows for co-oxidation of related compounds including alkanes, alkenes, and chlorinated hydrocarbons (DiSpirito, et al., 1992). A limited number of methanotrophic bacteria including *Methylobacterium*, *Methylosinus*, and *Methylococcus* (Patel and Savas 1987; Pikington et al., 1991; Stainethorp, et al., 1990) exhibit the ability to express either a membrane-associated (pMMO) or soluble (sMMO) form of the MMO. In addition to the differences in enzyme cellular location, the two MMO's have been shown to differ in substrate specificity (Green and Dalton, 1989; Prior and Dalton, 1985), apparent electron donor (Dalton, et al., 1984), and sensitivity to inhibitors (Stirling, et al., 1979). The expression of the soluble or particulate methane monooxygenase in methanotrophic bacteria has been shown to be regulated by the concentration of the copper ions in the growth medium. At growth medium copper concentrations below 0.2 μM, methanotrophs, such as *Methylomonas albus* BG-8, which lack genes for the sMMO demonstrate low cell viability or no growth. However, methanotrophs exhibiting genes for the sMMO, under copper deficient conditions, express the soluble form of the enzyme. The expression of the sMMO has been correlated to the loss of extensively paired intracytoplasmic membranes in type I and X methanotrophs and the loss of peripherally paired intracytoplasmic membranes in type II methanotrophs. Sodium dodecyl sulfate polyacrylamide gel electrophoresis (SDS-PAGE)

experiments comparing cell extracts grown in the absence of copper have correlated sMMO activity to the loss of the intracytoplasmic membranes and the disappearance of membrane-associated polypeptides with the apparent molecular mass of 47, 35, and 26 kDa and the appearance of polypeptides in the soluble fraction with the apparent molecular mass of 54, 44, 42, 20, and 17 kDa (Dalton, et al., 1984).

Progress toward the characterization and functional classification of switch-over polypeptides in the membranes of methanotrophs cultured in the presence of copper has been severely hindered due to the inability to maintain pMMO activity *in vitro*. A number of studies have addressed physiological changes associated with ultrastructure (Scott, et al., 1981; Stanley, et al., 1983), lipid content (Peltola, et al., 1993), copper and iron content (Nguyen, et al., 1994; Chan, et al., 1992), and MMO substrate specificity (Green and Dalton, 1989; Burrows, et al., 1984; Brusseau, et al., 1990; DiSpirito, et al., 1992) in methanotrophs with the ability to express either a soluble or membrane-associated MMO. However, the biochemical characterization of copper-regulated membrane-associated polypeptides in any methanotrophs have previously been ignored or unreported. This study describes the identity of major polypeptides associated with the expression of the pMMO in *M. capsulatus* Bath and describes additional biochemical alterations in soluble and membrane-associated heme-containing polypeptides which coincide with the switch-over event. Immunoblot analysis of Type I and Type II methanotrophs and of the nitrifying bacterium, *Nitrosomonas europaea*, with antibodies against the pMMO from *M. capsulatus* Bath has confirmed the presence of polypeptides in these organisms exhibiting structural homology to pMMO polypeptides in the Type X methanotroph, *M. capsulatus* Bath.

Materials and Methods

Organism and cultivation

M. capsulatus Bath and *Methylomonas* sp. MN were grown in nitrate mineral salts media (NMS) (Whittenburry and Dalton, 1981) plus 5μM $CuSO_4$, and a vitamin mixture (Lidstrom, 1988) at 37°C under an atmosphere of 40% methane and 60% (vol/vol) air. For expression of the soluble methane monooxygenase (sMMO), *M. capsulatus* Bath was cultured by a semi-chemostat method using NMS plus a vitamin mixture under copper limitation (<0.1 μM Cu^{2+}) at 37° C in a 12-liter fermentor sparged at flow rates between 80 and 150 ml/minute methane and 2000 to 2500 ml/minute air. Cell batches exhibiting less than 100% of the total methane monooxygenase activity associated with the soluble fraction were discarded (typically the first and second batches were discarded). The marine methanotroph, *Methylomonas* A45 was cultured at 37° C in NMS containing 5 μM $CuSO_4$, 1.5% NaCl, and a vitamin mixture under an atmosphere of 40% methane and 60% (vol/vol) air. *Methylocystis parvus* OBBP and *Methylomonas albus* BG8 were cultured at 30° C in NMS containing 5 μM CuSO4, and a vitamin mixture under an atmosphere of 40% methane and 60% air. Cells growth in a 12-liter fermentor were sparged at flow rates between 80 and 150 ml/minute methane and 2000 to 2500 ml/minute air at 42°C. *Nitrosomonas europaea* was a generous gift from Dr. A. B. Hooper (University of Minnesota).

Isolation of cells, soluble and membrane fractions

Cells were harvested by centrifugation at 13,000 x g for 15 minutes at 4° C, resuspended (1:5 w/v) in a buffer containing 10 mM Tris-HCl (pH 8.0) (Buffer A),

frozen in liquid nitrogen and stored at -80° C. All isolation steps were performed at 0 to 4° C. Freeze-thawed cells were passed three times through a French Pressure cell at 18,000 psi. Lysed cells were centrifuged at 13,000 x g for 30 minutes and the supernatant centrifuged at 150,000 x g for 2 hours. The supernatant ("soluble fraction")was decanted and the pellet was resuspended in a buffer containing buffer A plus 250 mM KCl using a dounce homogenizer. The solution was centrifuged at 150,000 X g for 2 hours and the supernatant ("salt-washed soluble fraction") was decanted and dialyzed 12 hours against three changes of buffer A . The washed membrane pellet ("salt-washed membrane fraction") was resuspended in 10mM Tris-HCl, pH 8.0 and dialized 12 hours against three changes of buffer A .

Protein and heme determinations

The concentrations of heme *a*, heme *b*, and heme *c* were measured by the pyridine hemochromogen method (DiSpirito, et al., 1990) using the $\Delta A_{587\ nm}$ of 21.7 $cm^{-1}mM^{-1}$ for heme *a* (DiSpirito, et al., 1994), the ΔA_{557nm} of 34.4$cm^{-1}mM^{-1}$ for heme *b* (Fuhrhop, 1975) and the ΔA_{550nm} of 29.1$cm^{-1}mM^{-1}$ for heme *c* (Fuhrhop, 1975). The simultanous determination of heme A, heme B, and heme C in washed membrane fractions was estimated using the method of Berry and Trumphower (1982). Protein was assayed by the method of Lowry *et al.* (1951) using bovine serum albumin as a standard.

The separation of extractable hemes was performed by reverse-phase high-performance liquid chromatography. Exactly 43.4 mg protein from isolated membrane fractions was extracted two times with a mixture of acetone/HCl (99:1 v/v) at -20° C. The combined extracts were partitioned into diethyl ether, washed

twice with H_2O, and dried in a stream of nitrogen. The hemes were solubilized with 2 ml of a mixture containing acetonitrile-water-trifluroacetic acid (50 : 49.92 : 0.08) and filtered through a 0.45 µm centrifugal filter (Millipore #UFC3OHV00). The filtered heme-containing solutions were separated by gradient reverse-phase HPLC using a (VyDac) semi-preparative C_{18} column (10 x 250 mm) (Cat. # 218TP510) at a flow rate of 4.0 ml/min using water-trifluroacetic acid (99.9 : 0.1) (buffer A) and acetonitrile-trifluroacetic acid (99.92 : 0.08) (buffer B) as the mobile phase. The linear gradient consisted of 40% buffer B at 10 minutes following injection to 100% buffer B at 40 minutes. Heme standards were composed of bovine hemoglobin (protoheme), and *M. capsulatus* Bath cytochrome *aa*3 (DiSpirito, et al., 1994). Fractions exhibiting an absorbance at 400 nm were collected and lyophilized to dryness for analysis of molecular mass by matrix assisted laser desorption/ionization (MALDI) time of flight mass spectroscopy on a Finnigan LASERMAT 2000 mass spectrometer using synapinic acid as a matrix (Baldwin, et al., 1993) .

Enzyme activity

Methane monooxygenase activity was determined by the epioxidation of propylene as previously described (DiSpirito, et al., 1990). Soluble methane monooxygenase activity was monitored spectrophotometrically by the formation of naphthol from naphthylene by the method of Brusseau et al., (1990). Oxidase activity was assayed by recording oxygen uptake at 37° C in the presence of Ascorbate/TMPD (DiSpirito, et al., 1994).

Spectroscopy

Optical absorption spectroscopy was performed with an Aminco DW-2000 spectrophotometer in the split-beam mode. The instrument was cablibrated upon start-up with a holium oxide filter or by the position of the ferrous minus ferric α-band of the pyridine ferrohemochrome of horse heart cytochrome *c* (550 nm).

X-band electron paramagnetic resonance (EPR) spectra were obtained on a Bruker ER 200 D spectrometer equipped with an Oxford Instruments liquid helium cryostat . Samples were placed in tubes with matched internal diameter (1.50 mm) and were maintained at 7.7° K during spectral aquisition. Comparsion of cellular extracts grown to express either the pMMO or sMMO was performed on membrane extracts containing 57.5 mg/ml protein and on soluble extracts containing 24.0 mg/ml protein in 10 mM Tris (pH 8.0). Operating parameters are as outlined in the figure legends.

Prepration of antibodies against pMMO and cytochrome caa_3 complex

Cytochrome caa_3 and pMMO were purified according to the method of DiSpirito et al., (1994), and Zahn and DiSpirito (1996), respectively. Polyclonal antibodies against purified enzymes from *Methylococcus capsulatus* Bath were raised in two 10-week-old female New Zealand White Rabbits. Each enzyme [0.6 mg per rabbit] was diluted in Ribi adjuvant according to the manufacturers recommendations and injected intradermally in 20 sites (150 - 200μL/site) across the back. Rabbits were given three 0.1 mg booster injections at 1 month intervals. Immunogloblin G was purified from serum using immobilized Protein A (Pierce) and concentrated using a Cenriprep 30 concentrator (Amicon).

Electrophoresis and immunoblot analysis

Sodium dodecyl sulfate (SDS)-polyacrylamide slab gel electrophoresis was carried out by the method of Laemmli (1970) on 12 to 15% gels using a Mini-Protean II electrophoresis cell (Bio-Rad Laboratories). Unless indicated, samples did not contain reducing agent and were incubated at room temperature prior to loading. Gels were stained for total protein with Coomassie brilliant blue R or by the diaminobenzidine method (McDonnel and Staehelin, 1981) for *c*-type cytochromes.

Immunoassays for cytochrome caa_3 and pMMO were completed by adding 12 µg protein of the membrane fraction, 16 µg protein of soluble fraction, or 8 µg protein of the salt wash fraction per well to 15% SDS-polyacrylamide gels. The protein concentration for corresponding gels stained for total protein with Coomassie R-250 were increased by three-fold. Electrophoretically resolved proteins were transferred to nitrocellulose using a Mini Trans-Blot electrophoretic transfer cell (Bio-Rad Laboratories, Richmond, CA). Following transfer, the blotted polypeptides were blocked for 1 hour with gentle agitation using a solution containing 5% non-fat dry milk, 1% bovine serum albumin, 500 mM NaCl, and 20 mM Tris (pH 7.5). Purified antibodies against 47-26 kDa switch-over complex or *caa*3 (Δ Abs. 280 nm = 0.32 abs. units - cm^{-1}) were added in a 1:1000 dilution to a solution containing 1% non-fat dry milk, 500 mM NaCl, 0.05% Tween-20, and 20 mM Tris (pH 7.5) and incubated for 1 hour. Antibodies were detected with conjugated goat anti-rabbit IgG alkaline phosphatase (Bio-Rad Laboratories, Richmond, CA) according to the protocol of the manufacturer.

Results

Characterication of copper-induced polypeptides

SDS-denaturing gels stained for total protein with Coomassie R-250 indicate major alterations in the expression of polypeptides in response to copper availability (Fig. 1). In the absence of copper, the soluble fraction (Fig. 1, Lane E) is dominated by polypeptides with the molecular masses of 54, 44, 42, 18, and 17 kDa. Immunoblot analysis with antibodies against the sMMO hydroxylase has confirmed the identity of the 54, 42, and 17 kDa polypeptides as components of the soluble methane monooxygenase (sMMO) hydroxylase. Immunoblot analysis of the soluble fraction of cells grown in the presence of 5 μM Cu^{2+} with antibodies against the sMMO hydroxylase indicates that this fraction is totally devoid of sMMO hydroxylase polypeptides. The membrane fraction from cells grown in the presence of 5 μM Cu^{2+} indicates the presence of three copper-induced polypeptides with molecular masses of 47, 27, and 25 kDa (Lane F). These polypeptides have previously been suggested to be components of the pMMO (Dalton, et al., 1984) The protein concentration utilized for SDS-PAGE analysis of the membrane fraction from cells grown under copper-limiting conditions (Lane G) has been increased by two-fold to emphasize the lack of pMMO-associated polypeptides.

SDS-denaturing gels stained for peroxidase-reactive polypeptides indicate the presence of two major high molecular mass polypeptides (>100 and 82 kDa) and three minor peroxidase-staining polypeptides with molecular masses of 28, 18, and 9 kDa in the membranes of cells grown in 5 μM Cu^{2+} (Fig. 1, Lanes H - M). Since the migration pattern and staining intensity of the 82 kDa polypeptide in this gel demonstrates simularities to peroxidase-staining polypeptides in purified samples of

FIG. 1. SDS-PAGE analysis of *M. capsulatus* Bath cell fractions exhibiting soluble or particulate MMO activity. Soluble KCl-wash fraction from cells expressing the pMMO (Lane B and H) and sMMO (Lanes C and I). Soluble fraction from cells expressing the pMMO (Lane D and J) and sMMO (Lane E and K). KCl-washed membranes from cells expressing the sMMO (Lane F and L) and sMMO (Lanes G and M). Lanes A though G were stained for total protein with Coomassie brilliant blue R-250 and Lanes H though M were stained for proxidase-reactive polypeptides with diaminobenzidine. Protein concentrations were as listed in the Materials and Methods. Molecular mass standards (Lane A): 92, 66.2, 45, 31, 21.5, and 14.4 kDa.


A
B
C
D
E
F
G
H
I
J
K
L
M

cytochrome *b*-559/569 (Zahn and DiSpirito, unpublished results), we have preliminarly assigned the identity of this polypeptide to aggregated protoheme. Evidence suggesting the identity of the 82 kDa polypeptide as aggregated protoheme is supported by the solvent extractable nature of this band (Fig. 2). Membrane extracts solublized in 2 M urea following extraction of non-covalently bound heme with acidified acetone (Fig. 2, lanes A - D) demonstrate the removal of the 82 kDa band and reduction in the intensity of the >100 kDa bands. The 11 kDa peroxidase-staining band found in the soluble fraction of cells grown in the presence or absence of Cu^{2+} (Fig. 1, Lanes J and K) is associated with the 11 kDa cytochrome *c*-555 and 9 kDa cytochrome *c*-553 (Zahn, et. al., 1994). This *c*-type cytochrome (Lanes J and K) is expressed at simular levels in cells expressing either the pMMO or sMMO. The identity of the >100 kDa heme-staining bands has recently been shown to be a novel 142 kDa cytochrome *c*-553 (Zahn, Unpublished results).

The α-band of the pyridine ferrohemochromogen absorption spectrum for soluble fractions expressing either the pMMO or sMMO demonstrates a dithionite-reduced minus ferricyanide oxidized absorption maximum at 550 nm. The content of heme C in the soluble fraction of cells expressing the sMMO was 1.63 μM heme C/mg protein and 1.12 μM heme C/mg protein for cells expressing the pMMO. These values indicate a 31% increase in the concentration of *c*-type cytochromes per mg protein in the soluble fraction during the expression of the sMMO. An increase in the concentration of *c*-type heme-containing polypeptides is also supported by analysis of the soluble fractions by EPR. The red shifted (552 nm) and broadened α-band of the pyridine ferrohemochromogen absorption spectrum of the membrane samples suggests the presence of heme B, or possibly heme O in these

FIG. 2. SDS-PAGE analysis of *M. capsulatus* Bath cell membrane fractions exhibiting soluble or particulate MMO activity. Non-covalently bound heme or metals were removed from each membrane sample by acid/acetone treatment. The heme/metal-free fraction was lyophilized to dryness and resuspended in SDS-PAGE buffer containing 6 M urea. Lanes A and C show the membrane fraction from cells expressing the sMMO. Lanes B and D show the membrane fraction from cells expressing the pMMO. Lanes A and B were stained for total protein with Coomassie brilliant blue R-250 and Lanes C and D were stained for peroxidase-reactive polypeptides with diaminobenzidine. Molecular mass standards (Lane A): 92, 66.2, 45, 31, 21.5, and 14.4 kDa.

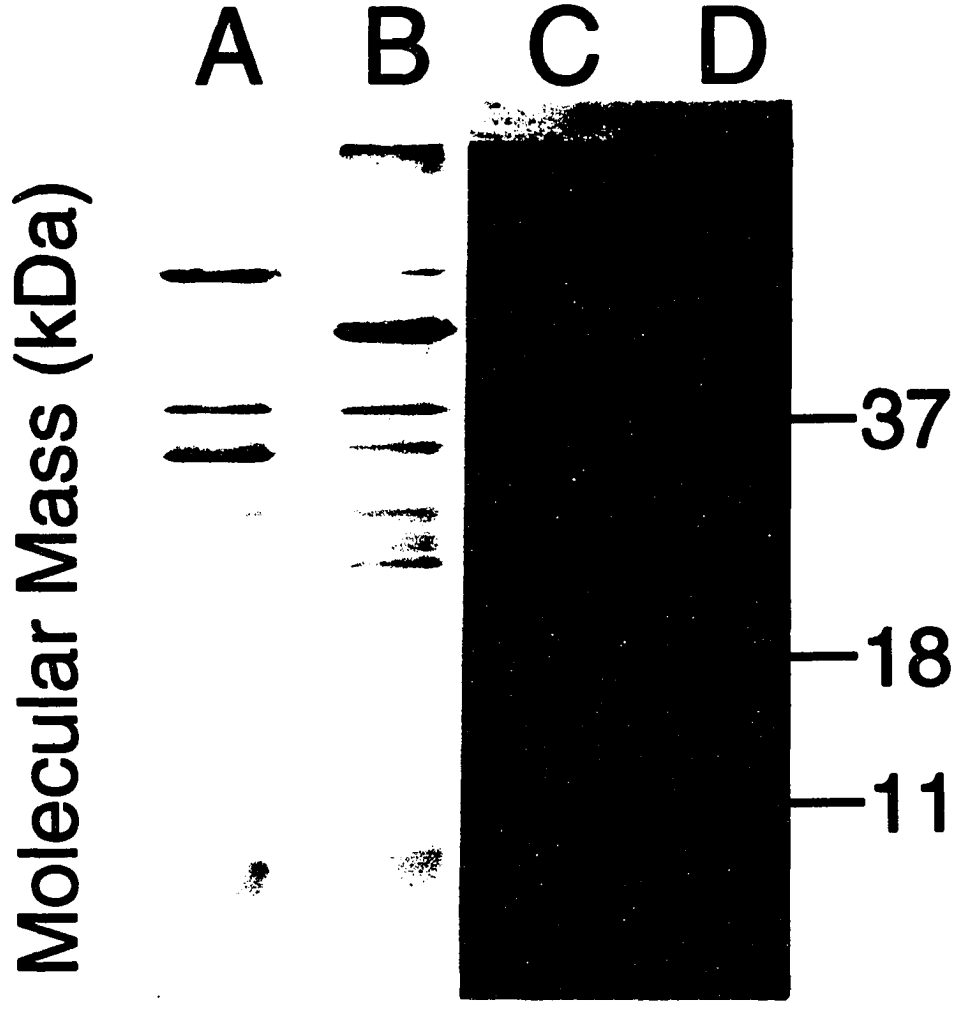
A
B
C
D
Molecular Mass (kDa)
37
18
11

samples. Since the identity of major extractable heme contributing to the red-shifted ferrohemochrome absorbance at 552 nm has subsequently been shown to be heme B (see Characterization of Membrane Extractable Heme), the concentration of heme A, heme B and heme C have been estimated by the method of Berry and Trumphower (1989). These results show that the concentration of heme A, heme B, and heme C from the membranes of cells expressing the sMMO are 0.065 μM heme A/mg protein, 0.392 μM heme B/mg protein, and 0.382 μM heme C/mg protein, and from the membranes of cells expressing the pMMO, 0.088 μM heme A/mg protein, 0.360 μM heme B/mg protein, and 0.353 μM heme C/mg protein, respectively. Comparsion of these values based on a mg protein ratio indicate that there is no significant change in the concentration of heme A, heme B, or heme C in the membranes of cells which express either the the pMMO or sMMO.

Characterization of membrane extractable heme

Heme extraction, HPLC purification, and characterization by mass spectrometery was utilized to remove spectral interferences of cytochrome c in the analysis of membrane samples. Figure 3 shows the elution profile recorded at 400 nm for extractable heme from the membranes of *M. capsulatus* Bath grown in the absence of copper and expressing 100% of the MMO activity in soluble fraction (B) and in the presence of 5 μM $CuSO_4$ and expressing 100% of the MMO activity in the membrane fraction (A). The elution profiles for the extracted heme were compared to standards composed of protoheme extracted from bovine hemoglobin and *M. capsulatus* Bath cytochrome aa_3. Peaks eluting at 20.9 minutes (61.8% solvent B) have been assigned to protoheme due to similarities in elution profile and molecular

FIG. 3. Reverse-phase HPLC profile of non-covalently bound heme in membrane fractions. Solvent extracted heme from the KCl-washed membranes of *M. capsulatus* Bath expressing the pMMO (A) and sMMO (B). HPLC instrument conditions were as follows: flow rate, 4 mL/min; detector wavelength, 400 nm; column, VyDac semi-preparative C_{18} column (10 x 250 mm).

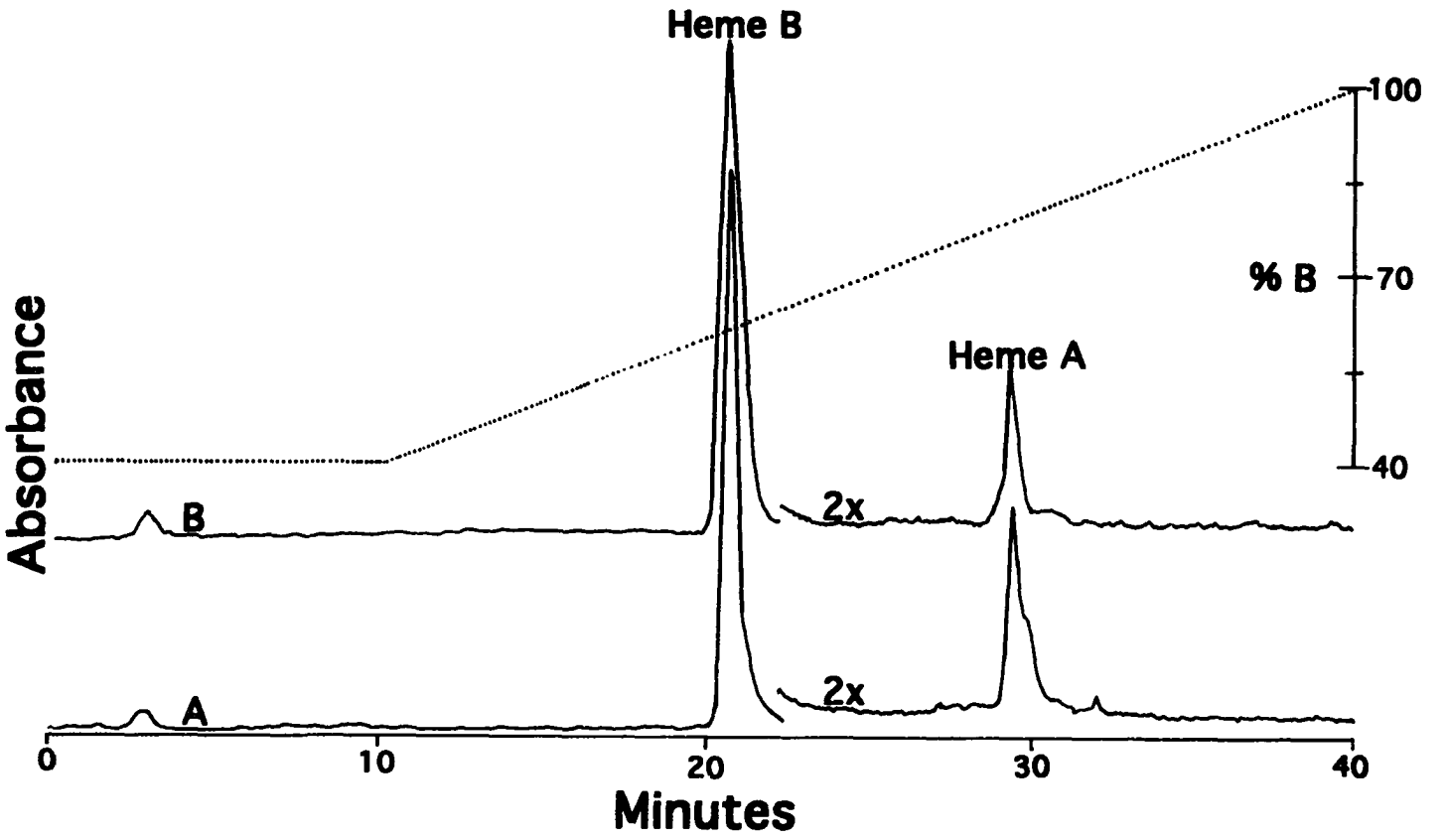
Heme B
Heme A
100
% B
70
40
Absorbance
B
A
2x
2x
0
10
20
30
40
Minutes

mass of extracted protoheme from bovine hemoglobin. Comparison of the mass spectra of the collected peaks at 20.9 minutes show that both samples have a molecular mass of 620 Da; this molecular mass value is in good agreement with the molecular mass of protoheme at 617 Da. Peaks eluting at 29.6 minutes (79.2% solvent B) have been assigned to heme A based on comparison of elution time to heme A extracted from *M. capsulatus* Bath cytochrome *aa*3, molecular mass (856 Da), and ferrohemochromagen spectral similarities to extracted heme A from *M. capsulatus* Bath cytochrome *aa*3. Comparison of total peak area of protoheme (35.88) and heme A (2.00) from the membranes of cells expressing the sMMO and protoheme (34.36) and heme A (2.27) from the membrane of cells expressing the pMMO suggests that the membrane concentration of each heme per mg protein is unaffected by the form of MMO expressed. This observation has been supported by the quantitative analysis of heme in membrane samples by the pyridine ferrohemochromagen assay.

EPR spectra

The electron paramagnetic spectrum of the resting soluble fraction from cells expressing the sMMO is dominated by a free radical signal at g = 2.011 which has previously been assigned to the sMMO hydroxylase (Woodland, et. al., 1984). The signal is also observed, although much weaker in intensity, in the washed membrane fraction (Fig 4, A). Subtraction of EPR spectra for the soluble fractions of cells expressing the sMMO or pMMO indicates an increase in the g = 4.05, g = 4.32, and g = 4.61 signals for cells expressing the sMMO. Preliminary studies of *b*-type cytochromes from *M. capsulatus* Bath have indicated that the signals (g = 4.05 and g

FIG. 4. Electron Paramagenic Resonance spectra for soluble cell extracts from *M. capsulatus* Bath expressing the sMMO (A) or the pMMO (B). Protein concentration was 24.0 mg/mL in 10 mM Tris, pH 8.0 at 7.7° K. Operating prameters were: modulation frequency, 100 kHz; modulation amplitude, 20 G ; time constant 100 ms. The microwave frequency was 9.421 GHz, microwave power 2.02 mW.

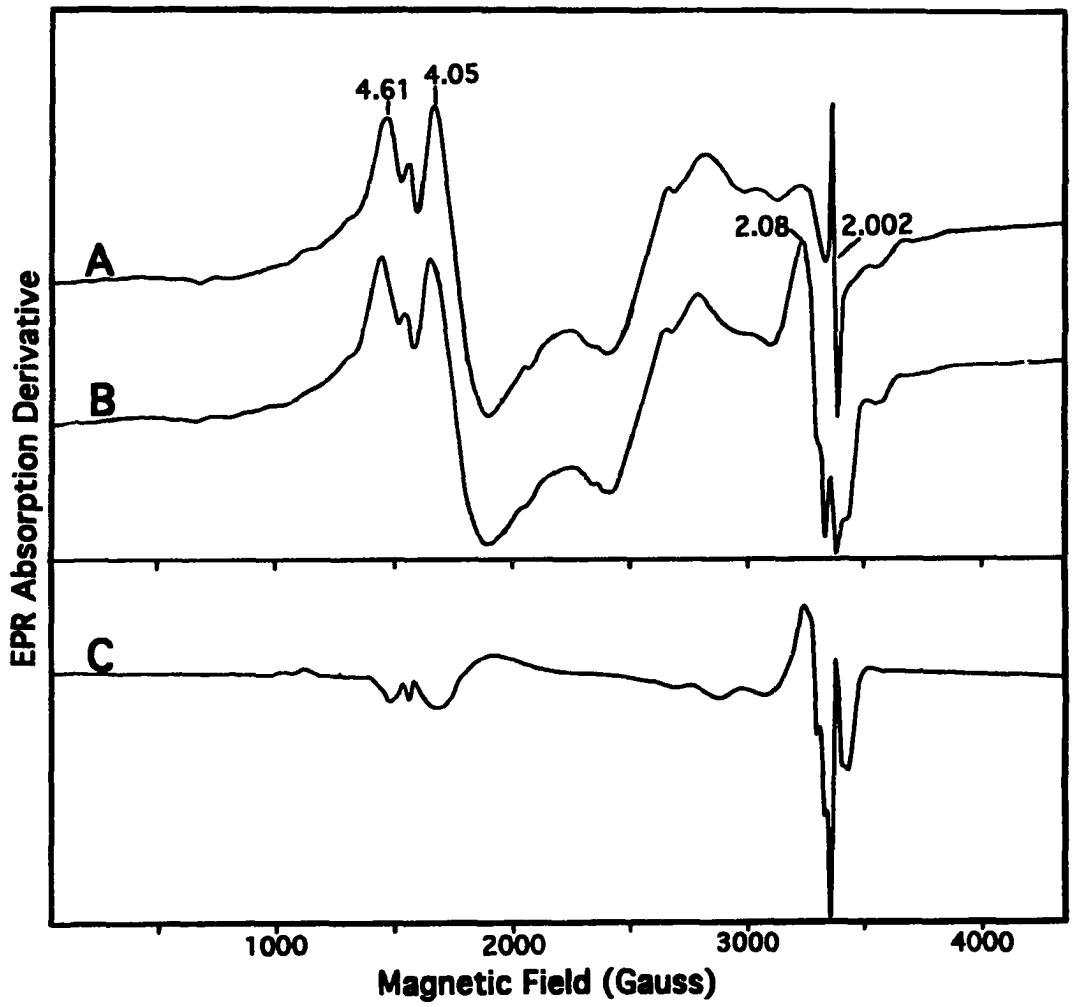
4.61
4.05
2.08
2.002
A
B
C
EPR Absorption Derivative
1000
2000
3000
4000
Magnetic Field (Gauss)

= 4.61) arise from cytochrome *b*559/569 (Zahn and DiSpirito, unpublished results). The signal at g = 4.32 is associated with adventitious ferric iron.

In agreement with Nguyen et al., (1994), we observe a very intense copper signal with a $g_{\perp}$ = 2.057 and hyperfine splitting constants of $g_{||}$= 2.27 and $|A_{||}|$= 174 [G] in the membranes isolated from cells grown in the presence of 5μM $CuSO_4$ (Fig. 5, B) No observable copper resonances were detectable in the membranes of cells expressing the sMMO (Fig. 5, A). Analysis of the isotropic copper signal occurring near g = 2.06 by using high microwave power was not performed; however, this signal has recently been shown to exhibit several similarities with a membrane-associated copper-binding cofactor isolated from copper-inducible polypeptides (Zahn and DiSpirito, 1996). Analysis of subtracted EPR spectra for membrane samples shows a minor increase for the g = 4.05 and g = 4.61 signals from the membranes of cells expressing the sMMO and a significant increase in the population of a g = 6.00 signal from the membranes expressing the pMMO. The signal at g = 6.00 appears to be associated with a non-heme species since the concentration of membrane-associated heme A, B, or C is not altered by supplementation of the growth medium with copper (Zahn and DiSpirito, 1996). Integration of the g = 6.00 signal from membranes exhibiting pMMO activity shows an increase in signal intensity of 55% as compared to the g = 6.00 from the membranes of cell expressing the sMMO . This EPR signal (g = 6.00) is observed with active preparations of purified pMMO (Zahn and DiSpirito, 1996). A minor signal arising from adventitious ferric iron ($g \approx 4.3$) was detected in both membrane isolations.

FIG. 5. Electron Paramagenic Resonance spectra for KCl-washed membrane cell extracts *M. capsulatus* Bath expressing the sMMO (A) or the pMMO (B). Protein concentration was 57.5 mg/mL in 10 mM Tris, pH 8.0 at 7.7° K. Operating prameters were: modulation frequency, 100 kHz; modulation amplitude, 10 G; time constant 100 ms. The microwave frequency was 9.421 GHz and the microwave power was 2.02 mW.

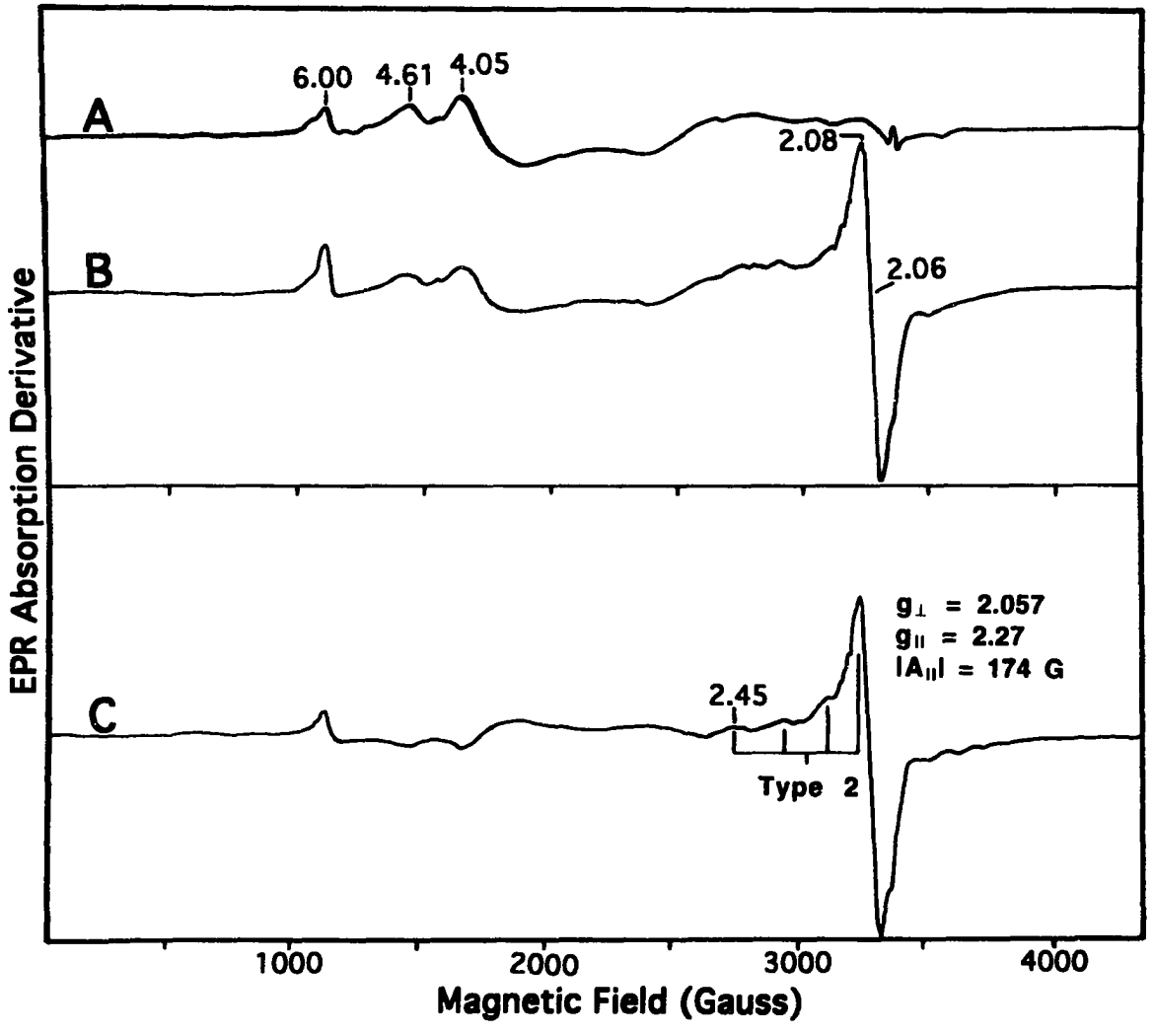
6.00
4.61
4.05
A
2.08
B
2.06
EPR Absorption Derivative
C
2.45
$g_\perp$ = 2.057
$g_{||}$ = 2.27
$|A_{||}|$ = 174 G
Type 2
1000
2000
3000
4000
Magnetic Field (Gauss)

Expression level of cytochrome *c*-557/cytochrome aa_3 complex in *Methylococcus capsulatus* Bath in response to copper availability

The isolation and properties of cytochrome *aa*3 from *M. capsulatus* Bath have recently been reported by our group (DiSpirito, et al., 1994). In the initial characterization of cytochrome aa_3-cytochrome *c*-557 complex, two structural polypeptides exhibiting similarities in molecular mass to putative pMMO polypeptides were observed, namely the 46 and 25 kDa polypeptides. Immunoblot analysis of membrane fractions isolated from cells expressing the sMMO or pMMO with antibodies against cytochrome aa3-cytochrome *c*-557 demonstrated that expression level of this complex was unchanged with respect to copper availability in the growth medium (Fig. 6).

Immunoblot analysis of methanotrophic and nitrifying bacteria

Recently, a three component particulate methane monooxygenase was isolated from the cell membranes of *M. capsulatus* Bath (Zahn and DiSpirtio, 1996). The pMMO consisted of polypeptides with a molecular mass of 47, 27, 25 kDa and contained 0.5 mol Cu, 0.7 mol Fe, and 0.5 mol sulfide per mol enzyme based on a holoenzyme molecular mass of 99,000 kDa and oxidized propylene and methane to propylene oxide and methanol, respectively. EPR spectra of the purified pMMO was similar to fractions of cell membrane and similarities in molecular mass to putative pMMO polypeptides strongly suggests the identity of structural polypeptides from this complex as putative pMMO polypeptides. Immunoblot analysis of *M. capsulatus* Bath cell extracts grown to express either the sMMO or pMMO with antibodies

FIG. 6. Immunoblot analysis of *M. capsulatus* Bath cell fractions exhibiting soluble or particulate MMO activity with antibodies against cytochrome aa_3-cytochrome *c*-557 complex. KCl-washed membrane fraction from cells expressing the sMMO (Lanes B and F) and pMMO (Lanes C and G). Soluble fraction from cells expressing the sMMO (Lane D and H) and pMMO (Lane E and I). Protein concentrations were as listed in the Materials and Methods. Molecular mass standards (Lane A): 92, 66.2, 45, 31, 21.5, and 14.4 kDa.


A
B
C
D
E
F
G
H
I

Table 1. Immunoblot analysis of methanotroph and nitrifier membrane polypeptides using antisera against pMMO isolated from the membranes of copper grown *Methylococcus capsulatus* Bath.

Organism	Cross-Reactive polypeptide(s) (kDa)	Relative Intensity of Cross-Reaction
Methylococcus capsulatus (Bath)	47; ≈ 2	++++
Methylomonas sp. MN	45; ≈ 2	+++
Methylomonas BG-8	44; ≈ 2	++
Methylomonas A-45	45; ≈ 2	+++
Methylocystis parvus OBBP	42; ≈ 2	++
Nitrosomonas europaea	42; ≈ 2	+

against the pMMO has confirmed that three polypeptides from this complex (47, 40, and < 5 kDa) are induced by copper availability (Zahn and DiSpirito, 1996).

The cross-reactivity of polyclonal antibodies raised against pMMO polypeptides from *M. capsulatus* Bath was investigated in other bacteria capable of methane oxidation. Immunoblot analysis of the type I methanotrophs, *Methylomonas* A45, *Methylomonas sp.* MN, and *Methylomonas albus* BG8, the type II methanotroph, *Methylocystis parvus* OBBP, and the nitrifying bacterium, *Nitrosomonas europaea* was performed on unboiled, KCl-washed membrane extracts with antibodies against pMMO from *M. capsulatus* Bath. Figure 7 and Table 1 show the results for this experiment. All strains tested show the presence of a high molecular weight (47 - 43 kDa) and low molecular weight (< 5 kDa) cross-reactive polypeptide, however, no cross-reactivity was observed for the 29 to 26 kDa polypeptide in any of the strains tested.

FIG. 7. Immunoblot analysis of the KCl-washed membrane fractions of Type 1 and Type 2 methanotrophs and of the nitrifying bacterium, *Nitrosomonas europaea* with antibodies against pMMO from *M. capsulatus* Bath. *Methylocystis parvus* OBBP (Lanes B and H); *Methylomonas* A45 (Lanes C and I); *Methylomonas* sp. MN (Lanes D and J); *Nitrosomonas europaea* (Lanes E and K); *Methylomonas albus* BG8 (Lanes F and L); and *M. capsulatus* (Bath) (Lanes G and M). Lanes H through M are a Western blot probed with antibodies against pMMO-A and pMMO-B. Lanes A through G are stained with Coomassie brilliant blue R-250. Protein concentrations were as listed in the Materials and Methods. Molecular mass standards (Lane A): 92, 66.2, 45, 31, 21.5, and 14.4 kDa.

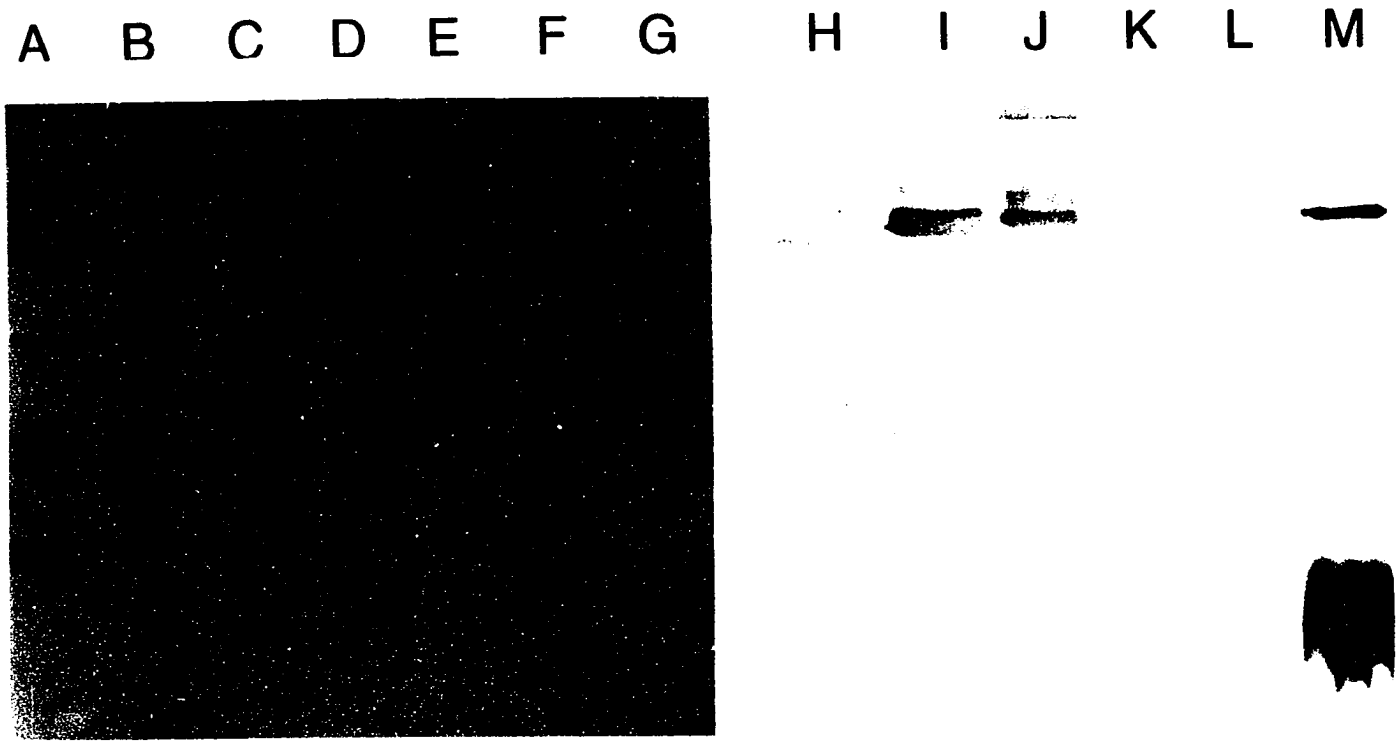
A B C D E F G H I J K L M

Discussion

The physiology of methane oxidizing bacteria has recently been reviewed by several authors (DeVries, et al., 1990; Fox, et al., 1991; Lidstrom and Semrau, 1995). These reviews reflect the general lack of knowledge concerning the physiology and biochemistry of obligate methylotrophs expressing the membrane-associated MMO. In contrast to the sMMO and components of the soluble methane oxidizing system, little is known concerning the bioenergetics of methane oxidation by the pMMO. The recent purification of the pMMO from *M. capsulatus* Bath has shown that prior problems in stabilizing the enzyme were due in part to the detergent-induced disruption of the electron transport chain (Zahn and DiSpirito, 1996). The most distinct indicator of this event was the complete loss of NADH + H^+-dependent pMMO activity following detergent solublization. This report describes an ongoing study concerned with characterizing the membrane-associated methane monooxygenase from *M. capsulatus* Bath and focuses on biochemical changes occurring in the membrane fraction which are associated with the copper-induced switch-over in methane oxidizing enzymes.

Immunoblot analysis of cell extracts with antibodies against pMMO polypeptides have confirmed the identity of two polypeptides (47 and 0.6 kDa) as the major copper-inducible membrane-associated polypeptides (Zahn and DiSpirito, 1996). The 47 and 0.6 kDa copper-induced polypeptides from the pMMO of *M. capsulatus* Bath appear to be highly conserved since antibodies against this complex demonstrate cross reactivity to other Type I and Type II methanotrophs and to the nitrifying bacterium, *Nitrosomonas europaea*. Although immunoblot analysis has failed to detect the 29 to 26 kDa polypeptide in all of the strains tested, it has

been previously shown that this polypeptide is poorly transferred to nitrocellulose membranes by the electroblotting procedure (Zahn and DiSpirito, 1996). As noted previously, the use of other buffer systems differing in ionic strength, pH, or in the absence of methanol were also found to be inadequate in increasing the transfer efficiency of the 29 to 26 kDa polypeptide.

Based on a mg protein comparison, the soluble fraction of *M. capsulatus* Bath cells expressing the sMMO shows a 31% increase in the concentration of C heme over the soluble fraction from cells expressing the pMMO (Zahn and DiSpirito, 1996). Comparison of peroxidase-reactive polypeptides by SDS-PAGE indicates that the increase in heme C in the soluble fraction of cells expressing the sMMO is associated with a general increase in all *c*-type cytochromes rather than an increase in concentration of any individual *c*-type cytochrome. This conclusion is supported by the comparison of EPR spectra presented in this study.

A comparison of membrane-associated heme A, B, and C from cell expressing the pMMO or sMMO indicates that there is no significant change in the concentration of these hemes in response to copper availability (Zahn and DiSpirito, 1996). EPR spectra indicate a significant increase in the concentration of a type 2 copper signal and a previously uncharacterized g = 6.0 signal. Since no increase in the concentration of heme is observed in the switch-over event, these results suggest that the g = 6.0 signal arises from a membrane-associated non-heme species. Nguyen et al., (1994) and Chan, et al., (1994) have reported that the switch-over event from sMMO to pMMO in *M. capsulatus* Bath is accompanied by an increase in the concentration of membrane-associated copper and iron as analyzed by elemental analysis. Although copper resonances were detected and were

presumed to be associated with the pMMO, no EPR signals were detected to support the observed increase in iron. The authors attributed the increase in iron to an increase in the expression of a membrane-associated cytochrome *c*-557; however, no data was given to support this conclusion. Immunoblot analysis of *M. capsulatus* Bath cell extracts from cells expressing the sMMO or pMMO with antibodies against cytochrome *c*-557/cytochrome aa_3 shows that neither cytochrome *c*-557 nor cytochrome oxidase is responsible for the increase in membrane-associated iron. Furthermore, these results suggest that cytochrome *c*-557 and cytochrome aa_3 are constitutively expressed in *M. capsulatus* Bath with respect to copper availability. This observation is supported by quantitative estimates of heme A in membrane fractions by the pyridine ferrohemochromagen assay and analysis of non-covalently bound heme by RP-HPLC. This result suggests that cytochrome oxidase has no specialized role in the oxidation of methane by either the pMMO or sMMO.

Based on previously reported data showing an increase in the concentration of membrane-associated iron, we suggest the origin of the g = 6.0 as being a non-heme iron center. We have confirmed the presence of a non-heme iron center as the prosthetic group in the purified pMMO (Zahn and DiSpirito, 1996). Due to the major differences in cell ultrastructure between cells expressing the pMMO and sMMO, these results, based on a per mg protein ratio, may greatly under-estimate the increase of respiratory/electron transfer polypeptides in the membrane fraction of *M. capsulatus* Bath cells expressing the pMMO. The increase in the intracytoplasmic membranes associated with the pMMO is expected to greatly increase the surface area of the cytoplasmic membranes exposed to both the

periplasm and cytoplasm and additionally, to increase the total protein concentration of the cytoplasmic membranes as compared to the cytoplasmic membranes found in *M. capsulatus* Bath cells expressing the sMMO. In this model, a comparison of respiratory/electron transfer polypeptides based on a per mg protein ratio between these cell types would not sufficiently account for biochemical changes associated with the switch-over event.

Finally, since cytochrome oxidase demonstrates constitutive expression with respect to MMO expression and the adventitious association of copper with purified enzymes is decreased with cells grown under low copper conditions, the membrane fraction isolated from cells expressing the sMMO would most likely serve as a more desirable source of cytochrome oxidase for future studies of this enzyme.

Acknowledgments

This work was supported by the Iowa State University Office of Biotechnology (ADS) and an Iowa State University Professional Advancement Grant (JAZ).

Literature Cited

Anthony C. (1982) The biochemistry of methylotrophs. Academic Press. Inc. New York.

Baldwin, M.A., R. Wang, K.-M. Pan, R. Hecker, N. Stahl, B.T. Chait and S.B., Prusiner (1993) Matrix-assisted laser desorption/ionization mass spectrometry of membrane proteins: the scrapie prion protein. Tech. Protein Chem. 9: 41-45.

Berry, E.A., and B.L. Trumphower (1987) Simultaneous determination of hemes *a*, *b*, and *c* from pyridine hemochrome spectra. Anal. Biochem. 161: 1-15.

Brusseau G.A., H.-C. Tsien , R.S. Hanson, and L.P. Wackett (1990) Optimization of trichloroethylene oxidation by methanotrophs and the use of colorimetric

assay to detect soluble methane monooxygenase activity. Biodegradation 1: 19-29.

Chan, S.I., Nguyen, H.T., Shiemke, A.K., and M.E. Lidstrom (1993) Biochemical and biophysical studies toward characterization of the membrane-associated methane monooxygenase. *In.* Microbial Growth on C_1 Compounds (JC Murrell & DP Kelly, eds) Intercept Ltd., Hampshire, UK.

Dalton H., Prior S.D., and S.H. Stanley (1984) Regulation and control of methane monooxygenase. *In*: R.L. Crawford and R.S. Hanson (eds) Microbial Growth on C_1 Compounds, (pp. 75-82) American Society for Microbiology Press, Washington, DC

DeVries, G.E., U. Kues, and U. Stahl (1990) Physiology and genetics of methylotrophic bacteria. FEMS Microbiol. Rev. 75: 57-102

DiSpirito A.A. (1990) Soluble cytochromes *c* from *Methylomonas* A4. Meth. Enzymol. 188: 289 - 297

DiSpirito A.A., Gulledge J.A., Shiemke A.K., Murrell J.C., Lidstrom M.E., and C.L. Krema (1992) Trichloroethylene oxidation by the membrane-associated methane monooxygenase in type I, type II and type X methanotrophs. Biodegradation 2: 151 -164

DiSpirito, A.A., A.K. Shiemke, S.W. Jordan, J.A. Zahn, and C.L. Krema. (1994) Cytochrome *aa*3 from *Methylococcus capsulatus* Bath. Arch. Microbiol. 161: 258 - 265.

Drummond D., Smith S. and H. Dalton (1989) Solublization of methane monooxygenase from *Methylococcus capsulatus* (Bath). Eur.J.Biochem. 182: 667-671

Fox, B.G., W.A. Froland, and J.D. Lipscomb (1991) Biochemistry of the bacterial oxidation of methane. Annal. Rev. Microbiol. *in press.*

Fuhrhop, J-H (1975) Laboratory method in porphyrin and metalloporphyrin research. Elsevier Scientific Publishers, New York

Green J., and H. Dalton (1985) Protein B of soluble methane monooxygenase from *Methylococcus capsulatus* (Bath). A novel regulatory protein of enzyme activity. J.Biol.Chem. 260: 15795-15802

Green J., and H. Dalton (1989) Substrate specificity of soluble methane monooxygenase: mechanistic implication. J.Biol.Chem. 264: 17698-17703

Laemmli U.K. (1970) Cleavage of structural proteins during the assembly of the head of bacteriophage T4. Nature (London) 227: 680 - 685

Lidstrom, M.E. (1988) Isolation and characterization of marine methanotrophs. Ant.v. Leew. J. Microbiol. Serol 54: 189 - 199

Lidstrom, M.E., and J.D. Semrau (1995) Metals in Microbiology: The influence of copper on methane oxidation, *In* Aquatic Chemistry, American Chemical Society

Lowry, O.H., Rosebrough N.J., Farr A.L., and R.J. Randall (1951) Protein measurement with the Folin phenol reagent. J. Biol. Chem. 193: 265 - 275

McDonnel A., and L.A. Staehelin (1981) Detection of cytochrome *f*. a *c*-class cytochrome, with diaminobenzidine in polyacrylamide gels. Anal.Biochem. 117: 40 - 44

Nguyen, H-HT., A.K. Shiemke, S.J. Jacobs, B.J. Hales, Lidstrom, M.E., and S.I. Chan (1994) The nature of the copper ions in the membranes containing the particulate methane monooxygenase from *Methylococcus capsulatus* Bath. J. Biol. Chem. 269: 14995-15005

Patel R.N., and J.C. Savas (1987) Purification and properties of the hydroxylase component of methane monooxygenase. J.Bacteriol. 169: 2313-2317

Pilkington S.J., and H. Dalton (1991) Purification and characterization of the soluble methane monooxygenase from *Methylosinus trichosporium* demonstrates the highly conserved nature of this enzyme in methanotrophs. FEMS Microbiol. Lett. 78: 103-108

Prior S.D., and H. Dalton (1985) The effect of copper ions on membrane content and methane monooxygenase activity in methanol-grown cells of *Methylococcus capsulatus* (Bath). J.Gen.Microbiol. 131: 155-163

Scott D., Brannan J., and I.J. Higgins (1981) The effect of growth conditions on intracytoplasmic membranes and methane monooxygenase activities in *Methylosinus trichosporium* OB3b. J. Gen. Microbiol. 125: 63-72

Stainethorp A.C., Salmond G.P.C., Dalton H., and J.D. Murrell (1990) Screening of obligate methanotrophs for soluble methane monooxygenase genes. FEMS Microbiol.Lett. 70: 211-216

Stanley S.H., Prior S.D., Leak D.J., and H. Dalton (1983) Copper stress underlies the fundamental change in intracellular location of methane mono-oxygenase

in methane-oxidizing organisms: studies in batch and continuous cultures. Biotechnol. Lett. 5: 487-492

Stirling D.I., Colby J., and H. Dalton (1979) A comparison of the substrate and electron-donor specificity of the methane mono-oxygenase from three strains of methane-oxidizing bacteria. Biochem.J. 177: 362-364

Whittenbury R., Phillips K.C., and J.F. Wilkinson (1970) Enrichment, isolation, and some properties of methane utilizing bacteria. J.Gen. Microbiol. 61: 205 - 218.

Whittenbury R., and H. Dalton (1981) The methylotrophic bacteria. *In.* M.P.Starr, H.G. Truper, A. Balows, and H.G. Schlegel (eds) The Prokaryotes, Vol.I (pp 894-902) Springer-Verlag, New York

Woodland M.P., and H. Dalton (1984) Purification and characterization of component A of the methane monooxygenase from *Methylococcus capsulatus* Bath. J.Biol.Chem. 259:53-60

Zahn J.A., C. Duncan, and A.A. DiSpirito (1994) Oxidation of hydroxylamine by cytochrome P-460 of the obligate methylotroph *Methylococcus capsulatus* Bath. J. Bacteriol. 176: 5879 - 5887.

Zahn J.A., and A.A. DiSpirito (1996) Membrane-associated methane monooxygenase from *Methylococcus capsulatus* Bath. 178: 1018-1029

CHAPTER 4. OXIDATION OF HYDROXYLAMINE BY CYTOCHROME P-460 OF THE OBLIGATE METHYLOTROPH *Methylococcus capsulatus* Bath

A paper published in the Journal of Bacteriology[3]

James A. Zahn , Christy Duncan and Alan A.DiSpirito

ABSTRACT

The enzyme responsible for the oxidation of hydroxylamine to nitrite was isolated from the obligate methylotroph, *Methylococcus capsulatus* Bath. Absorption spectra in cell free extracts, electron paramagnetic resonance spectra, molecular weight, covalent attachment of heme group to polypeptide, and enzymatic activities suggest that the enzyme is similar to cytochrome P-460, a novel iron-containing protein previously observed only in *Nitrosomonas europaea*. The native and subunit molecular masses of the *M. capsulatus* Bath protein were 38,900 and 16,800 Da, respectively; the isoelectric point was 6.98. The enzyme has approximately one iron and one copper atom per subunit. The electron paramagnetic resonance spectrum of the protein showed evidence for a high spin ferric heme. In contrast to the enzyme from *N.europaea*, a 13 nm blue shift in the soret band of the ferrocytochrome (463 nm in cell extracts to 450 nm in the final sample) occurred during purification. The amino acid composition and *N*-terminal amino acid sequence of the enzyme from *M.capsulatus* Bath was similar, but not identical to cytochrome P-460 of *N.europaea*.

---

[3] Reprinted with permission from the Journal of Bacteriology, **176**, 5879-5887.

In cell-free extracts, the identity of the biological electron acceptor is as yet unestablished. Cytochrome *c*-555 is able to accept electrons from cytochrome P-460, although the purified enzyme required phenazine methosulfate (PMS) for maximum hydroxylamine oxidation activity (specific activity 366 mol. O_2/sec•mol enzyme). With PMS as the electron acceptor, the purified enzyme could account for hydroxylamine oxidase activity *in vivo*. Hydroxylamine oxidation rates were stimulated approximately 2-fold by 1mM cyanide and 1.5 fold by 0.1mM 8-hydroxyquinoline.

Key Words: Methanotrophs, methylotroph, *Methylococcus capsulatus* Bath, nitrification, cytochrome P-460, cytochrome *c'*, cytochrome P-450, hydroxylamine oxidoreductase.

Abbreviations: Tris, Tris[hydroxymethyl]aminomethane; HAO, hydroxylamine oxidoreductase; PMS, phenazine methosulfate; SDS, sodium dodecyl sulfate; DEAE, diethylaminoethyl; MMO, methane monooxygenase; sMMO, soluble methane monooxygenase; pMMO, membrane-associated methane monooxygenase; AMO, ammonia monooxygenase.

INTRODUCTION

Methanotrophs and ammonia oxidizing bacteria show a number of morphological, physiological, and biochemical similarities (7). Both groups of bacteria have been shown to oxidize a variety of non-growth substrates, including alkanes, alkenes, carbon monoxide, and halogenated hydrocarbons as well as methane and ammonia (4, 7, 11, 13, 17, 29, 30, 31, 32, 33, 48, 62, 64, 66). In

methanotrophs, as in the nitrifiers, the oxidation of ammonia is a two step process (Fig. 1). The first step is the energy-dependent oxidation of ammonia to hydroxylamine, catalyzed by the methane monooxygenase (MMO) (11,13). Both forms of the MMO, soluble MMO (sMMO) and membrane associated MMO (pMMO), have been shown to catalyze this reaction (11, 13, 49, 60). The second step involves the four electron oxidation of hydroxylamine to nitrite (13, 57). Little is known concerning the enzyme catalyzing this reaction. In cell free extracts, hydroxylamine oxidation rates are stimulated by cyanide, 8-hydroxyquinoline, and phenazine methosulfate (13). Inhibitor and cell fractionation activities have shown hydroxylamine oxidation activity is separate from MMO and methanol dehydrogenase activities (13, 57). This activity has been partially purified from *Methylococcus thermophilus* and identified as a hydroxylamine oxidoreductase-like enzyme, although no evidence was given for this conclusion (57).

In ammonia oxidizing bacteria, two different enzymes have been found which oxidize hydroxylamine to nitrite, hydroxylamine oxidoreductase (HAO) and cytochrome P-460 (20, 23,46). HAO is the periplasmic enzyme responsible for the energy yielding step in ammonia oxidation (14, 23, 47, 68). The physiological role of cytochrome P-460 in nitrifiers has not been resolved, but may serve to protect the cell from this toxic and mutagenic intermediate (Hooper, personal communication). Both enzymes contain a novel chromophore with an absorption maximum at 463 nm (2, 3, 20, 23,43). In *Nitrosomonas europaea*, 95% of the chromophore absorbing at 463 nm is associated with hydroxylamine oxidoreductase (20). Each subunit of HAO contains 7 *c*-type hemes and one P-460 heme group (5). Arciero et al. (6) have recently determined the structure of heme P-460 in HAO to be an iron

FIG. 1. Proposed mechanism of ammonia oxidation by methanotrophs. Abbreviations: sMMO, soluble methane monooxygenase; pMMO, membrane-associated methane monooxygenase.

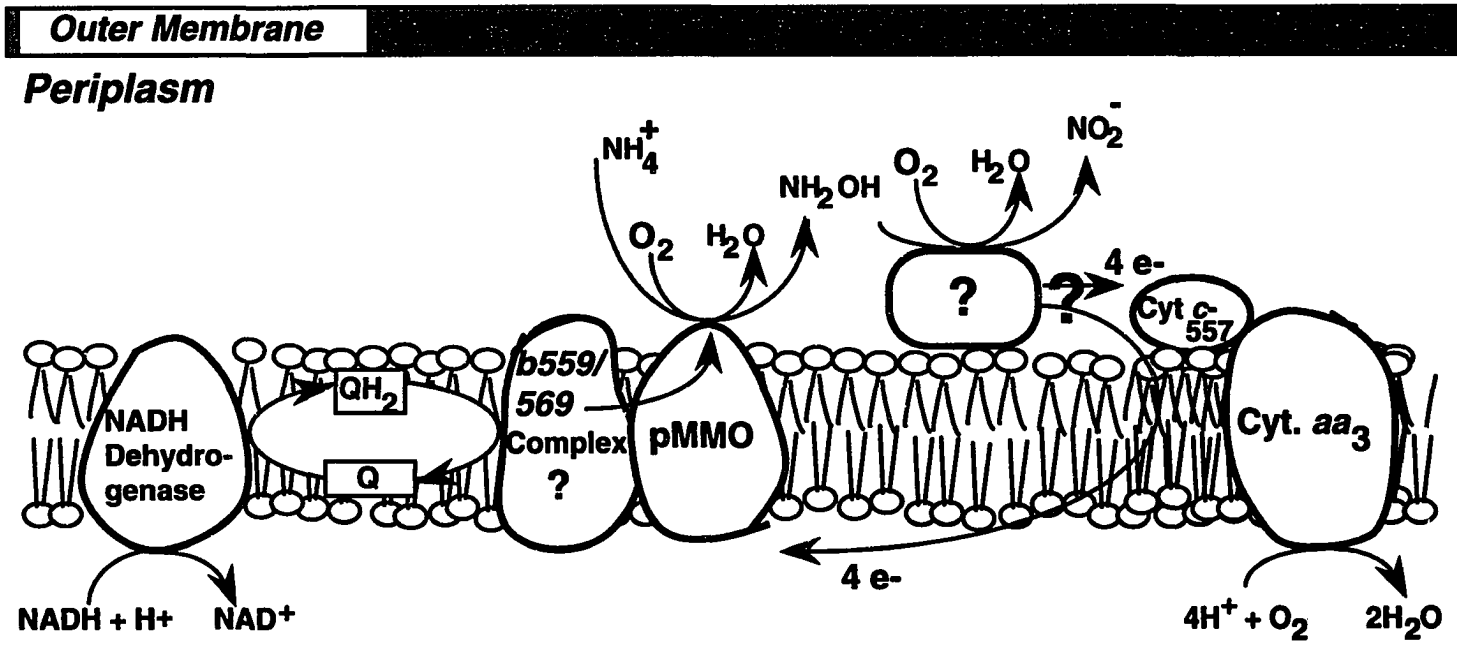
Outer Membrane
Periplasm
NH_4^+
NO_2^-
NH_2OH
O_2
H_2O
O_2
H_2O
?
?
4 e-
Cyt c_{557}
NADH Dehydro-genase
QH_2
Q
b559/ 569 Complex
?
pMMO
Cyt. aa_3
4 e-
NADH + H+
NAD^+
$4H^+ + O_2$
$2H_2O$

protoporphyrin IX bound to the peptide by two thioether bridges and by a covalent bond between a meso heme carbon and an aromatic ring carbon on a tyrosyl-residue. All available evidence indicates the P-460 heme of HAO is involved in the catalytic function of the enzyme (25). During hydroxylamine oxidation, electrons pass from hydroxylamine though the P-460 chromophore to the *c*-hemes of HAO (6, 25, 27, 28).

The second chromophore with an absorbance at 463 nm in *N.europaea* is associated with a low molecular weight (M_r 17,000 - 18,400) protein called cytochrome P-460 (20). Initially believed to be a solubilized heme P-460-containing fragment of HAO and called the "P460 fragment," cytochrome P-460 has been shown to be a different polypeptide from HAO (41, 53). The absorption maximum of the ferrocytochrome, resonance Raman spectroscopy, and hydroxylamine oxidation activity suggest the chromophore in cytochrome P-460 is structurally very similar to heme P-460 in HAO (3). In addition, as observed with the heme P-460 in HAO, the heme group is not extracted with acid acetone, ethyl acetate, Ag_2SO_4, *o*-nitrophenylsulfenyl chloride or SDS-urea-mercaptoethanol which suggests additional covalent linkages beyond thioether bonds (6, 20, 46). However, other spectral evidence (Mössbauer, EPR and optical) and redox properties have indicated structural differences in the chromophore in HAO and cytochrome P-460 (2, 6, 12, 38). The structure of the 463 nm chromophore in cytochrome P-460 has not been determined.

The present report describes the first purification of a hydroxylamine oxidizing enzyme from a methylotroph. The enzyme is similar, but not identical to cytochrome

P-460 from *N. europaea*. It describes a purification procedure, molecular weight, subunit composition, metal composition, N-terminal amino acid sequence, optical absorption and electron paramagnetic resonance spectra. The electron donor and acceptor specificity of the enzyme are also considered.

MATERIALS AND METHODS

Culture conditions. *Methylococcus capsulatus* Bath was grown in nitrate mineral salts media (67) plus 5μM $CuSO_4$, and a vitamin mixture (37) at 37°C under an atmosphere of 40% methane and 60% (vol/vol) air. Cells growth in a 12-liter fermentor were sparged at flow rates of 80 to 150 ml/minute methane and 2000 to 2500 ml/minute air at 42°C. Cells were harvested by centrifugation at 13,000 x g for 15 minutes at 4°C, resuspended (1:5 w/v) in a buffer containing 10 mM Tris-HCl (pH 8.2) (Buffer A), and centrifuged at 13,000 x g for 15 minutes at 4°C. The cell pellet was resuspended (1:1 w/v) in buffer A containing 1μg/ml deoxyribonuclease (Sigma), frozen in liquid nitrogen, and stored at -80° C.

Isolation of Cytochrome P-460. All procedures were performed at 4°C. Freeze-thawed cells were passed through a French pressure cell three times at 15,000 lb/in^2. The cell suspension was centrifuged at 13,000 x g for 15 minutes to remove unlysed cells and debris. The supernate (cell extract) was centrifuged at 155,000 x g for 1.5 hours. The supernate (soluble fraction I) was saved and the pellet resuspended with a Dounce homognizer in buffer A and 500 mM KCl. The sample was centrifuged at 155,000 x g for 1.5 hours, and the supernate (soluble fraction II) pooled with soluble fraction I. The combined soluble fractions were

dialyzed for 6 hours against 3 changes of buffer A and loaded on a 5.0 x 30 cm DEAE-cellulose column equilibrated with buffer A. The sample did not bind to DEAE-cellulose and eluted with buffer A. This fraction was brought to 40% saturation with ammonium sulfate, stirred for 1 hour, and centrifuged at 13,000 x g for 30 minutes. The pellet was discarded, and the concentration of ammonium sulfate in the supernatant raised to 60% saturation. The solution was then stirred for 1 hour and centrifuged at 13,000 x g for 30 minutes. The pellet (40 - 60% ammonium sulfate fraction) was resuspended in a minimal volume of buffer A, and dialyzed against three changes of buffer A. Following dialysis, the sample was concentrated on a stirred cell (YM10 filter) and loaded on a preparative isoelectric focusing bed (15 x 30 cm) containing 4% Ultrodex and 2% ampholyte (pH 5-8) and electrophoresed for 16 hours at 4°C. The cytochrome P-460 fraction appeared as a green band focusing at pH 6.98. The band was eluted from the Ultradex with buffer A, concentrated with a stirred cell (YM-10 filter) and loaded a 2.5 x 96 cm Sephadex G-75 column equilibrated with 25 mM Tris-HCl (pH 8.2), 100 mM KCl buffer (buffer B). The 25,000 to 45,000 Da fractions were pooled, and loaded on a 1.25 x 20 cm Phenyl-Sepharose CL-4B column equilibrated with buffer B. The sample was washed with 2 bed volumes of buffer B and eluted with 10 mM Tris-HCl, 25 mM KCl buffer (pH 8.2) buffer. The sample was dialyzed with 3 changes of buffer A, then loaded on a DEAE-Sepharose CL-6B column (1.25 x 60 cm) equilibrated with buffer A. Cytochrome P-460 appeared as an intense green band on the top of the column. The column was washed with 4 bed volumes of buffer A and the purified cytochrome P-460 slowly eluted with approximately 4 bed volumes of 10 mM Tris-HCl (pH 8.2), 25 mM KCl buffer. The sample was concentrated with a stirred cell (YM10 filter) and

dodecyl-β-D- maltoside or dodecyl-β-D-glycopyranoside added to a final concentration of 100 μM.

Electrophoresis. Sodium dodecyl sulfate (SDS)-polyacrylamide slab gel electrophoresis was carried out by the Laemmli method on 10 to 16% gels (36). Gels were stained for total protein with Coomassie brilliant blue R, or by the silver stain method of Nielsen and Brown (44). Proteins with peroxidative activity in SDS-polyacrylamide gels were stained by the diaminobenzidine method (40).

Mass spectrometry. Molecular mass of cytochrome P-460 was determined by time of flight mass spectrometry on a Kratos MALDI (Matrix Assisted Laser Desorption Ionization) III mass spectrometer using a sinapinic acid matrix, and a laser power setting of 39 (Kratos Analytical, Ramsey NJ).

Enzyme Activity. Whole cell ammonia oxidation was measured by the rate of oxygen utilization (Clark oxygen electrode, Yellow Springs, Ohio) or nitrite production at 37°C. Reaction mixtures contained 1 to 5 mg cell protein, 2 mM ammonium sulfate, 5 mM sodium formate in 10 mM Tris-HCl buffer, pH 8.0. The electrode was calibrated by the method of Robinson and Cooper (51). Nitrite was determined by the sulphanilamide/*N*-(1-naphthyl) ethylene diamine hydrochloride method of Nicholas and Nason (45) and measured at 540 nm. Spectral assays were performed on 1 ml samples containing 5 mM hydroxylamine hydrochloride (pH 8), 10 mM Tris (pH 8), approximately 50 μg sample protein. Reactions were initiated by the addition of PMS, cytochrome *c*-555, cytochrome *c*-557, and/or cytochrome *c'* from *M.capsulatus* Bath.

Hydroxylamine oxidation was measured as the rate of oxygen utilization or nitrite production in the presence of phenazine methylsulfate as described by Dalton

(13). Assays were run in 10 mM Tris-HCl buffer, pH 8.0, or 10 mM NaK-phosphate buffer, pH 7.0, containing 5 mM hydroxylamine and 100 μM PMS or one or more of the soluble ferricytochromes from *M.capsulatus* Bath; cytochrome *c*-555, cytochrome *c'* or cytochrome *c*-557.

Spectroscopy. Optical absorption spectroscopy was performed with an SLM Aminco DW-2000 spectrophotometer in the split-beam mode.

Electron paramagnetic resonance spectra were recorded at X-band on a Bruker ER 200D EPR spectrometer equipped with an Oxford Instruments ESR-900 liquid helium cryostat. Operating parameters were as follows: modulation frequency 100 kHz, modulation amplitude 4 G, microwave frequency 9.422 GHz, time constant 100 ms, and sweep time 50 seconds. Samples were maintained at 8°K during spectral acquisition.

Heme and Protein Determination. The optical extinction coefficient values for cytochrome P-460 were quantified using absorption maximum of the soret band and protein determinations by the Lowry method (39) using bovine serum albumin as a standard. Heme composition was determined from the pyridine ferrohemochrome method (15). The acid acetone method was used to determine covalent linkage of the prosthetic groups to the polypeptide (21).

Metal Analysis. Protein samples were dialyzed for 18 hours against five changes of 5 mM NaEDTA. Protein (10 - 25 nmol) samples were analyzed for zinc, copper and iron using a Perkin Elmer model 5100 graphite furnace atomic absorption spectrophotometer.

Amino Acid Sequence and Analysis. Amino acid analysis was carried out with an Applied Biosystems 420A derivatizer coupled to an Applied Biosystems 130A separation system. Samples were hydrolyzed in 6 M HCl plus trace amounts of phenol in HCl vapors for 1 h, then in a vacuum at 150°C. After hydrolysis, norleucine was added as an internal standard.

The N-terminal amino acid sequence of cytochrome P-460 was analyzed by Edmond degradation on a Applied Biosystems 477A protein sequencer/120A analyzer.

Other Methods. Tetraacetyl-α-D-glucopyranosyl bromide was synthesized by the method of Jeremias et al. (34) and used in the synthesis of dodecyl-β-D-glycopyranoside. Dodecyl-β-D-glycopyranoside was synthesized as described previously (65).

Cytochrome cytochrome *c*-557 was isolated by the method of DiSpirito *et al.*, (18).

Cytochrome *c'* was separated from cytochrome P-450 on the 1.52 x 20 cm Phenyl-Sepharose CL-4B column (see isolation of cytochrome P-460). Cytochrome *c'* remained bound to the column as a visible brown-red band following elution of cytochrome P-460 and was eluted with 6 column volumes of buffer A. This fraction was electrophoretically homogenous, and had an apparent molecular mass of 16,700 Da on SDS-polyacrylamide gels and a pI of 7.0. The optical spectra and ligand binding properties of cytochrome *c'* were similar to other *c'*-type cytochromes (35, 42, 54).

Cytochrome *c*-554 was isolated from the soluble cell fraction by precipitation with ammonium sulfate using a 50-70% saturation. The pellet was resuspended in a

minimual volume of buffer A, and dialyzed against three changes of buffer A. Following dialysis, the sample was concentrated by ultrafiltration and loaded on a preparative isoelectric focusing bed using 4% Ultradex (Pharmacia) and 2% ampholine (pH 3.5-10) and electrophoresed for 16 hours at 4°C. Cytochrome *c*-554 appeared as a light pink band with a pI of 8.83. The cytochrome migrated on SDS-denaturing gels with an apparent molecular mass of 10.7 kDa and had a dithionite-reduced α-maximum at 553.7 nm.

Cytochrome *c*-555 was isolated from the soluble 70% ammonium sulfate fraction as described previously in the isolation of cytochrome *c*-554. The sample was applied to a phenyl sepharose column (2.5 x 20 cm) equilibrated in 70% ammonium sulfate and washed with 1 column volume of 70% ammonium sulfate. Cytochrome *c*-555 was eluted from the column with 6 column volumes of 35% ammonium sulfate and was dialized against three changes of buffer A. Cytochrome *c*-555 migrated on SDS-denaturing gels with an apparent molecular mass of 14.1 kDa and had a dithionite-reduced α-maximum at 555.4 nm.

RESULTS

Purification. Hydroxylamine oxidation activity in cells lysed in 10 mM Tris-HCl was distributed evenly between the soluble and membrane fractions. A high salt wash (500 mM KCl) was required to solubilize the membrane-associated activity. Lower salt washes of 10 mM Tris-HCl buffers containing 100 or 250 mM KCl only solublized a small fraction of the membrane-associated hydroxylamine oxidation activity. Once solublized, the cytochrome P-460 in the soluble fraction and in the sample solubilized in the high salt washes behaved similarly during purification.

FIG. 2. SDS-polyacrylamide slab gel electrophoresis of (*Lane A*) molecular mass standards, 92, 66.2, 45, 31, 21.5, and 14.4 kDa; (*Lanes B and D*) following chromatography on Phenyl Sepharose (8.3 µg protein); (*Lanes C and E*) purified cytochrome P-460 (2.8 µg protein); and heme-stained standards (*Lane F*): Cytochrome *c'* 16.7 kDa (2.5 µg protein); Cytochrome *c*-555 14.1 kDa (1.7 µg protein); and Cytochrome *c*-554 10.7 kDa (2.0 µg protein). Lanes A through C are stained with Coomassie blue R-250 and lanes D through F are stained with diaminobenzidine.

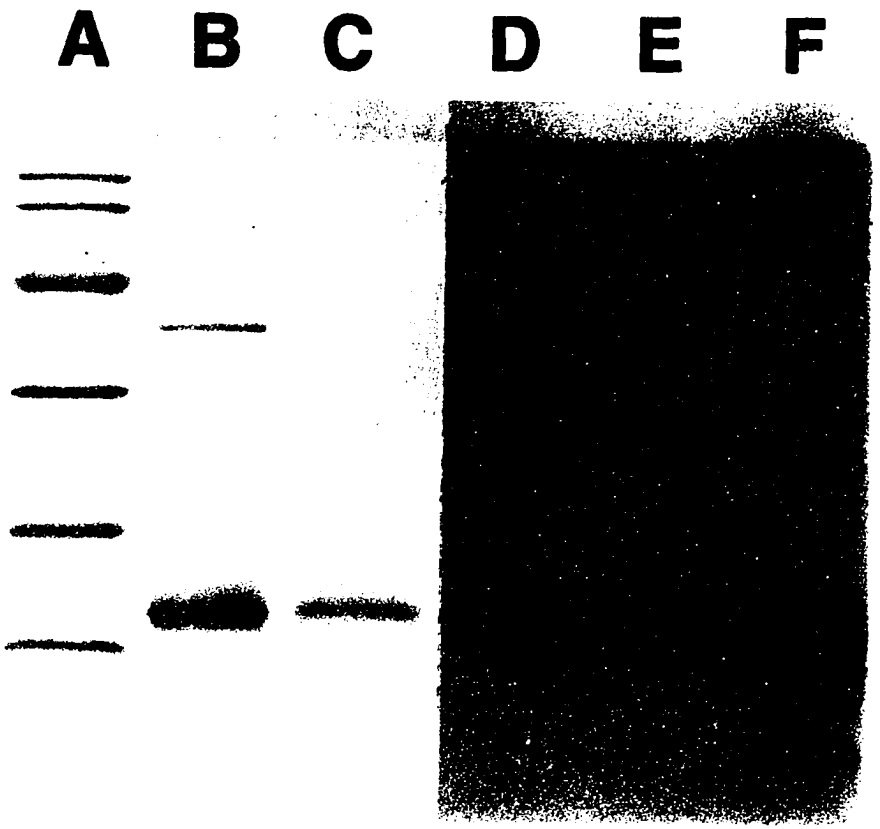
A
B
C
D
E
F

An unusual feature of the purification was a 13 nm blue shift in absorption maxima of the soret band of ferrocytochrome P-460 during the final purification steps (Table 1). The major spectral shift (463 nm to 452) was observed following gel filtration on Sephadex G-75 (Table 1). Electrophoretic and spectral analysis of proteins separated at this step indicated the separation of two minor polypeptides with subunit molecular mass of 61,200, and 39,700 Da, a peroxidase-staining heat-labile 47,000 Da polypeptide, and cytochrome *c'* (M_r 16,700 Da) from cytochrome P-460. The 47,000 Da polypeptide stained positive with diaminobenzidine (Fig. 2). When together on SDS-denaturing gels, cytochrome *c'* could not be distinguished from cytochrome P-460. The concentration of cytochrome *c'* in these samples was estimated from absorption and EPR spectra.

In an attempt to stabilize the spectral characteristics of cytochrome P-460, four different purification procedures were developed. The results from the different purification procedures associated the spectral shifts with the separation of cytochrome *c'* and the 47,000 Da heme-staining polypeptide from cytochrome P-460. Reconstitution experiments using proteins separated at this step, alone and/or in different combinations, did not alter spectral or enzymatic properties of the cytochrome P-460. Although the isolated ferrocytochrome P-460 showed an absorption maxima at 450 nm we will refer to the sample as "cytochrome P-460" (see Discussion).

Cytochrome P-460 also became labile with the separation of cytochrome *c'* and the 47,000 Da polypeptide. The sample lost distinguishing spectral characteristics and PMS-dependent hydroxylamine oxidase activity within 48 hours

of purification. The spectral properties and enzyme activity in this sample could be stabilized by the addition of 100 μM dodecyl-β-D-maltoside or dodecyl-β-D-glucopyranoside to the purified cytochrome. However, separation of cytochrome *c'* from cytochrome P-460 resulted in a spectral shift in the soret band of the ferrocytochrome to 454 nm (results not shown).

Table 1. Isolation and purification of cytochrome P-460 from *M. capsulatus* Bath

Fraction	Protein		Absorption Maxima Shift		
	Total (mg)	%	Oxidized (nm)	Reduced (nm)	Reduced+CO (nm)
Cell Extract	24252	100	-	-	-
Soluble S-155K	16909	69.7	N.D.§	N.D.	N.D.
DEAE-Cellulose	9563	39.4	N.D.	N.D.	N.D.
40-60% $(NH_4)_2SO_4$	1649.6	6.8	N.D.	463	N.D.
Isoelectric Focusing (pH 3-10)	582	2.4	N.D.	461	442
Sephadex G-75	34.1	0.14	421	452	436
Phenyl Sepharose CL-4B	18.2	0.08	419	450	435
DEAE-Sepharose CL-6B	6.4	0.03	419	450	435

§ Not Detectable

Purified Triton X-100 (Boehringer Mannheim Biochemicals) was also tested as a stabilizing agent on cytochrome P-460, but this detergent caused a rapid loss of hydroxylamine oxidation activity and loss of the spectral properties of the enzyme.

Properties of cytochrome P-460. The properties of cytochrome P-460 are summarized in Tables 2 - 4.

Molecular Mass. The molecular mass of cytochrome P-460 was determined to be 38,900 ± 6,100 Da on a Sephadex G-75 column (2.5 x 96 cm). Reference proteins were horse heart cytochrome *c* (M_r 12,400), lysozyme (M_r 14,300), horse

FIG. 3. Absorption spectra of the cytochrome P-460 containing fraction from the preparative isoelectric focusing flat bed in 25 mM Tris-HCl, 100 mM KCl, buffer (pH 8.2). Absorption of the resting enzyme (·····) and following reduction with dithionite (———).

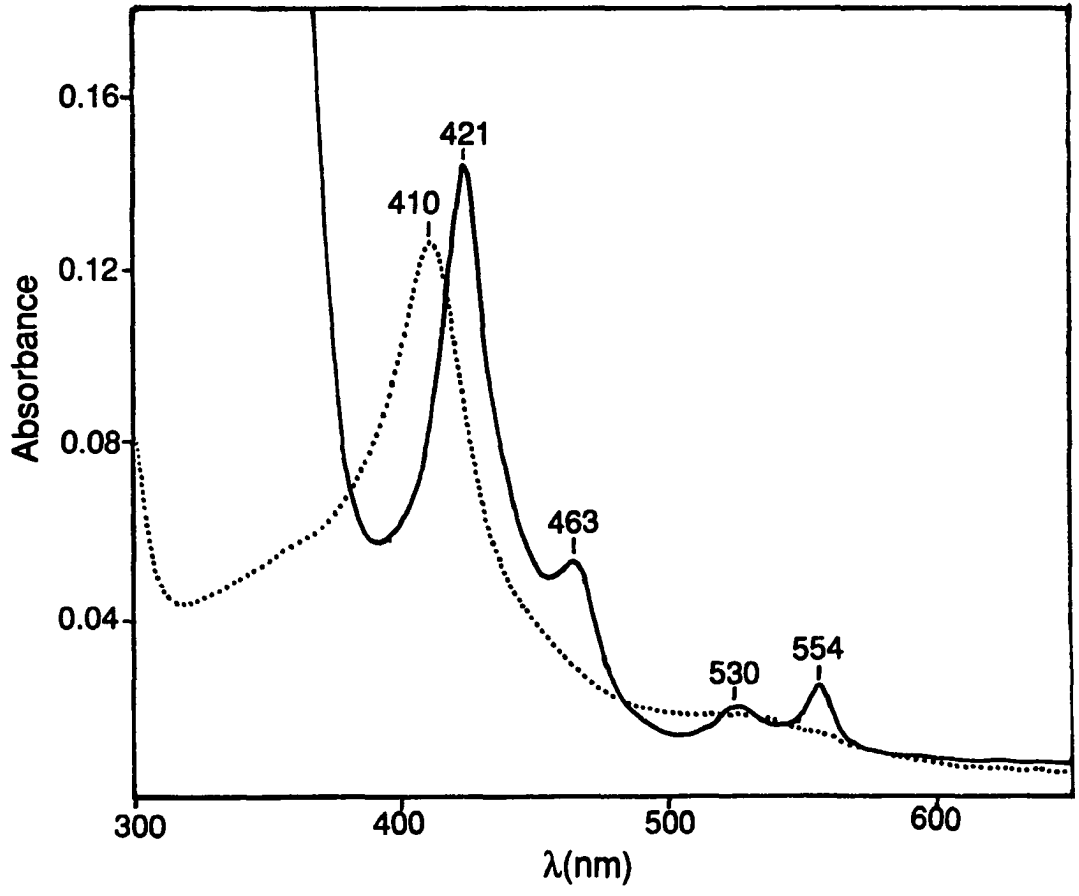
0.16
0.12
0.08
0.04
Absorbance
421
410
463
530
554
300
400
500
600
λ(nm)

heart myoglobin (M_r 18,800) carbonic anhydrase (M_r 29,000) and bovine hemoglobin (64,500). In sodium dodecyl sulfate (SDS)-polyacrylamide gels cytochrome P-460 migrated as a single band corresponding to a molecular mass of 16,800 ± 100 Da (Fig. 2). The results suggest the enzyme is a dimer composed of two identical subunits. The sample did not require β-mercaptoethanol nor heat treatments before loading on SDS-polyacrylamide gels for subunit separation (results not shown). Thus, the interaction between subunits appears to be non-covalent.

The molecular mass of the purified sample was also analyzed by mass spectroscopy and showed major M/z peaks at 16,391 ($[M + 1H]^+$) and 8,151 ($[M + 2H]^{2+}$) which were similar to the subunit molecular mass determined on SDS-polyacrylamide gel (Fig. 8).

Amino acid analysis and sequence. The minimum molecular mass determined from the amino acid composition and iron concentration was similar to that determined by SDS-polyacrylamide gels or by mass spectroscopy (Table 3).

The data presented in table 2 suggests that the cytochrome P-460 from *M.capsulatus* Bath is similar but not identical to the enzyme from *N. europaea.*

Heme and Metal Components. As reported for the cytochrome P-460 from *N. europaea* (20), the prosthetic group of cytochrome P-460 was not extracted with acid acetone. The heme also remained associated with the polypeptide in SDS-polyacrylamide gels in samples incubated in sample buffers containing 1.5% β-mercaptoethanol at room temperature, and stained weakly with diaminobenzidine (40). The absorption spectrum of the pyridine ferrohemochrome of cytochrome P-

460 was similar, but not identical to the enzyme from *N.europaea* with absorption maxima at 420, 528 and 556 nm (Table 4).

As determined by atomic absorption in conjunction with the Lowry protein procedure (39) using bovine serum albumin as a standard, the content of iron and copper of the purified enzyme was 51.2 and 51.4 nmol/mg protein, respectively. Based on the molecular mass as determined by SDS-gel electrophoresis (16,800 Da) or by mass spectroscopy (16,390) a protein containing 1 iron should have a metal content of 59.5 or 61 nmol/mg protein, respectively. The lower value of copper and iron/mg protein may be the result of extensive dialysis agents NaEDTA or that the Lowry method overestimates the protein content. Comparison of protein concentration by the Lowry method using bovine serum albumin as the standard and amino acid analysis indicates the Lowry method over estimates the protein concentration by a factor of 1.4. The *M. capsulatus* Bath enzyme contained less than 12 molar % zinc.

Spectral Properties. Cytochrome P-460 was first detected by absorption spectroscopy in the 40 - 60% ammonium sulfate fraction. As described by Sokolov et al. (57), the optical spectra of this fraction is similar to HAO (Fig. 3; 26), however, unlike HAO, the *c*-type cytochromes could be separated from cytochrome P-460.

The spectral properties of the dithionite reduced and reduced plus CO samples isolated in the presence of cytochrome *c'* and the 47,000 Da polypeptide were similar to the sample isolated from *N.europaea* (Fig 4; 46). The absorption maximum at 418 nm was associated with contaminating cytochrome *c'* in this sample. In the presence of these two polypeptides the resting spectrum of cytochrome P-460 showed a significant population in the ferrous form. Whether this

Table 2. N-terminal amino acid sequences of cytochrome P-460 from *M. capsulatus* Bath, cytochrome P-460 from *N. europaea* (46).

N.europaea Cytochrome P-460:	Ala-	Glu-	Val-	**Ala-**	Glu-	Phe-	**Asn-**	Asp-	**Ile-**	Gly
	1	2	3	4	5	6	7	8	9	10
M.capsulatus Bath Cytochrome P-460:	Glu-	Pro-	?	**-Ala-**	Ala-	Pro-	**Asn-**	Gly-	**Ile-**	Ser
	1	2	3	4	5	6	7	8	9	10

Table 3. Amino Acid Composition of *M. capsulatus* Bath cytochrome P-460.

Amino Acid	*M. capsulatus* Bath		*N. europaea*[a]	
	mol %	Residues (per Fe atom)	mol %	Residues (per Fe atom)
Asx	10.3	15	12.2	15
Ser	5.1	7	4.1	5
Glx	11.1	16	10.6	13
Pro	7.4	10	7.3	9
Gly	11.8	17	9.8	12
Ala	15.5	22	12.2	15
Cys	ND[b]	-	1.6	2
Val	5.7	8	6.5	8
Met	0.9	1	1.6	2
Ile	4.6	6	0.8	1
Leu	7.2	10	5.7	7
Tyr	0.8	1	4.1	5
Phe	3.6	5	4.9	6
His	2.1	3	1.6	2
Lys	7.4	10	7.3	9
Arg	2.9	4	3.3	4
Thr	3.6	5	6.5	8
Trp	ND	-	ND	-
Minimum molecular weight[c]	14,345		13,200	

[a]46

[b]not determined

[c]Based on iron concentration (assuming 1 iron/subunit)

FIG. 4. Absorption spectrum of the final step in the purification of cytochrome P-460 in the presence of dodecyl-β-D-glycopyranoside. Absorption of the resting enzyme (– – – –), following oxidation with ferricyanide (–·–·–·–), following reduction with dithionite (————), and dithionite reduced plus CO (·····).

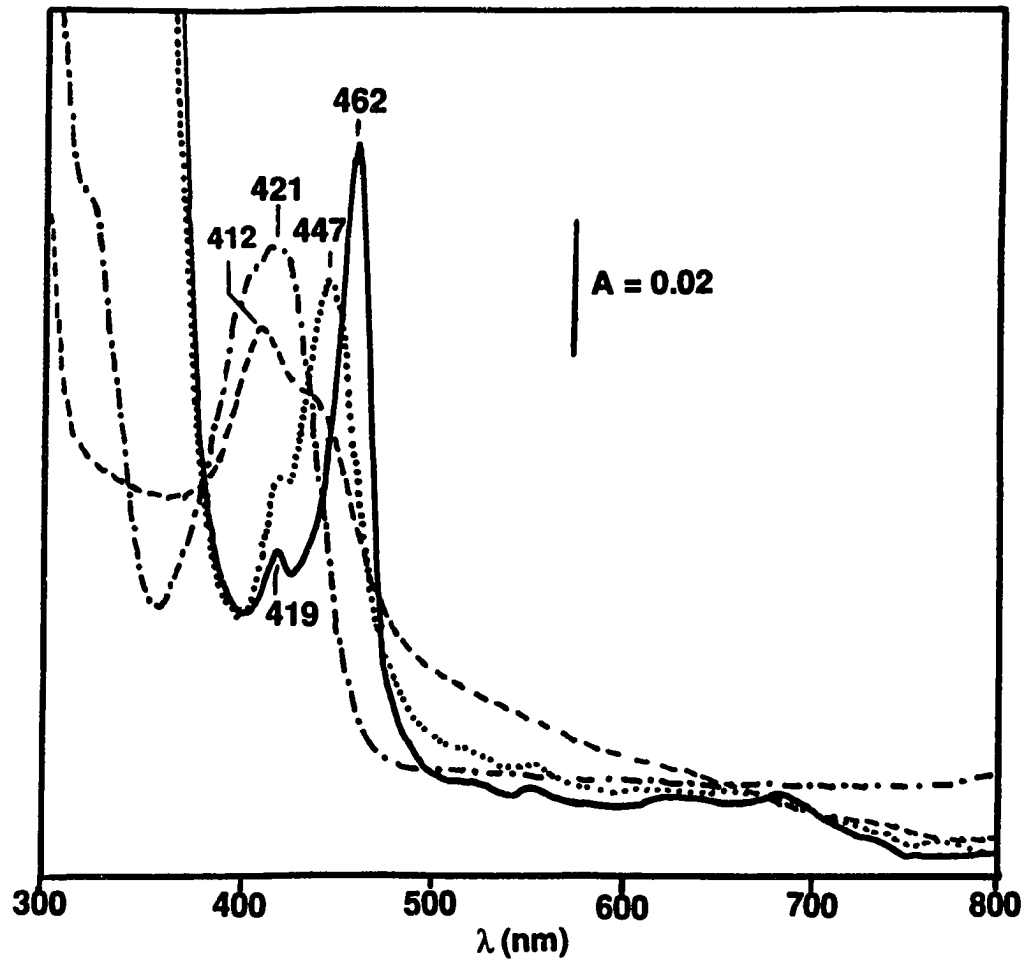
462
421
412
447
A = 0.02
419
300
400
500
600
700
800
λ (nm)

spectrum is the result of interactions between heme P-460 and the chromophores in the 47,000 Da polypeptide and cytochrome *c'*, or to a difference in the heme environment has not been determined.

Separation of the 47,000 Da polypeptide and cytochrome *c'* from cytochrome P-460 resulted in a 13 nm spectral shift in the soret band of the ferrocytochrome spectrum (Figs. 4 - 6). In the absence of dodecyl-β-D-maltoside or dodecyl-β-D-glycopyranoside, reduction of the purified sample by $Na_2S_2O_3$ in the presence of oxygen lowered the absorbance 70 - 80% compared to the absorbance observed under anaerobic conditions (data not shown). Reduction under anaerobic conditions or in the presence of dodecyl-β-D-maltoside or dodecyl-β-D-glycopyranoside protected the enzyme from destruction by $Na_2S_2O_3$ and O_2. The addition of carbon monoxide, cyanide or azide before addition of dithionite also protected the enzyme from the effects of $Na_2S_2O_3$ and O_2. Addition of KCN or NaN_3 to the resting enzyme resulted in a shift of the soret band to 435 and 432 nm, respectively. Reduction of KCN and NaN_3-treated cytochrome P-460 with $Na_2S_2O_3$ (in the presence of O_2) resulted in absorption maxima at 441 and 437 nm, respectively.

Addition of KCN or NaN_3 to cytochrome P-460 following reduction with dithionite in the presence of oxygen resulted in similar spectra, but the absorbance was 70 - 80% less than when the ligands were added before reduction (results not shown). The addition of CO to the resting enzyme had no effect on the spectrum, but protected the enzyme from the absorbance decrease resulting from reduction

Table 4. Properties of purified cytochrome P-460 from *M. capsulatus* Bath.

Property	*M.capsulatus* Bath	*N.europaea*
Molecular Mass		
Enzyme [a]	38,900 ± 6,100	36,000 - 60,000[b,c,d]
Subunit		
a. SDS-PAGE	16,800 ± 100	17,000 - 18,500[b,c,d]
b. mass spectrum	16,312	nd
c. Amino Acid Analysis	14,345	13,200
Isoelectric Point (pI)	6.98	n.d.[e]
Metal concentration (mol/mol enzyme[f])		
Fe	1.72	2.6[b]
Cu	1.72	nd[g]
Absorption Maxima (nm)		
Oxidized	419	435[c,d]
a. plus NaN_3	432	n.d.
b. plus KCN	435	447[d]
Reduced	450,653	460,688[d]
a. plus CO	435	448[d]
b. plus NaN_3	437	n.d.
c. plus KCN	441	455[b]
d. plus $NaNO_2$		454[a]
Ferrohemochromagen	420, 528, 556	433, 530, 560
Optical extinction coefficients (cm^{-1} mM^{-1})		
Reduced: 450 - 600 nm	54.5	nd
Resting : 419 - 600 nm	56.1	nd
EPR (*g* values)	6.19, 5.70, 2.0	5.92, 5.63, 1.99[a]
		6.15, 5.70, 2.0[h]
Hydroxylamine Oxidase[i]		
(mol O_2/sec/mol enzyme)	366[g]	6[j]
a. plus 1 mM CN	770	nd
b. plus 100 µM 8-HQ	514	nd

[a] Determined by gel filtration on Sephadex G-75. [b]46 ; [c]20; [d]2; [e]43; [f]assuming a molecular weight of 33,600 for the *M.capsulatus* Bath enzyme and 34,600 for the *N.europaea* enzyme; [h]38; [i] phenazine methosulfate as electron acceptor; [j] cytochrome *c*-552 as electron acceptor.

FIG. 5. Absorption spectrum of cytochrome P-460; 26 μg protein per ml, in 10 mM Tris-HCl (pH 8.2). Absorption of the resting enzyme (·····), dithionite reduced (———), and dithionite reduced plus CO (– – – –).

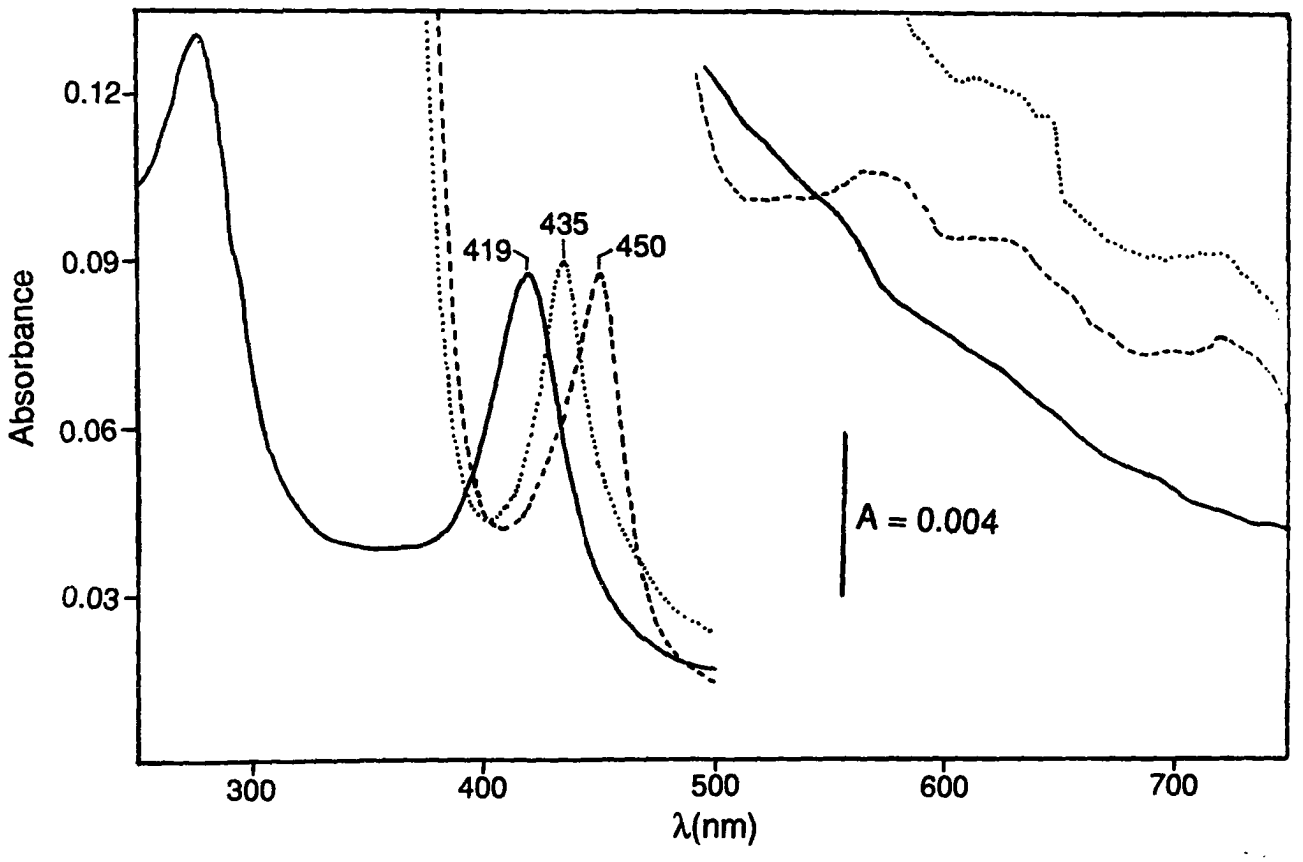
0.12
0.09
0.06
0.03
Absorbance
419
435
450
A = 0.004
300
400
500
600
700
λ(nm)

FIG. 6. Electron paramagnetic resonance spectrum of A) sample following chromatography on Phenyl Sepharose (84 μg protein) and B) purified cytochrome P-460 (180 μM) in 10 mM Tris-HCl (pH 8.2) at 8° K. Instrumental conditions were the following: modulation frequency 100 kHz, modulation amplitude 4 G, microwave frequency 9.422 GHz, time constant 100 ms.

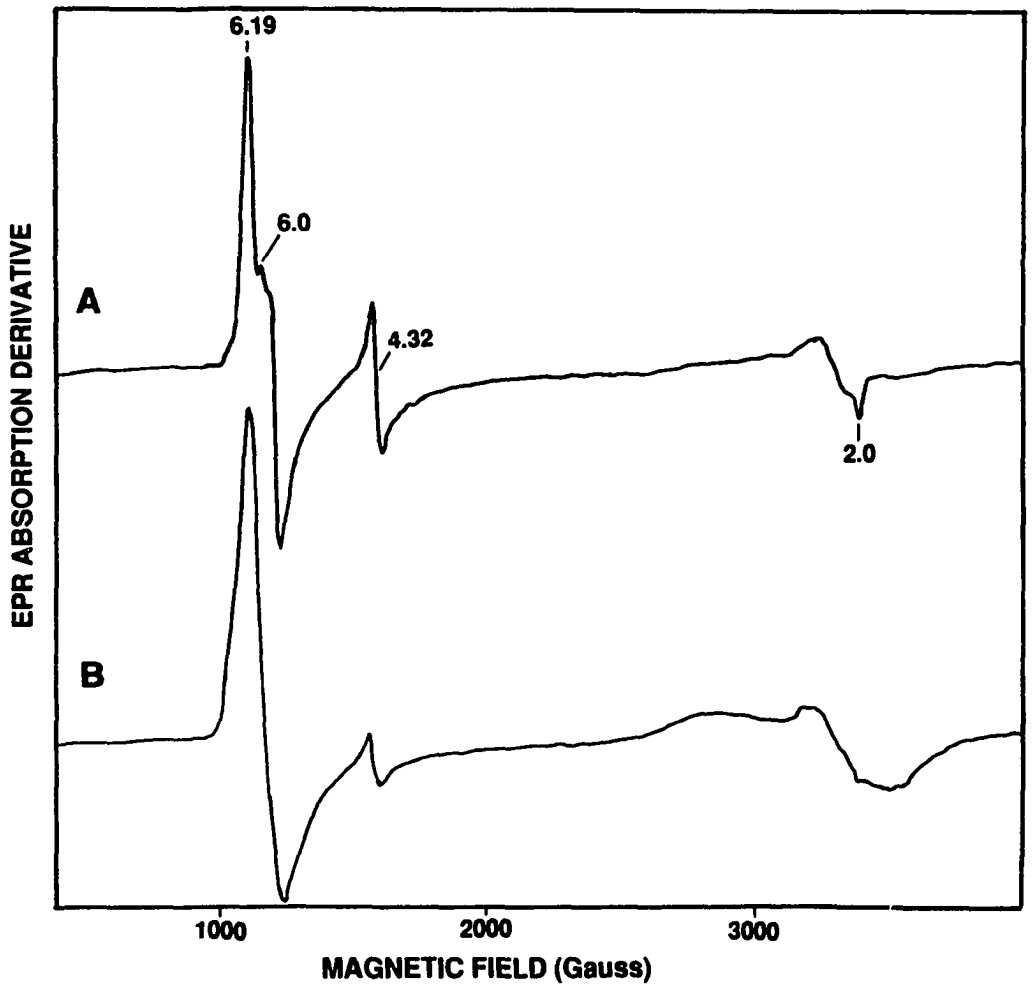
6.19
6.0
4.32
2.0
A
B
EPR ABSORPTION DERIVATIVE
1000
2000
3000
MAGNETIC FIELD (Gauss)

with $Na_2S_2O_3$ in the presence of O_2 and resulted in absorption maxima at 435 nm (Fig.6). As in the case of KCN and NaN_3, addition of CO to the enzyme after reduction in the presence of O_2 resulted in a similar spectrum but with diminished absorbance. The addition of 5 mM copper sulfate to samples caused an approximate 7% increase in the absorption of the soret band of both the oxidized and reduced enzymes (data not shown).

The absorption spectrum of the purified cytochrome P-460 from *M. capsulatus* Bath differed from the enzyme of *N. europaea* in several ways. First, the ferricytochrome from *M.capsulatus* Bath lacked the 535 nm absorption maximum observed in the *N.europaea* enzyme. Second, the cytochrome from *M.capsulatus* Bath showed complete reduction with dithionite in less than 30 seconds. This is in contrast to the cytochrome from *N.europaea* which requires approximately 16 minutes for complete reduction (20, 46). Lastly, the soret band of the ferricytochromes of the two purified enzymes differed by 10 - 13 nm.

EPR spectrum. Low temperature X-band EPR spectra of the resting cytochrome P-460 in the presence and absence of cytochrome *c'* and the 47,000 Da polypeptide are shown in figure 7. The purified cytochrome P-460 as typical of a high spin ferric heme (g = 6.19) and showed a marked similarity to cytochrome P-460 from *N.europaea* (2, 46; Fig. 7B). In contrast to the spectral changes observed in the absorption spectra, the separation of cytochrome *c'* and the 47,000 Da polypeptide had little effect on the EPR spectra of cytochrome P-460 (Fig. 7A). The second high spin ferric heme signal at g=6.0 is associated with cytochrome *c'*. The copper associated with cytochrome P-460 is apparently EPR silent. Future studies will examine the nature copper in this enzyme.

FIG. 7. Hydroxylamine-reduced minus resting absorption spectra of the cytochrome P-460 containing fraction from the Sephadex G-75 column in 25 mM Tris-HCl, 100 mM KCl, buffer (pH 8.2).

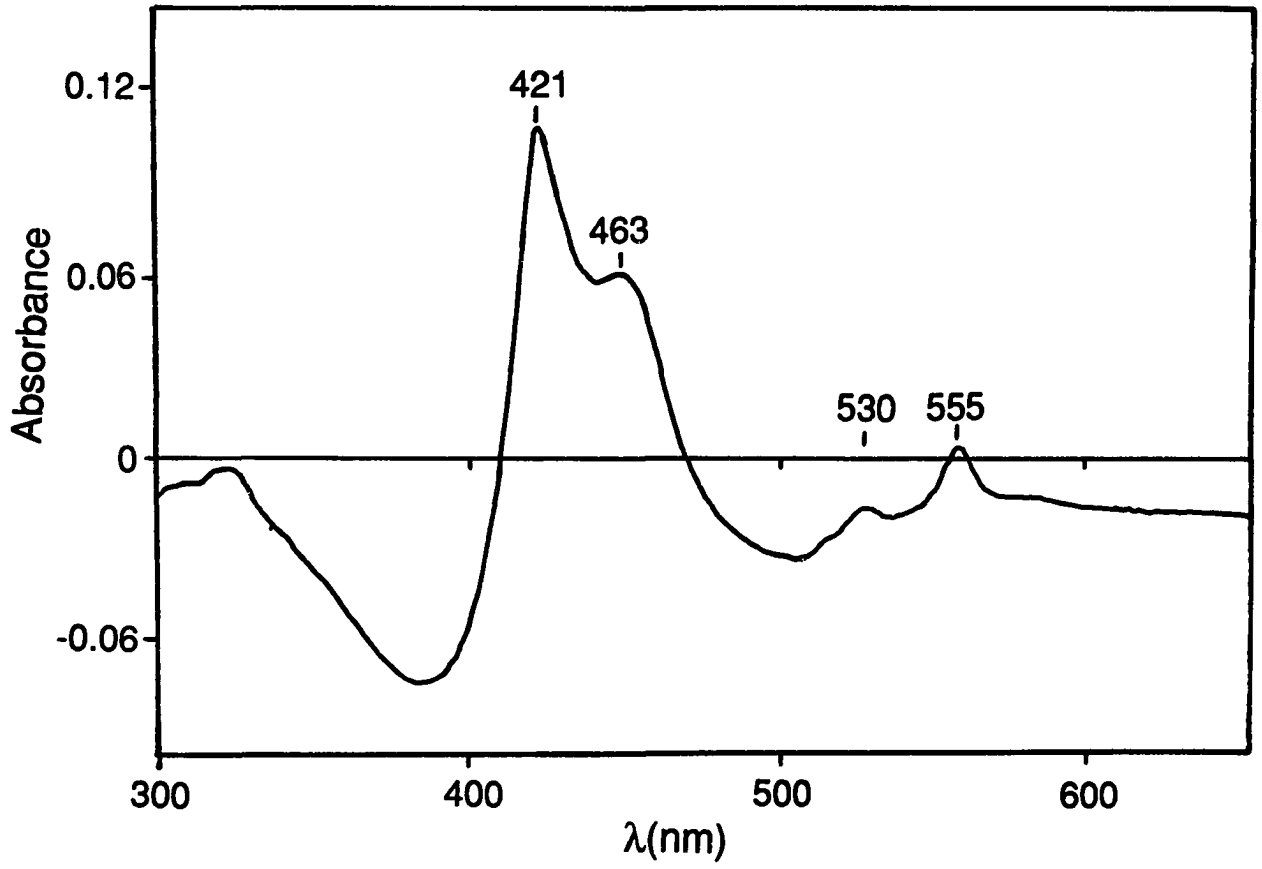
0.12
0.06
0
-0.06
Absorbance
421
463
530
555
300
400
500
600
λ(nm)

FIG. 8. Matrix-Assisted Laser Desorption/Ionization mass spectrum of cytochrome P-460 from *M. capsulatus* Bath.

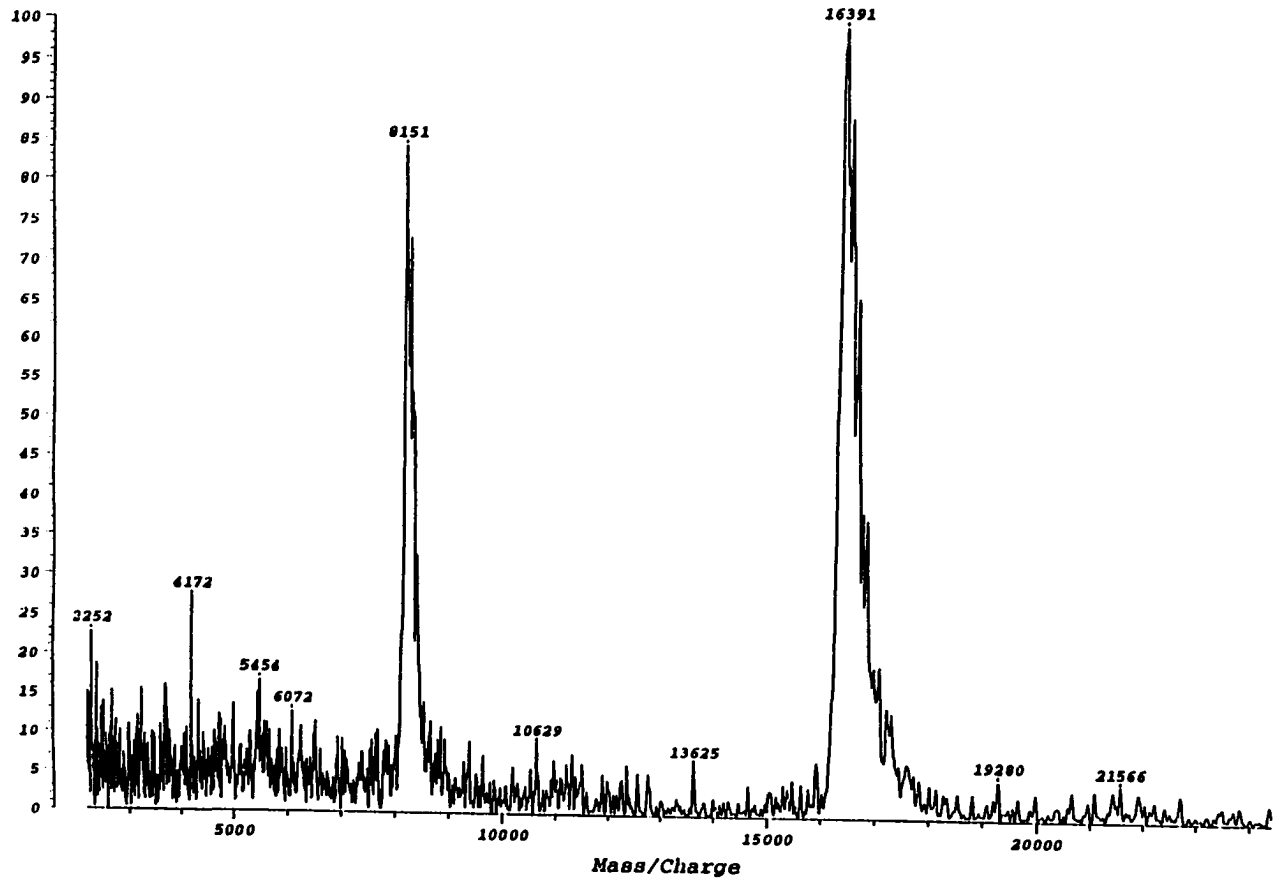
100
95
90
85
80
75
70
65
60
55
50
45
40
35
30
25
20
15
10
5
0
3252
4172
5456
6072
8151
10629
13625
16391
19280
21566
5000
10000
15000
20000
Mass/Charge

Enzyme Activity. As described by Dalton (13), cell free extracts of *M.capsulatus* Bath oxidized hydroxylamine to nitrite, at rates of 0.6 ± 01 nmol nitrite produced/min•mg protein, and was stimulated over 20-fold by the addition of PMS. As shown in figure 8, the addition of hydroxylamine to the cell free extracts resulted in the reduction of cytochrome P-460 and cytochrome *c*-555. However, in the absence of an additional electron acceptor such as PMS, no detectable nitrite is formed.

The purified enzyme was active with PMS as an electron acceptor (Table 4), but inactive with cytochrome *c*-555, cytochrome *c*-554, cytochrome *c*-557 (18) or cytochrome *c'* from *M.capsulatus* Bath. As in cell free extracts (13), the hydroxylamine oxidation activity by the purified enzyme was stimulated 2-fold by low concentrations of cyanide (0.7 mM) and 1.5 fold by 8-hydroyquinoline (100 μM)(Table 4). Higher concentrations (10 mM) of cyanide inhibited hydroxylamine oxidation by 90%.

The rate of enzyme turnover is rapid enough to account for the *in vivo* rates at the observed cellular concentrations (Table 4). The turn over rates were higher than observed with the enzyme from *N.europaea* and were surprisingly close to the turnover rates observed with HAO (28).

DISCUSSION

The relative ecological role of the methanotrophs and nitrifiers in the oxidation of methane and ammonia has yet to be resolved . A problem in field studies is in separating the contribution of ammonia-oxidizing and methane-oxidizing bacteria in the global carbon and nitrogen cycles (7). The similarities in the membrane-associated MMO (pMMO) and the AMO have made the development of a simple

procedure for differentiating between the two groups of microorganisms impossible. Although neither enzyme has been purified, all available evidence indicate both enzymes are copper proteins, are coupled to membrane component of the electron transport chain and may have similar polypeptides (10, 17, 19, 25, 32, 41, 49, 50, 55, 58, 59). In addition, both enzymes (AMO and pMMO) will catalyze the energy-dependent oxidation of ammonia to hydroxylamine and methane to methanol. After the initial oxidation step, the similarities between ammonia and methane oxidation between these two groups of bacteria end. High concentrations (up to 500 μM) of methanol accumulate during methane oxidation by nitrifiers. The methanol is slowly oxidized to CO_2 with formaldehyde and formate as intermediates (30, 33, 63, 64). The enzyme(s) responsible for the oxidation of methanol, formate and formaldehyde in whole cell studies may prove to be the AMO, but this has yet to be determined. During ammonia oxidation by methanotrophs, hydroxylamine accumulates, and is subsequently oxidized to nitrite (13). The results presented in this paper identify, for the first time, the enzyme responsible for hydroxylamine oxidation in methanotrophs and shows that the enzyme, cytochrome P-460, is different from the major enzyme responsible for *in vivo* oxidation in nitrifiers. This information may provide the needed method of separating the contributions of methanotrophs and nitrifiers in field studies.

Hydroxylamine oxidation to nitrite by methanotrophs has been examined by several authors; the activity has been described as insensitive to the MMO inhibitor acetylene and stimulated by phenazine methosulfate, cyanide, and 8-hydroxyquinoline (13, 29, 48, 57, 66). In keeping with earlier observations, the

purified enzyme presented in this study is insensitive to acetylene and stimulated by phenazine methosulfate, cyanide and 8-hydroxyquinoline. The results presented in this study shows the enzyme catalyzing this activity appears to belong in the cytochrome P-460 class of enzymes. This is the first report of a P-460-type enzyme outside of the ammonia-oxidizing bacteria.

In crude cell extracts, the optical absorption spectra of cytochrome P-460 from *M.capsulatus* Bath was similar to the enzyme observed in *N.europaea* (2, 46). The enzyme also showed similar molecular weight (*Mr* 38,000), subunit composition (α_2), ligand binding, and electron paramagnetic resonance spectra to cytochrome P-460 from *N. europaea*. The two enzymes also showed similar amino acid composition and N-terminal sequence. However, the optical spectrum and metal composition of the purified enzymes from *M.capsulatus* and *N. europaea* differed. In addition to iron, the enzyme from *M. capsulatus* Bath also contained equimolar levels of copper. Copper analysis of cytochrome P-460 from *N.europaea* has either not been determined or has not been published. The EPR spectra of cytochrome P-460 from *N. europaea* does indicate that copper is either not present or like the enzyme from *M. capsulatus* Bath is EPR silent (3, 46). Also in contrast to the enzyme from *N. europaea*, cytochrome P-460 from *M. capsulatus* Bath was very unstable in the absence of detergents. The addition of 100µM dodecyl-β-D-maltoside or dodecyl-β-D-glucopyranoside was found to stabilize the enzyme to storage at 0 - 4°C (over 14 days), or to freeze-thawing of the sample. The optical spectra was also stabilized by the addition of these detergents.

The spectral shift in the soret band from 463 to 450 nm makes nomenclature of the hydroxylamine-oxidizing enzyme from *M.capsulatus* Bath problematic. Cytochrome P-450, which has a protoporphyrin IX as a prosthetic group, has an absorption maxima at 450 nm in the reduced plus CO form (8, 22). The purified cytochrome P-460 from *M.capsulatus* Bath has an absorption maxima at 450 nm but is observed in the absence of carbon monoxide Furthermore, in contrast to cytochrome P-450, the heme group in cytochrome P-460 from is not extracted with acid acetone (21). The enzyme also shows other molecular and spectral differences (optical and EPR) to bacterial cytochrome P-450's (22, 52,55). The enzyme from *M.capsulatus* Bath is similar, to cytochrome P-460 from *N.europaea* (table 4) and has few common properties with the cytochrome P-450 class of enzymes. Thus, the enzyme from *M.capsulatus* Bath is tentatively called cytochrome P-460.

The enzyme functions well as a hydroxylamine oxidoreductase and probably functions to protect the cell from this toxic compound. The cellular concentration of cytochrome P-460 from *M.capsulatus* Bath is similar to the levels observed in *N. europaea* (20). The function may also prove to be similar in both groups of microorganisms. The cellular location of cytochrome P-460 in *N. europaea* is unknown, a cytoplasmic location would support a protective function.

ACKNOWLEDGMENTS

We thank A.B. Hooper (U. Minnesota), R.G. Lulich (ISU), and C.L. Krema (U. Iowa) for their evaluation of this manuscript and useful suggestions. The authors would also like to thank Shirley Elliott, Iowa State University (ISU), for amino acid analysis, Dr. H.M. Starr (ISU) for metal analysis, and Roger Greathead (Kratos Inc.) for mass spectral analysis.

This work was supported by the Iowa State University Office of Biotechnology (ADS) and Howard Hughes Assistantships (CD). Partial funding for the amino acid sequence was provided through the Iowa State University Graduate Student Senate Professional Advancement Grant (JZ).

LITERATURE CITED

1. **Ambler, R.P., H.Dalton, T.E. Meyer, R.G. Bartsch, and M.D. Kamen.** 1986. The amino acid sequence of cytochrome *c*-555 from the methane-oxidizing bacterium *Methylococcus capsulatus.* Biochem. J. **233:** 333 - 337.
2. **Andersson, K.K., T.A.Kent, J.D. Lipscomb, A.B. Hooper, and E. Münck.** 1984. Mössbauer, EPR and Optical studies of the P-460 center of hydroxylamine oxidoreductase fro *Nitrosomonas.* **259:** 6833 - 6840.
3. **Andersson, K.K., G.T. Babcock, and A.B. Hooper.** 1991. P460 of hydroxylamine oxidoreductase of *Nitrosomonas europaea*: soret resonance Raman evidence for a novel heme-like structure. **174:** 358 - 363.
4. **Arciero, D.M., T. Vannelli, M. Logan, and A.B. Hooper.** 1989. Degradation of trichloroethylene by the ammonia-oxidizing bacterium *Nitrosomonas europaea.* Biochim. Biophys. Res. Commun. **159:** 640 - 643.
5. **Arciero, D.M. and A.B. Hooper. 1993.** Hydroxylamine oxidoreductase from *Nitrosomonas europaea* is a multimer of an octa-heme subunit. J. Biol. Chem. **268:** 14645 - 14654.
6. **Arciero, D.M., A.B. Hooper, M. Cai, and R.Timkovich.** 1993. Evidence for the structure of the active site of heme P-460 in hydroxylamine oxidoreductase of *Nitrosomonas.* Biochemistry **32:** 9370 - 9378.
7. **Bédard, C., and R.Knowles.** 1989. Physiology, biochemistry and specific inhibitors of CH_4, NH_4^+ and CO oxidation by methanotrophs and nitrifiers. Microbiol. Rev. **53:** 68 - 84.
8. **Berg, A., M. Ingelman-Sundberg, and J.-Å. Gustafsson.** 1979. Purification and characterization of cytochrome $P\text{-}450_{meg}$. J. Biol. Chem. **254:** 5264 - 5271.
9. **Burrows, K.J., A. Cornish, DD. Scott, and I.J. Higgins.** 1984. Substrate specificities of the soluble and methane monooxygenase of *Methylosinus trichosporium* OB3b. J. Gen. Microbiol. **130:** 3327 - 3333.
10. **Chan, S.I., H.T. Nguyen, A.K. Shiemke, and M.E. Lidstrom.** 1993. Biochemical and biophysical studies toward characterization of the membrane-associated methane monooxygenase. p. 93 - 108. *In* J.C. Murrell and D.P. Kelly (eds), Microbial Growth on C_1 Compounds. Intercept Limited, Hampshire, UK.
11. **Colby, J., D,.I. Stirling, and H. Dalton.** 1977. The soluble methane monooxygenase from *Methylococcus capsulatus* Bath. Its ability to oxygenate *n*-alkanes, *n*-alkenes, ethers, and alicyclic, aromatic and heterocyclic compounds. Biochem. J. **165:** 395 - 402.

12. **Collins, M.J., D.A. Arciero, and A.B. Hooper**. 1993. Optical spectrophotometric resolution of the hemes of hydroxylamine oxidoreductase. J. Biol. Chem. **268:** 14655 - 14662.
13. **Dalton, H.** 1977. Ammonia Oxidation by the methane oxidizing bacterium *Methylococcus capsulatus* strain Bath. Arch. Microbiol. 114: 273-279.
14. **DiSpirito, A.A., L.R. Taaffe, and A.B. Hooper.** 1985. Localization and concentration of hydroxylamine oxidoreductase and cytochromes *c*-552; *c*-554, c_m-553; c_m-552 and *a*. in *Nitrosomonas europaea*. Biochim. Biophys. Acta **806:** 320 - 330.
15. **DiSpirito, A.A.** 1990. Soluble cytochromes from *Methylomonas* A4. Meth. Enzymol. **188:** 289 - 297.
16. **DiSpirito A.A., J.D. Lipscomb, and A.B. Hooper.** 1986. Cytochrome aa_3 from *Nitrosomonas europaea*. J. Biol. Chem. 261: 17048 - 17056.
17. **DiSpirito, A.A., J. Gulledge, A.K. Shiemke, J.C. Murrell, M.E. Lidstrom, and C.L. Krema.** 1992. Trichloroethylene oxidation by the membrane-associated methane monooxygenase in type I, type II and type X methanotrophs. Biodegradation **2:** 151 - 164.
18. **DiSpirito, A.A., A.K. Shiemke, S.W. Jordan, J.A. Zahn, and C.L. Krema.** 1994. Cytochrome aa_3 from *Methylococcus capsulatus* Bath. Arch. Microbiol. **161:** *in press.*
19. **Ensign, S.A., M.R. Hyman, and D.J. Arp.** 1993. In vitro activation of ammonia monooxygenase from *Nitrosomonas europaea* by copper. J. Bacteriol. **175:** 1971 - 1980.
20. **Erickson, R.H., and A.B. Hooper.** 1972. Preliminary characterization of a variant co-binding heme protein from *Nitrosomonas*. **275:** 231 - 244.
21. **Fuhrhop, J.-H.** 1975. Laboratory methods in porphyrin and metalloporphyrin research. Elsevier Scientific Publishers, New York.
22. **Gunsalus, I. C., J. R. Meeks, J. D. Lipscomb, P. DeBrunner, E. Münck.** 1974. Bacterial Monooxygenases. p. 559-613. *In.* O. Hayaishi (ed.), The P-450 Cytochrome System, Molecular Mechanisms of Oxygen Activation, Academic Press, New York, New York.
23. **Hooper, A.B., and A. Nason.** 1965. Characterization of hydroxylamine-cytochrome *c* reductase from the chemoautotrophs *Nitrosomonas europaea* and *Nitrosocytic oceanus*. J. Biol. Chem. **240:** 4044 - 4057.
24. **Hooper, A.B., and K.R. Terry.** 1973. Specific inhibitors of ammonia oxidation in *Nitrosomonas*. J. Bacteriol. **115:** 480 - 485.
25. **Hooper, A.B., and K.R. Terry**. 1977. Hydroxylamine oxidoreductase from *Nitrosomonas*: Inactiviation by hydrogen peroxide. Biochemistry **16:** 455 - 459.
26. **Hooper, A.B., P.C. Maxwell, and K.R. Terry. 1978**. Hydroxylamine oxidoreductase from *Nitrosomonas*: Absorption spectra and content of heme and metal. Biochemistry **17:** 2984 - 2989.
27. **Hooper, A.B., and C. Balny**. 1982. Reaction of oxygen with hydroxylamine oxidoreductase of *Nitrosomonas*. Fast kinetics. FEBS Lett. **144:** 299 - 303.

28. **Hooper, A.B., V.M. Tran, and C. Balny,** 1984. Kinetics of reduction by substrate or dithionite and heme-heme electron transfer in the multiheme hydroxylamine oxidoreductase. **141:** 565 - 571.
29. **Hutton, W.E., and C.E. ZoBell.** 1953. Production of nitrite from ammonia by methane oxidizing bacteria. J. Bacteriol. **65:** 216 - 219.
30. **Hyman, M.R., and P.M. Wood.** 1983. Methane oxidation by *Nitrosomonas europaea*. Biochem. J. **212:** 31 - 37.
31. **Hyman, M.R., and P.M. Wood.** 1984. Ethylene oxidation by *Nitrosomonas europaea*. Arch. Microbiol. **137:** 155 - 158.
32. **Hyman, M.R., and D.J. Arp.** 1992. $^{14}C_2H_2$- and $^{14}CO_2$-labeling studies of the *de novo* synthesis of polypeptides by *Nitrosomonas europaea* during recovery from acetylene and light inactivation of ammonia monooxygenase. J. Biol. Chem. **267:** 1534 - 1445.
33. **Jones, R.D., and R.Y. Morita.** 1983. Methane oxidation by *Nitrosococcus oceanus* and *Nitrosomonas europaea*. Appl. Environ. Microbiol. **45:** 401 - 410.
34. **Jeremias, C.G., G.B. Lucas and C.A. MacKenzie.** 1948. Preparation of tetraacetyl-a-D-glucopyranosyl bromide. **70:** 2076.
35. **Kassner, R.J.** 1991. Ligand binding properties of cytochromes *c'*. Biochim. Biophys. Acta. **1058:** 8 - 12.
36. **Laemmli U.K.** 1970 Cleavage of structural proteins during the assembly of the head of bacteriophage T4. Nature (London) **227:** 680 - 685.
37. **Lidstrom, M.E.** 1988. Isolation and characterization of marine methanotrophs. Antonie van Leewenhoek J. Microbiol. Serol. **54:** 189 - 199.
38. **Lipscomb, J.D., and A.B. Hooper**. 1982. Resolution of multiple heme centers of hydroxylamine oxidoreductase fro *Nitrosomonas*. 1. Electron paramagnetic resonance spectroscopy. Biochemistry **21:** 3965 - 3972.
39. **Lowry, O.H., N.J. Rosebrough, A.L. Farr, and R.J. Randall.** 1951. Protein measurement with the Folin phenol reagent. J. Biol. Chem. **193:** 265 - 275.
40. **McDonnel A., and L.A. Staehelin.** 1981. Detection of cytochrome *f.* a *c*-class cytochrome, with diaminobenzidine in polyacrylamide gels. Anal.Biochem. **117**: 40 - 44.
41. **McTavish, F. LaQuier, D. Arciero, M. Logan, G. Mundfrom, J.A. Fuchs, and A.B. Hooper**. 1993. Multiple copies of genes coding for electron transport proteins in the bacterium *Nitrosomonas europaea*. J. Bacteriol. **175:** 2455 - 2477.
42. **Meyer, T.E., and M.D. Kamer.** 1982. New perspectives on *c*-type cytochromes. Adv. Protein Chem. **35:** 105 - 212.
43. **Miller, D.J., P.M. Wood, and D.J.D. Nicholas**. 1984. Further characterization of cytochrome P-460 in *Nitrosomonas europaea*. J. Gen. Microbiol. **130:** 3049 - 3054.
44. **Nielsen, B. L., and L. R. Brown.** 1983 The basis for colored silver-protein complex formation in stained polyacrylamide gels. Anal. Biochem. **141:** 311-315
45. **Nicholas, D.J.D., and A. Nason**. 1957. Determination of nitrate and nitrite. Meth. Enzymol. *3:* 981 - 984.

46. **Numata, M. T.Saito, T.Yamazaki, Y.Fukumori, and T.Yamanaka.** 1990. Cytochrome P-460 of *Nitrosomonas europaea*: further purification and further characterization. J. Biochem. **108:** 10116 - 1021.
47. **Olson, T.C. and A.B. Hooper.** 1983. Energy coupling in the bacterial oxidation of small molecules: an extracytoplasmic dehydrogenase in Nitrosomonas. FEMS Microbiol. Lett. **19:** 47 - 50.
48. **O'Neill, J.G., and J.F. Wilkinson.** 1977. Oxidation of ammonia by methane-oxidizing bacteria and effects of ammonia on methane oxidation. J. Gen. Microbiol. **100:** 407 - 412.
49. **Prior, S.D., and H. Dalton.** 1985. The effect of copper ions on membrane content and methane monooxygenase activity in methanol-grown cells of *Methylococcus capsulatus* (Bath). J. Gen. Microbiol. **131:** 155 - 163.
50. **Prior, S.D., and H. Dalton.** 1985. Acetylene as a suicide substrate and active site probe for membrane monooxygenase from *Methylococcus capsulatus* (Bath). FEMS Microbiol. Lett. **29:** 105 - 109.
51. **Robinson J. and J.M. Cooper.** 1970. Method of determining oxygen concentrations in biological media, suitable for calibration of oxygen electrode. Anal. Biochem. **33:** 390 - 399
52. **Sato, R. and T Omura.** 1978. Cytochrome P-450, Academic Press, New York, New York.
53. **Sayavedra-Sota, L.A., N. Hommes, and D.L. Arp.** 1994. Characterization of the gene encoding hydroxylamine oxidoreductase in *Nitrosomonas europaea*. J. Bacteriol. **176:** 504 - 510.
54. **Schmidt, T.M. and A.A. DiSpirito.** 1990. Spectral characterization of *c*-type cytochromes purified from *Beggiatoa alba*. **154:** 453 - 458.
55. **Scott, D., J. Brannan, and I.J. Higgins.** 1981. The effect of growth conditions on intracytoplasmic membranes and methane monooxygenase activities in *Methylosinus trichosporium* OB3b. J. Gen. Microbiol. **125:** 63 - 72.
56. **Sligar, S. G., and R. I. Murray.** 1986. Cytochrome $P\text{-}450_{cam}$ and Other Bacterial P-450 Enzymes, pp. 429-503 *In* P. R. Ortiz de Montellano (ed.) Cytochrome P-450: Structure, Mechanism, and Biochemistry, Plenum Press, New York.
57. **Sokolov, I.G., V.A. Romanovskaya, Y.B. Shkurko and Y.R. Malashenko.** 1980. Comparative characterization of the enzyme systems of methane-utilizing bacteria that oxidize NH_2OH and CH_3OH. Microbiology **49:** 202 - 209.
58. **Stanley, S.H., S.D.Prior, D.J. Leak, and H. Dalton.** 1983. Copper stress underlines the fundamental change in intracellular location of methane mono-oxygenase in methane utilizing organisms: studies in batch and continuous cultures. Biotechnol. Lett. **5:** 487 - 492.
59. **Stirling, D.I., and H. Dalton.** 1977. Effect of metal-binding agents and other compounds on methane oxidation by two strains of *Methylococcus capsulatus*. Arch. Microbiol. **114:** 71 - 776.
60. **Stirling D.I., J.Colby, and H. Dalton.** 1979. A comparison of the substrate and electron-donor specificity of the methane mono-oxygenase from three strains of methane-oxidizing bacteria. Biochem. J. **177:** 362 - 364.

61. **Topp, E., and R. Knowles.** 1982. Nitropyrin inhibits the obligate methylotrophs *Methylosinus trichosporium* and *Methylococcus capsulatus.* FEMS Microbiol. Lett. **14:** 47 - 49.
62. **Vannelli, T., M. Logan, D.M. Arciero, and A.B. Hooper.** 1990. Degradation of halogenated aliphatic compounds by the ammonia-oxidizing bacterium *Nitrosomonas europaea.* Appl. Environ. Microbiol. **56:** 1169 - 1171.
63. **Voysey, P.A., and P.M. Wood.** 1987. Methanol and formaldehyde oxidation by an autotrophic nitrifying bacterium. J. Gen. Microbiol. **133:** 2833 - 290.
64. **Ward, B.B.** 1987. Kinetic studies on ammonia and methane oxidation by *Nitrosomonas oceanus.* Arch. Microbiol. **147:** 126 - 133.
65. **Weber, N. and H. Benning.** 1982. Synthesis of alkyl b-glycosides. Chem. Phys. Lipids. **31:** 325 - 329.
66. **Whittenbury, R., K.C. Phillips, and J.F. Wilkinson.** 1970. Enrichment, isolation, and some properties of methane utilizing bacteria. J.Gen. Microbiol. **61:** 205 - 218.
67. **Whtitenbury R., and H. Dalton.** 1981. The methylotrophic bacteria. pp 894-902. *In* M.P.Starr, H.G. Truper, A. Balows, and H.G. Schlegel (eds) The Prokaryotes, Vol.I Springer-Verlag, New York.
68. **Yamanaka, T., and Y. Sakano.** 1980. Oxidation of hydroxylamine to nitrite catalyzed by hydroxylamine oxidoreductase purified from *Nitrosomonas europaea.* **4:** 239 - 244.
69. **Zahn, J.A. and A.A. DiSpirito.** Unpublished data.

CHAPTER 5. CYTOCHROME c' FROM *Methylococcus capsulatus* Bath

A paper submitted for publication in the European Journal of Biochemistry

[4]James A. Zahn[A,B], David M. Arciero[C], Alan B. Hooper[C,D], and Alan A. DiSpirito[A,B]

SUMMARY

A cytochrome *c'* was isolated from the obligate methylotroph *Methylococcus capsulatus* Bath. The native and subunit molecular masses of the cytochrome were 34,855 and 16,186 Da, respectively, with an isoelectric pH of 7.0. The amino acid composition and N-terminal amino acid sequence are consistent with identification as a cytochrome *c'*. The electron paramagnetic resonance spectrum of the mono heme cytochrome indicated the presence of a high spin, S = 3/2, heme center diagnostic of cytochromes *c'*. The optical absorption spectra of ferric or ferrous cytochrome*c'* were also characteristic of cytochromes *c'*. The ferrocytochrome bound carbon monoxide and nitric oxide, but not isocyanide, cyanide or azide. Changes in physical properties due to binding of CO or NO to some other *c'* -type cytochromes have been interpreted as dimer dissociation. In the case of

---

[4] [A] Department of Microbiology, Immunology, and Preventive Medicine and [B] Graduate Program in Toxicology Iowa State University Ames, IA 50011, USA. [C]Department of Genetics and Cell Biology and [D]Graduate Programs in Biochemistry and Microbiology, University of Minnesota, St. Paul, MN 55108, USA.

cytochrome *c'* from *M. capsulatus* Bath, analytical ultracentrifugation of the ferricytochrome, the ferrocytochrome and the ferrocytochrome-plus-CO complex indicate that the changes induced by binding of CO are conformational and are not consistent with dimer dissociation.

EPR spectra show that cytochrome *c'* was reduced in the presence of hydroxylamine only when in a complex with cytochrome P-460. The value of midpoint potential, $E_{m\ 7.0}$, was - 205 mV for cytochrome *c'* from *M. capsulatus* Bath, well below the range of values reported for other cytochromes *c'*. The values of midpoint potentials for cytochrome P-460 ($E_{m\ 7.0}$ = - 300 to -380 mV) and cytochrome *c*-555 ($E_{m\ 7.0}$ = + 175 to + 195 mV) bracket the value for cytochrome*c'* and support the possibility that the latter can function as an electron shuttle between cytochrome P-460 and cytochrome *c*-555.

Abbreviations: AMS, ammonium mineral salts; EDTA, ethylaminediamine-tetraacetic acid; EPR, electron paramagnetic resonance; MALDI, matrix-assisted laser desorption ionization; NMS, nitrate mineral salts; pMMO, membrane-associated methane monooxygenase; PMS, phenazine methosulfate; SDS, sodium dodecyl sulfate; sMMO, soluble methane monooxygenase.

Key Words: Methanotroph, methylotroph, cytochrome *c'*, *Methylococcus capsulatus* Bath, hydroxylamine oxidation, ammonia oxidation, cytochrome P-460.

INTRODUCTION

In methanotrophs, the oxidation of ammonia to nitrite is a two step process [1]. The energy dependent oxidation of ammonia to hydroxylamine is catalyzed by the methane monooxygenase [2, 3]. This is followed by the four electron oxidation of hydroxylamine to nitrite, catalyzed by cytochrome P-460 [1]. During purification of cytochrome P-460, a major blue-shift (463 nm to 450 nm) in the ferrous soret maximum was observed following the separation of cytochrome *c'* and two non-heme proteins with molecular masses of 61,200 and 26,000 Da from cytochrome P-460. The spectral shift was accompanied by enzymatic changes in cytochrome P-460. Before separation, cell free hydroxylamine-dependent reduction of cytochrome P-460 and cytochrome c_{555} in was observed in cell free extracts cell free extracts [1]. Following separation, phenazine methosulfate (PMS) was required to support hydroxylamine oxidation. Several lines of evidence (electron paramagnetic resonance spectroscopy, SDS-polyacrylamide gel electrophoresis, and visible absorption spectroscopy) have suggested that the change in enzymatic properties of cytochrome P-460 may be due to the separation of cytochrome *c'* from cytochrome P-460. In order to further understand the association between cytochrome *c'* and cytochrome P-460, the properties of purified cytochrome *c'* and cytochrome P-460 - cytochrome *c'* complex from *Methylococcus capsulatus* Bath have been examined. The results support the role of cytochrome *c'* as the initial electron acceptor to cytochrome P-460.

Cytochromes *c'* belong to a unique subclass of *c*-cytochromes which are believed to function in electron-transfer reactions in diverse groups of eubacterial species. Despite the apparent widespread nature of the cytochrome in eubacteria

including sulfur-oxidizing [4], photosynthetic [5, 6], denitrifying [7], and nitrogen-fixing bacteria [8], the specific physiological or biochemical role of any cytochrome *c'* has remained elusive. Cytochromes *c'* have the following conserved physiochemical and structural properties. The heme is covalently bound at a Cys-X-X-Cys-His site near the carboxy terminus and has a value of midpoint oxidation-reduction potential between -10 and 202 mV [7, 9]. The cytochromes are generally dimers which may or may not be dissociated into monomers by carbon monoxide [10, 11, 12]. In this report, we describe the purification and properties of cytochrome *c'* from the obligate methane oxidizing bacterium, *M. capsulatus* Bath. The cytochrome from *M. capsulatus* Bath is related to other *c'*-type cytochromes in amino acid composition, spectral properties, and ligand binding properties, but not in molecular weight, midpoint oxidation-reduction potential or structural changes resulting from reaction with carbon monoxide. The latter data suggests that a revaluation of previous studies of the reaction of cytochrome *c'* with CO may be appropriate.

MATERIALS AND METHODS

Culture conditions

M. capsulatus Bath was grown in nitrate mineral salts media (NMS) plus 5 μM $CuSO_4$, and a vitamin mixture at 37°C as previously described [13]. Ammonium chloride (5 mM) was substituted for sodium nitrate for cultures grown in ammonium minimal salts (AMS) media and the pH adjusted during growth to 7.0 with KOH. Cells grown for expression of the soluble methane monooxygenase (sMMO) were cultured in low copper NMS as described previously [13]. Cells were harvested at

late log phase (OD_{600nm} = 1.4 - 1.7) by centrifugation at 13,000 x g for 15 minutes at 4°C, and resuspended (1:5 w/v) in 10 mM Tris-HCl , pH 8.0 (buffer A).

Isolation of cytochrome *c'* from cells cultured in NMS

All procedures were performed at 0 to 4°C. Cells were lysed in a French pressure cell at 18,000 lb/in^2. The homogenate was centrifuged at 12,000 x g for 20 minutes. The supernate was centrifuged at 140,000 x g for 2 hour. The 140,000 x g supernate (soluble fraction I) was saved and the pellet resuspended with a Dounce homognizer in buffer A plus 1 M KCl. The sample was centrifuged at 155,000 x g for 2 hours, and the supernate (soluble fraction II) pooled with soluble fraction I. The combined soluble fractions were brought to 35% saturation with ammonium sulfate, stirred for 1 hour, and centrifuged at 13,000 x g for 30 minutes. The pellet was discarded, and the concentration of ammonium sulfate in the supernatant raised to 75% saturation. The solution was then stirred for 1 hour and centrifuged at 13,000 x g for 30 minutes. The pellet (35 - 75% ammonium sulfate fraction) was resuspended in a minimal volume of 25 mM Tris-HCl, (buffer B) plus 150 mM KCl (pH 8) buffer (buffer C) and loaded on a 5 x 96 cm Sephadex G-75 gel-filtration column equilibrated in buffer C. The 25,000 to 45,000 Da fraction containing cytochrome P-460 and cytochrome *c'* were pooled and dialyzed against three changes of buffer C plus 2 mM glycine. Following dialysis, the sample was concentrated on a stirred cell (YM10 filter) and loaded on a preparative isoelectric focusing bed (15 x 30 cm) containing 4% Ultrodex and 2% ampholyte (pH 5-8) and electrophoresed for 16 hours at 4°C. The band containing cytochrome P-460 and cytochrome *c'* appeared dark green and focused at pH 7.0. The band was eluted from the Ultradex with

buffer A and concentrated with a stirred cell (YM-10 filter). The concentrated fraction was brought to 30% saturation with ammonium sulfate and loaded on a 2.5 x 18 cm Phenyl Sepharose CL-4B column equilibrated with buffer A plus 1.25 M ammonium sulfate (buffer D). The sample was washed with one column volume of buffer D and cytochrome P-460 eluted with buffer A plus 400 mM ammonium sulfate. Cytochrome *c'* remained bound to the column as a visible brown-red band following elution of cytochrome P-460. The column was washed with one bed volume of buffer A and cytochrome *c'* was eluted with buffer A plus 0.4% deoxycholate. The detergent was removed from the cytochrome on a 1.25 x 8 cm Extracti-gel (Pierce Chemical Co, Rockford, IL) column.

Isolation of cytochrome *c'* from cells cultured in AMS

The initial purification of cytochrome *c'* from cells cultured in AMS, were identical to the procedure described above. Following the Sephadex G-75 column step, the 25,000 to 45,000 Da fraction were pooled and dialyzed against three changes of 15% ammonium sulfate. The sample was loaded on a 2.5 x 20 cm Phenyl Sepharose CL-4B column equilibrated with 15% ammonium sulfate. The sample was washed with one column volume of 0.15% ammonium sulfate, one column volume of water and eluted with 0.5% deoxycholate. The detergent was removed from the cytochrome on a 1.25 x 8 cm Extracti-gel and the sample dialyzed against buffer A.

Isolation of the cytochrome *c'* - cytochrome P-460 complex and cytochrome c_{555}.

Cytochrome *c'* - cytochrome P-460 complex and cytochrome c_{555} were purified as previously described by Zahn, et al. [1]. Samples of cytochrome *c'*-cytochrome P-460 complex utilized for EPR experiments showed an absorption maxima at 463 nm in the dithionite-reduced state.

Electrophoresis

Sodium dodecyl sulfate (SDS)-polyacrylamide slab gel electrophoresis was carried out by the Laemmli method on 15% gels [14]. Gels were stained for total protein with Coomassie brilliant blue R. Proteins with peroxidative activity (heme proteins) were stained by the diaminobenzidine method in SDS-polyacrylamide gels [15].

Mass spectroscopy

Molecular mass of cytochrome *c'* was determined by time of flight mass spectrometry on a Finnigan (Matrix Assisted Laser Desorption Ionization) mass spectrometer using sinapinic acid as the matrix.

Analytical ultracentrifugation

Sedimentation velocity and equilibrium experiments were performed on a Beckman Optima XL-A analytical ultracentrifuge equipped with a Beckman An-60 Ti rotor. Samples of cytochrome *c'* were dialyzed against three changes of buffer containing either 5 mM Tris-HCl (pH 8) or buffer B plus 125 mM KCl. The sample and reference cell assembly were monitored using a wavelength of 410 nm for ferricytochrome *c'* or 426 nm for ferrocytochrome *c'* and ferrocytochrome *c'* plus

CO. Sedimentation velocity experiments were performed at 45,000 rpm and sedimentation equilibrium experiments at initial rotor speeds of 18,000 and 25,000 rpm. Following equilibrium, the rotor speed was increased to 45,000 rpm to obtain a baseline (E) value. Rotor temperature was maintained at 20°C during sedimentation experiments. Partial specific volume (v) and maximum hydration of dimeric *M. capsulatus* Bath cytochrome *c'* were calculated from the amino acid composition using the method of Cohn and Edsall [16] using the sedimentation formula, M = RTs/D(1-Vp), of Svedberg [21] where M is the mass of the polypeptide in Daltons, R is the gas constant, T is the absolute temperature, s, is the sedimentation constant, D is the diffusion constant, V is the partial specific volume of the polypeptide, and p is the solution density. Solution density (p) was corrected for buffer concentration by the method of Laue, et al. [16].

Spectroscopy

Optical absorption spectroscopy was performed with an SLM Aminco DW-2000 spectrophotometer in the split-beam mode. Low-temperature (77 K) spectra were recorded with a 2 mm light path low-temperature attachment for the Aminco DW-2. Electron paramagnetic resonance spectra were recorded at X-band on a Bruker ER 200D EPR spectrometer equipped with an Oxford Instruments ESR-900 liquid helium cryostat. Operating parameters were as listed in the figure legends. Samples were maintained at 8°K during spectral acquisition.

Spectroelectrochemical analysis

Spectroelectrochemistry was carried out in 50 mM MOPS buffer, pH 7.00 containing 0.1 M KCl using an optically transparent thin layer electrode (OTTLE) cell described previously [20]. Two sets of mediator dyes were employed for either the

low potential or high potential ranges. Low potential redox mediator dyes used were indigo trisulfonate (TCI America, Inc. (Portland OR); $E^{o'}$ = -80 mV), indigo carmine (BDH Chemicals, Ltd. (Poole, UK); $E^{o'}$ = -125 mV), anthraquinone-2,6-disulfonate (Aldrich Chemical (Milwaukee, WI); $E^{o'}$ = -170 mV), anthraquinone-2-sulfonate (Aldrich Chemical; $E^{o'}$ = -230 mV), safranine T (Aldrich Chemical; $E^{o'}$ = -290 mV), and benzyl viologen (Aldrich Chemical; $E^{o'}$ = -350 mV). High potential redox mediator dyes used were ferrocene acetic acid (Aldrich Chemical; $E^{o'}$ = +375 mV), 2,6-dibromo-indosalicylic acid (TCI America, Inc.; $E^{o'}$ = +275 mV), dichlorophenol-indophenol (BDH Chemicals, Ltd.; $E^{o'}$ = +215 mV), 2,6-dibromo-3'-methoxy-idophenol (TCI America, Inc.; $E^{o'}$ = +160 mV), phenazine-methosulfate (Sigma Chemical (St. Louis, MO); $E^{o'}$ = +80 mV), and gallocyanine (Sigma Chemical; $E^{o'}$ = +20 mV). Spectroelectrochemical titrations of cytochrome *c'* and cytochrome P460 were carried out in the presence of the low potential dyes. Spectroelectrochemical titration of cytochrome c_{555} was carried out in the presence of the high potential dyes.

Heme and protein determination

The optical extinction coefficient values for cytochrome *c'* were quantified using the subunit molecular weight of 16,186 Da and protein determinations via amino acid analysis. Protein concentration was also determined by the Lowry method [17] using either bovine serum albumin or horse heart cytochrome *c* as standards. Heme composition was determined by the pyridine ferrohemochrome method [18, 19]. The acid acetone method was used to determine covalent linkage of the prosthetic groups to the polypeptide [19].

Metal analysis

Protein samples (1 ml, 10 -25 nmol) were diluted in 8 M nitric acid to a final volume of approximately 10 ml. The samples were then sealed in teflon-lined digestion cylinders and digested for 18 hours at 100°C. The digested samples were diluted to a total volume of 25 ml in H_2O and were analyzed for zinc, copper and iron using a Perkin Elmer model 5100 graphite furnace atomic absorption spectrophotometer.

Amino acid analysis and sequence analysis

Amino acid analysis was carried out with an Applied Biosystems 420A derivatizer coupled to an Applied Biosystems 130A separation system. Samples were hydrolyzed in 6 M HCl containing trace amounts of phenol in HCl vapors for 1 h, then in a vacuum at 150°C. After hydrolysis, norleucine was added as an internal standard. Amino acid sequence analyses was performed by Edman degradation with an Applied Biosystems 477A Protein Sequencer coupled to a 120A Analyzer.

RESULTS

Purification of cytochrome *c'*

The purification of cytochrome *c'* from *M. capsulatus* Bath was performed as described under Materials and Methods. The cytochrome was non-covalently associated with cytochrome P-460 and the two cytochromes separated by hydrophobic interaction chromatography on Phenyl Sepharose CL-4B [1]. As noted previously by Ambler, et al. [21] cytochrome *c'* was present at high concentrations in cells of *M. capsulatus* Bath expressing the sMMO in AMS medium. The results from

FIG. 1. Molecular mass determination of *M. capsulatus* Bath cytochrome *c'* by matrix-assisted laser desorption/ionization mass spectroscopy and by SDS-polyacrylamide slab gel electrophoresis (insert). Insert, purified *M. capsulatus* Bath cytochrome*c'* stained for heme with diaminobenzidine, (*Lane 1*) and for total protein with Coomassie R-250 (*Lane 2*). Molecular mass standards, 92, 000, 66,200, 45,000, 31,000, 21,5000, and 14,400 Da are shown in *Lane 3*.

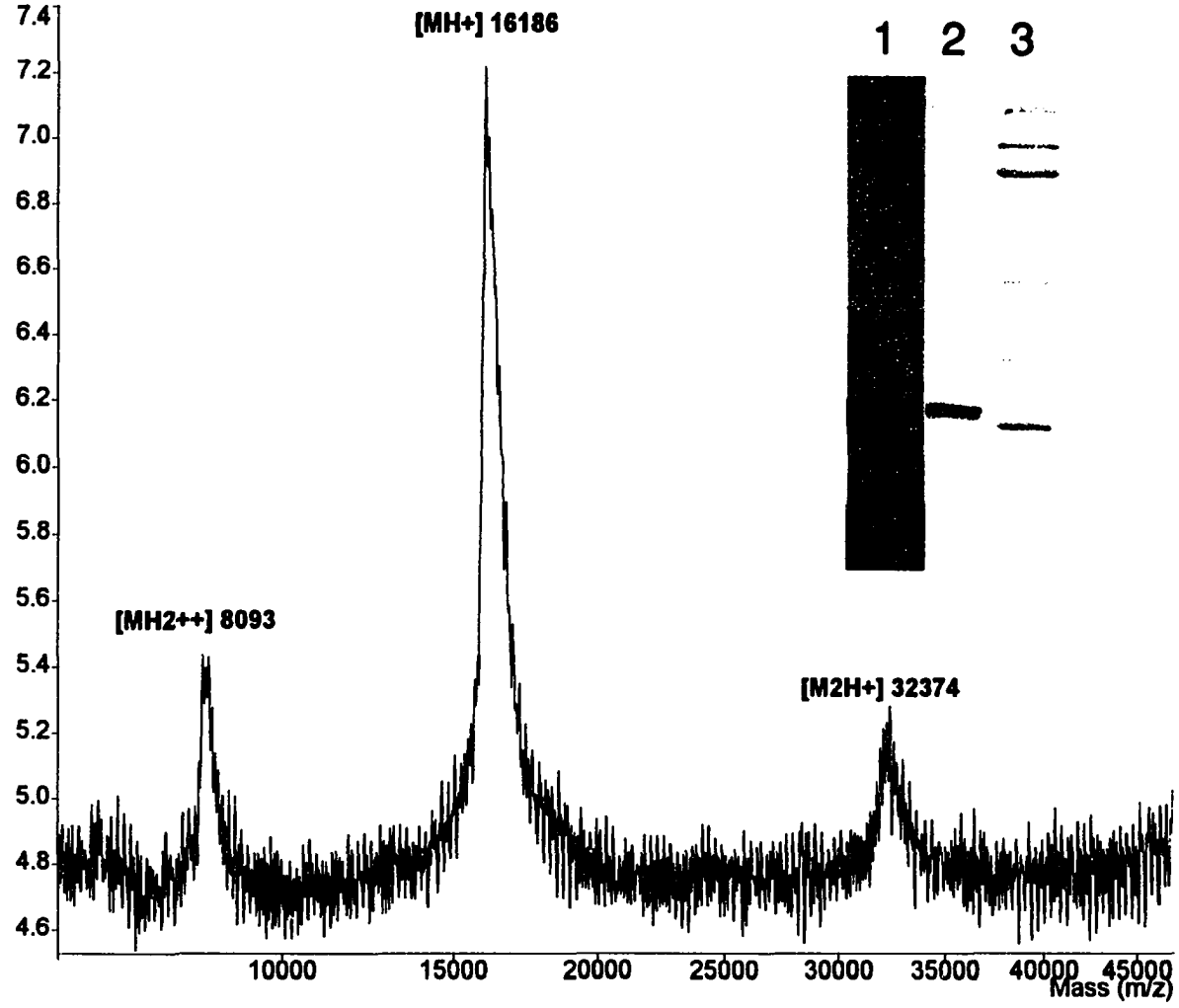
[MH+] 16186
[MH2++] 8093
[M2H+] 32374
1
2
3
7.4
7.2
7.0
6.8
6.6
6.4
6.2
6.0
5.8
5.6
5.4
5.2
5.0
4.8
4.6
10000
15000
20000
25000
30000
35000
40000
45000
Mass (m/z)

this study show cytochrome *c'* is also present in cells of *M. capsulatus* Bath expressing the pMMO with either nitrite or ammonia as the nitrogen source. While the physical properties of cytochrome *c'* from cells cultured under different conditions are identical, cells cultured on AMS media show two different physiological properties with respect to this cytochrome. The cytochrome *c'* concentration was at least 3-fold higher (0.14 nmol/mg cell protein vs. 0.04 nmol/mg cell protein) in cells grown in AMS and expressing either MMO. Further, the majority of the cytochrome *c'* isolated from cells grown in AMS

Table 1. Properties of purified cytochrome *c'* from *M. capsulatus* Bath.

Property	
Molecular Mass (Da)	
Cytochrome	
a. Gel filtration	38,900 ± 6,100
b. Ultracentrifugation	34,885
Subunit	
a. SDS-PAGE	16,000
b. Mass spectroscopy	16,186
isoelectric Point (pi)	7.0
Heme C concentration (mol/mol enzyme)	0.78 ± 0.15
Fe concentration (mol/mol enzyme[f])	1.12 ± 0.28
Absorption Maxima (nm)	
Oxidized	401, 502, 638
Dithionite-Reduced	433, 552
Reduced plus NO	418, 430, 562
Reduced plus CO	420, 435, 561
Ferrohemochromagen	512, 520, 550
Optical extinction coefficients (cm^{-1} mM^{-1})	
ferrochrome plus CO: (ε 420-700nm)	143.8
ferrichrome : (ε 419 - 700 nm)	66.6
Ferrohemochromagen: (ε 550 - 600 nm)	21.0
EPR (*g* values)	6.27, 6.06, 5.57, 5.43, 2.00
Purity Index (Abs. 401 nm/A 280 nm)	2.21

FIG 2. The N-terminal amino acid sequence of *M. capsulatus* Bath cytochrome *c'*.

Ala-Glu-Thy-Lys-Val-Lys-Tyr-Pro-Asp-Gly-Phe-Arg-Ser-Trp-Tyr-
1 5 10 15

His-Val-Lys-Ser-Met-Val-Ile-Gln-Pro-Gly-His-Pro-Leu-Glu-Asn-
16 20 25 30

Cytochrome *c'* was purified as described in the "materials and methods" section. The yield for the PTH-derivative of the listed amino acids are given in picomoles. The N-terminal amino acid sequence of *M. capsulatus* Bath cytochrome *c'*.

Cycle	Residue	Yield	Cycle	Residue	Yield
1	Ala	602	16	His	55
2	Glu	380	17	Val	112
3	Thr	374	18	Lys	61
4	Lys	310	19	Ser	61
5	Val	419	20	Met	66
6	Lys	293	21	Val	86
7	Tyr	261	22	Ile	75
8	Pro	262	23	Gin	52
9	Asp	138	24	Pro	62
10	Gly	251	25	Gly	92
11	Phe	216	26	His	34
12	Arg	302	27	Pro	48
13	Ser	114	28	Leu	43
14	Trp	10	29	Glu	31
15	Tyr	88	30	Asn	52

media was not associated with cytochrome P-460. The concentration of cytochrome *c'* did not change significantly with the expression of the different MMO's.

Molecular mass of cytochrome *c'*

The molecular mass of native cytochrome *c'* was determined to be 38,900 ± 6,100 Da on a Sephadex G-75 column (2.5 x 96 cm). Reference proteins were horse heart cytochrome *c* (M_r 12,400), lysozyme (M_r 14,300), horse heart myoglobin (M_r 18,800) carbonic anhydrase (M_r 29,000) and bovine hemoglobin (64,500). This value differed slightly from the native molecular mass of 34,885 Da determined at sedimentation equilibrium by analytical ultracentrifugation. In sodium dodecyl sulfate (SDS)-polyacrylamide gels, cytochrome *c'* migrated as a single band corresponding to a molecular mass of 16,000 ± 100 Da (Fig. 1). The results suggest the enzyme is a dimer composed of two identical subunits. The sample did not require b-mercaptoethanol or heat treatments before loading on SDS-polyacrylamide gels for subunit separation (results not shown). Thus, the interaction between subunits appears to be non-covalent.

MALDI mass spectroscopy of cytochrome *c'* showed major Me peaks at 32,272 ($[2MH]^+$), 16,186 ($[MH]^+$) and 8,114 ($[MH2]^{2+}$(Fig. 1) . The mass of the molecular ion was similar to the subunit molecular mass determined on SDS-polyacrylamide gels. The subunit molecular mass of 16,186 Da was used further in the calculation of the molar extinction coefficients and calculation of molecular volume through the sedimentation formula of Svedberg [22].

FIG. 3. Absorption spectra of 4.64 μM cytochrome *c'* in10 mM Tris-HCl buffer (pH 8). Absorption of resting *M. capsulatus* Bath cytochrome *c'* (– · – · – · –), following reduction with dithionite (·····), following the addition of carbon monoxide to the ferrocytochrome (– – – –), and following addition of Nitric oxide to the ferrocytochrome (———).

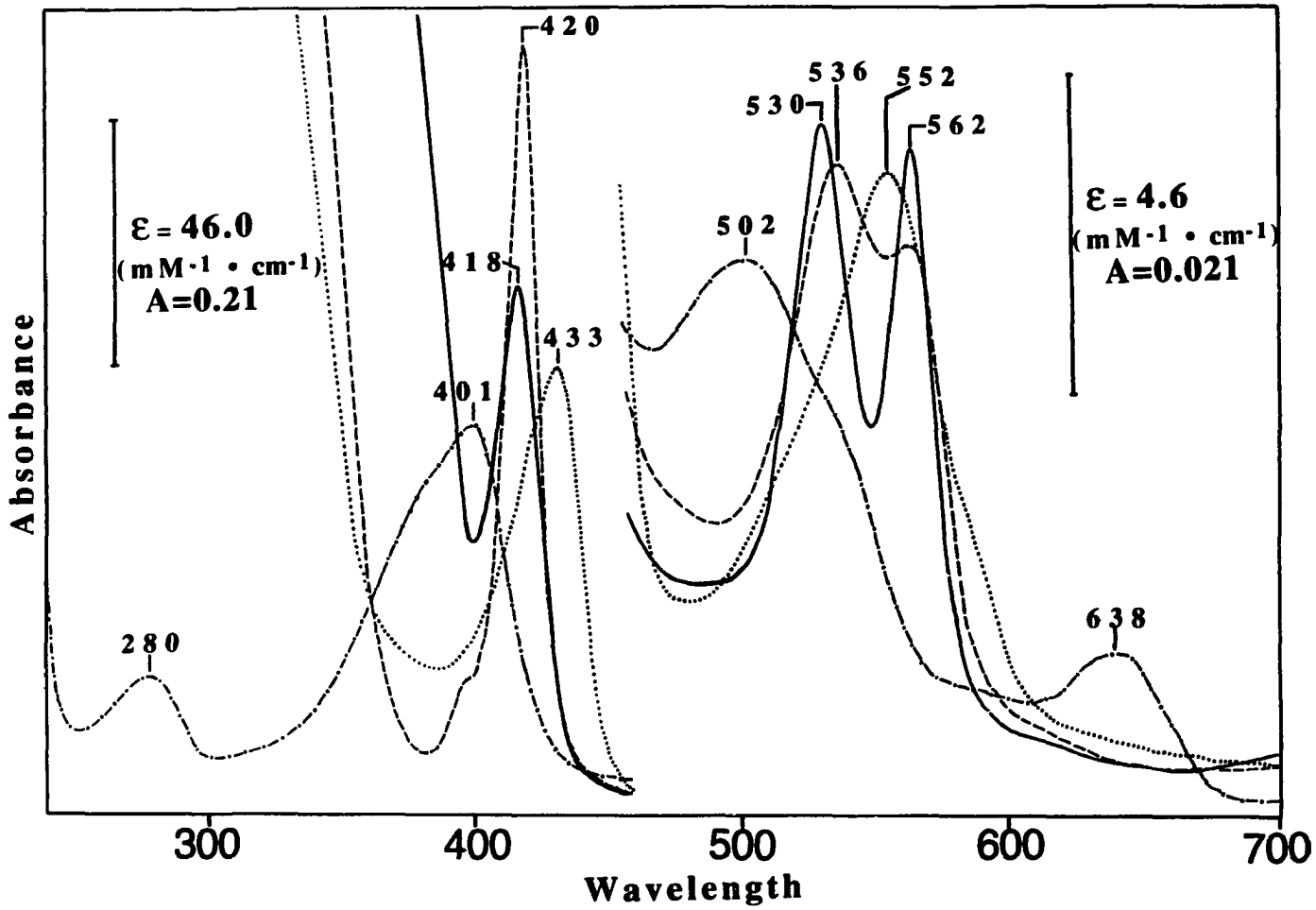
420
536
552
530
562
502
418
433
401
280
638
ε = 46.0
(mM-1 • cm-1)
A=0.21
ε = 4.6
(mM-1 • cm-1)
A=0.021
Absorbance
300
400
500
600
700
Wavelength

Amino acid and N-terminal sequence analysis

The amino acid composition of *M. capsulatus* Bath cytochrome *c'* (Table 1) was similar to the amino acid composition of cytochrome *c'* present in photosynthetic and denitrifying bacteria [7]. The minimum molecular mass determined from the amino acid composition was nearly identical to that determined by SDS-polyacrylamide gels or by mass spectroscopy.

The N-terminal amino acid sequence of cytochrome *c'* from *M. capsulatus* Bath is shown in Fig. 2. As with all previously sequenced *c'*-type cytochromes, an arginine was present within the 7th to 12th amino acid residues [23].

Table 2. Amino acid composition of *M. capsulatus Bath* cytochrome *c'*.

Amino Acid	mol %	mole amino acid/mole heme
Asx	10	15
Ser	3.1	7
Glx	11.7	17
Pro	4.7	7
Gly	15.5	23
Ala	8.1	12
Cys	ND[1]	-
Val	7.5	11
Met	0.4	1
Ile	3	5
Leu	6.1	9
Tyr	4.7	7
Phe	5.6	8
His	4.5	7
Lys	7.1	11
Arg	5.4	8
Thr	2.4	4
Trp	ND[1]	-
Estimated Number of Amino Acid Residues/Mole Heme C		152
Minimum Molecular Mass (Da)		16,204

[1]Cysteine and Tryptophan residues were not determined.

FIG. 4. Reduced-*minus*-oxidized difference spectra (A) and Absorption-Potential plot (B) for cytochrome *c*' derived from spectropotentiometric titration at pH 7.00. A) Oxidized spectrum recorded at -117 mV; reduced spectra recorded at 10 mV increments between -117 and -317 mV. B) Absorbance (430 nm)-*minus*-absorbance (398 nm) plotted at 5 mV increments. Solid line is a theoretical curve for a one electron Nernst center with midpoint potential of -204 mV. Inset shows Nernst plot of optical data; solid line is best fit line by linear regression with slope of 60 mV/decade.

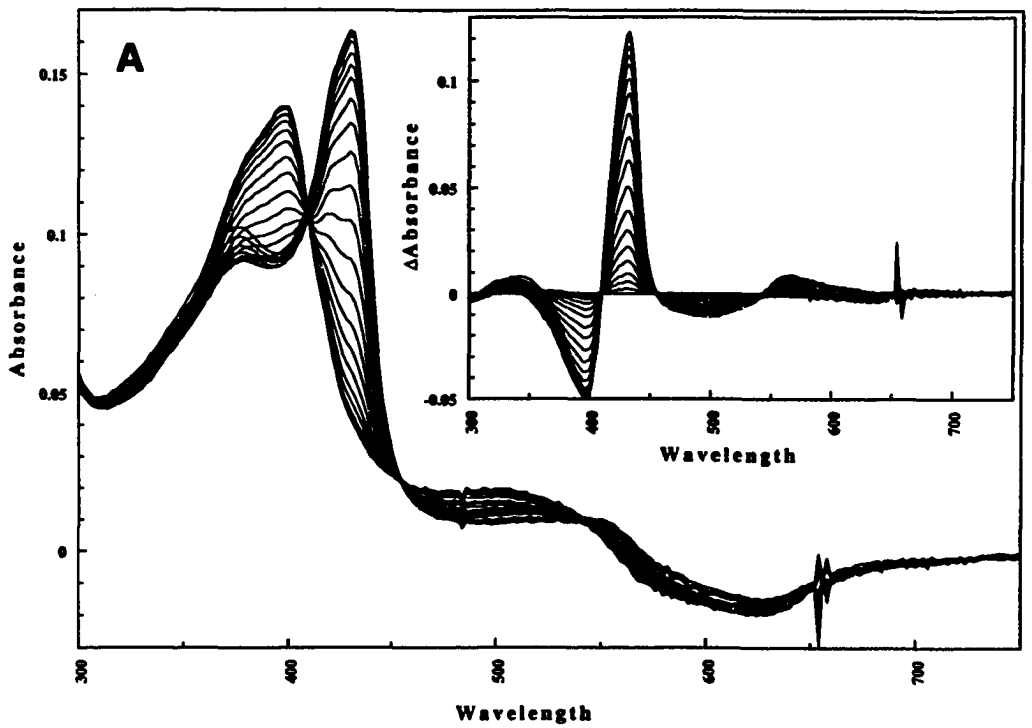
A
Absorbance
0.15
0.1
0.05
0
300
400
500
600
700
Wavelength
ΔAbsorbance
0.1
0.05
0
-0.05
300
400
500
600
700
Wavelength

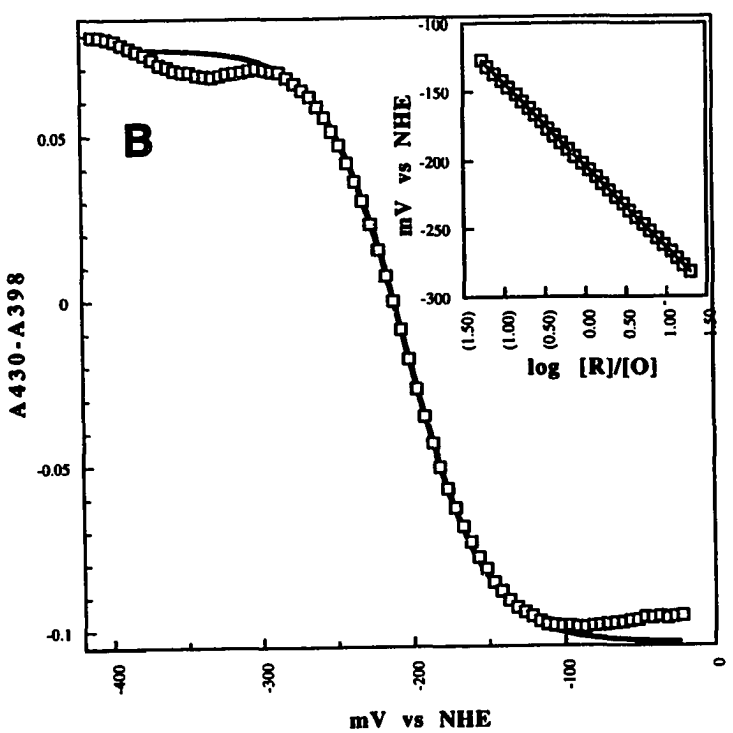
B
A430-A398
0.05
0
-0.05
-0.1
-400
-300
-200
-100
0
mV vs NHE
mV vs NHE
-100
-150
-200
-250
-300
(1.50)
(1.00)
(0.50)
0.00
0.50
1.00
1.50
log [R]/[O]

This arginine residue has been shown to form a hydrogen bond to one of the heme propionates in cytochromes *c'* [23]. As with the *c'*-type cytochromes from several photosynthetic bacteria, the cytochrome from *M. capsulatus* Bath contains a lysine residue at position 4. The general sequence alignment of the first 30 amino acids of cytochrome *c'* from *M. capsulatus* Bath revealed no significant correlations to other *c'*-type cytochromes. However, the N-terminal region is very poorly conserved in this class of cytochromes [23].

Heme and metal components

The prosthetic group of cytochrome *c'* was not extracted with acid acetone and the ferrohemochromogen spectra showed absorption maxima at 401, 520 and 550nm. Thus, the cytochrome was identified as a *c*-type.

Protein concentration was determined from amino acid analysis, since the Lowry method was found to under-estimate protein concentration of cytochrome *c'* by 33% when bovine serum albumin or by 24% when horse heart cytochrome *c* were used as standards. Based on the molecular mass as determined by mass spectroscopy (16,186 Da), a protein containing 1 iron should have a metal content of 3.45 μg Fe/mg protein. The similarity of the estimated value to the experimentally derived value for iron concentration of 3.87 ± 0.97 μg Fe/mg protein (Table 1) suggests that the cytochrome contains one heme per subunit (1.12 ± 0.28 mol Fe/mol cytochrome *c'*). Using an extinction coefficient for the pyridine ferrochrome of heme C of 29.1 mM-1• cm-1, the heme C concentration was estimated to be 0.78 ± 0.15 mol heme C/mol cytochrome *c'* based on a molecular mass of 16,186 Da.

FIG. 5. Reduced-*minus*-oxidized difference spectra (A) and Absorption-Potential plot (B) for cytochrome c_{555} derived from spectropotentiometric titration at pH 7.00. A) Oxidized spectrum recorded at +283 mV; reduced spectra recorded at 10 mV increments between +283 and +83 mV. B) Absorbance (420 nm)-*minus*-absorbance (404 nm) plotted at 5 mV increments. Solid line is a theoretical curve for a one electron Nernst center with midpoint potential of +174 mV. Inset shows Nernst plot of optical data; solid line is best fit line by linear regression with slope of 63.8 mV/decade.

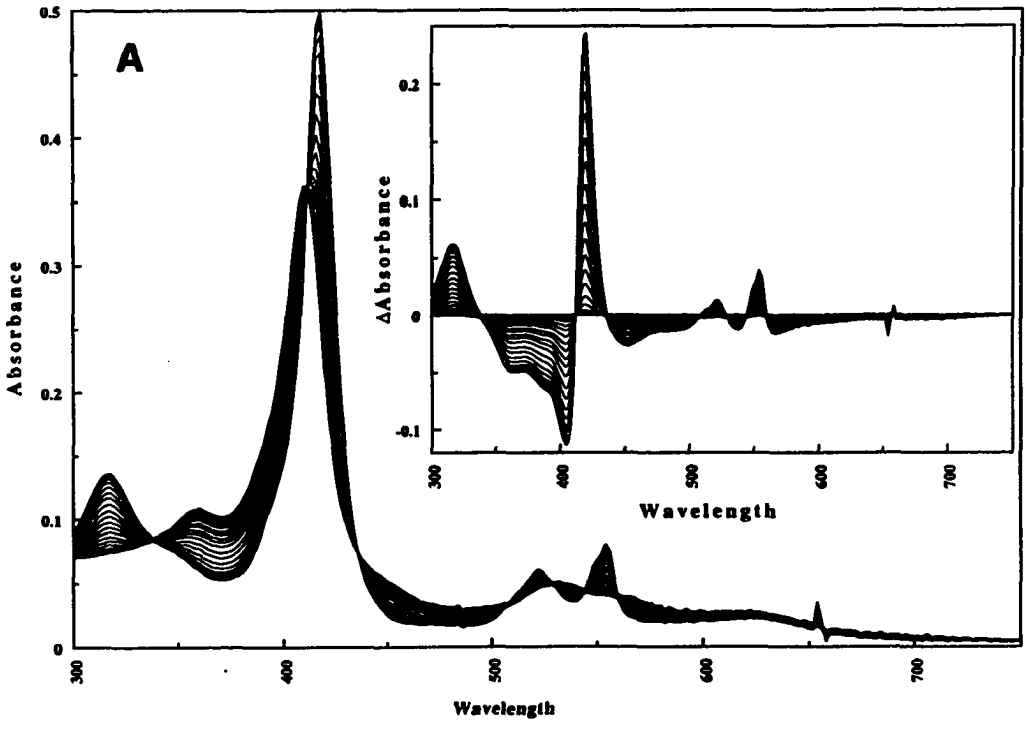
A
Absorbance
Wavelength
ΔAbsorbance
Wavelength

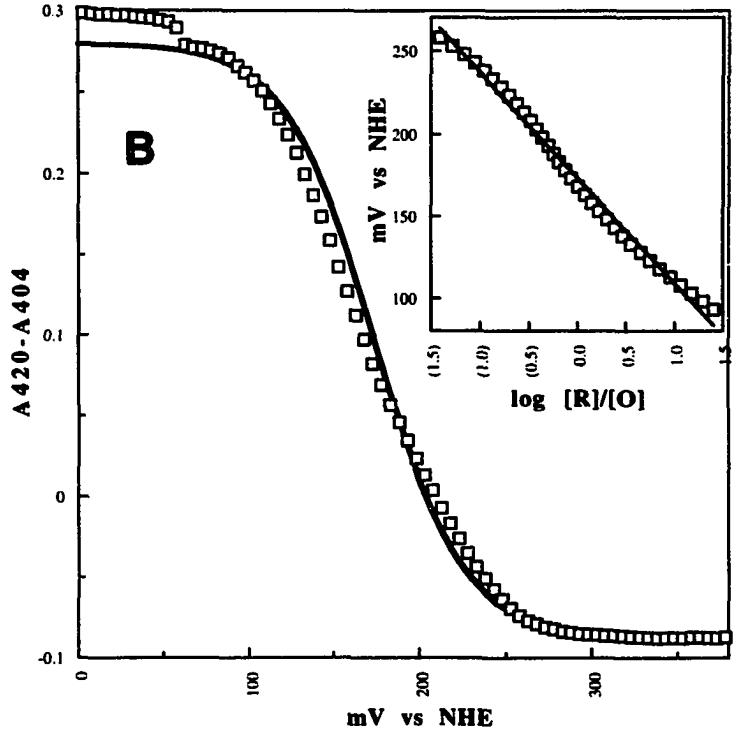
B
A420-A404
mV vs NHE
mV vs NHE
log [R]/[O]

Spectral properties

Cytochrome *c'* from *M. capsulatus* Bath exhibited optical spectral characteristics which were similar to other *c'*-type cytochromes [24, 25]. The major distinguishing features of this group are the lack of a and b bands, and the blue shifted soret absorbance maxima (Fig. 3) The ferrocytochrome bound carbon monoxide and nitric oxide (Fig. 3), but not ethyl isocyanide, cyanide, or azide.

Electrochemical properties

The redox behavior of cytochrome *c'* was analyzed spectroelectrochemically using an OTTLE cell and mediator dyes. Optical changes associated with the potentiometric titration and a Nernst plot of the data is shown in figure 4. The cytochrome followed Nernstian behavior for a single one electron redox site. The midpoint potential was determined to be -205 mV.

The probable electron donor and acceptor of cytochrome *c'*, cytochrome P460 and cytochrome c_{-555}, respectively [1], were also analyzed spectroelectrochemically. Although neither protein exhibited true Nernstian behavior, a midpoint potential range for the redox center of each of the proteins was still obtainable. Midpoint potential ranges for cytochrome P460 and cytochrome c_{555} were found to be -300 to -380 mV and +175 to +195 mV, respectively. The optical changes and titration curve for cytochrome c_{555} is shown in figure 5. These ranges are consistent with the functions proposed for the two cytochromes.

FIG. 6. Electron paramagnetic resonance spectrum of purified *M. capsulatus* Bath. [A] Cytochrome *c'* in 10 mM Tris-HCl (pH 8.2) at 8°K. [B] Cytochrome c' in 50 mM acetate buffer (pH 4.0) at 8° K. Instrumental conditions were as follows: modulation frequency 100 kHz, modulation amplitude 4 G, microwave frequency 9.422 GHz, time constant 100 ms, microwave power 2.02 mW. Temperature was maintained at 8°K during spectral acquisition.

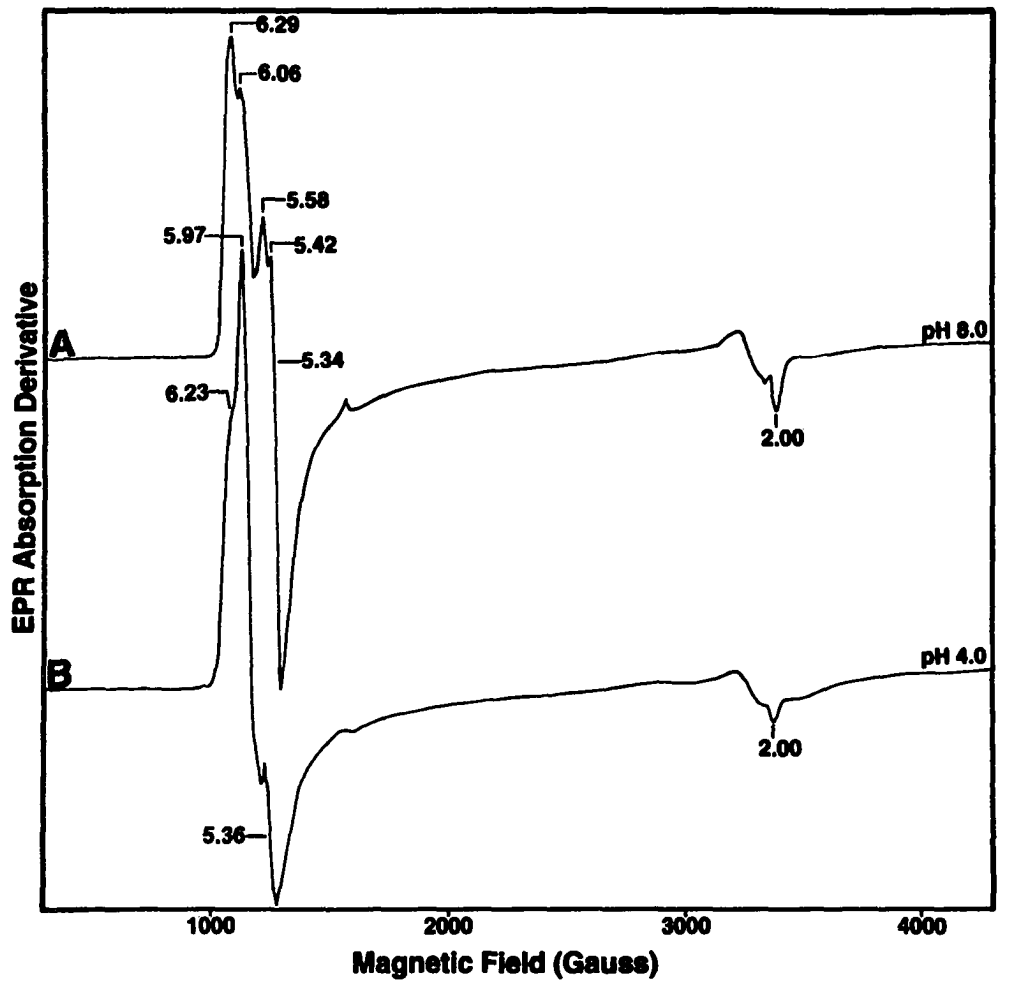
6.29
6.06
5.58
5.97
5.42
A
5.34
6.23
pH 8.0
2.00
B
pH 4.0
2.00
5.36
EPR Absorption Derivative
1000
2000
3000
4000
Magnetic Field (Gauss)

EPR spectrum

The low temperature X-band EPR spectra of oxidized cytochrome *c'* from *M. capsulatus* Bath at pH 8.0 and 4.0 are shown in Fig. 6. The EPR spectrum of the cytochrome shows the presence of two high-spin ferric iron EPR signals at pH 8 in 20 mM Tris buffer: Species 1 demonstrates g-values at $g_y = 6.29$, $g_x = 5.70$, and $g_z = 2.0$; and species 2 at $g_y = 5.58$, $g_x = 5.34$ and $g_x = 2.0$ (Fig. 6A). Two species are also observed at pH of 4.0 in 20 mM acetate buffer although the ratio of each species varied (Fig. 6B). The results are similar to those observed by in Empitage et al. [26] in *Rhodospirillum rubrum*. However, the spectra from *M. capsulatus* Bath cytochrome *c'* was more rhombic than in the cytochrome from *R. rubrum*. The EPR spectrum of the *M. capsulatus* Bath cytochrome differs from previously characterized cytochromes *c'* [5, 26] in that the g_y component of the major high-spin species was above g = 6 ($g_y = 6.27$). Additionally, the signals associated with each species clearly deviate from the axial symmetry present in other cytochromes *c'*. Integration of the signals arising from each species indicate that species 1 accounts for at least 60% of the total high-spin iron in the sample at pH 8. As with cytochromes *c'* from in *R. rubrum* and *Chromatium vinosum*, the origin of species 2 is most likely the result of a admixture of the S = 5/2 ground state with a S = 3/2 excited state [5, 26]. This assignment of a quantum mechanical admixture in the *M capsulatus* Bath cytochrome is supported by: 1) the 1:1 heme to subunit stoichiometry present in the sample of cytochrome *c'* and 2) analysis of the absorption spectrum and redox titration data, which show no significant perturbations due to a possible second heme species or population in the sample. Furthermore, the signal is not likely to be

the result of a heterogeneous sample, since all samples from 6 different purification procedures yielded similar EPR spectra. A precise assignment of the origin of species 2 however, must await investigation by Mössbauer spectroscopy.

Ligand-induced structural perturbation of cytochrome *c'*

The degree of apparent association between the subunits of cytochrome *c'* has been found to vary considerably among the bacterial sources [10, 11, 12, 27]. The subunits of cytochrome *c'* from *Rhodospirillum mosischianum* and *Rhodospirillum rubrum* exhibit a tight interaction and are shown to resist dimer dissociation in 6 M urea [10, 11, 27]. In the opposite extreme, the subunits of ferrocytochrome *c'* from *Chromatium vinosum* apparently undergo a unique CO-induced dimer dissociation. [27]. It has been suggested that ligand-induced dimer dissociation of cytochrome *c'* from *C. vinosum* was mediated by molecular volume constraints imposed by aromatic residues positioned near the 6th coordinate position of the heme [12]. These studies also suggested that the presence of an aromatic residue at position 16 caused structural perturbations at the dimer interface upon carbon monoxide ligation to the heme, which led to the dissociation of the dimers. By analogy to *C. vinosium* cytochrome *c'*, the presence of the aromatic residue, histidine at position 16 in *M. capsulatus* Bath cytochrome *c'*, suggested that ferrocytochrome *c'* from *M. capsulatus* Bath would undergo carbon monoxide or nitric oxide-mediated dimer dissociation.

Sedimentation equilibrium and velocity experiments were conducted on ferricytochrome *c'*, ferrocytochrome *c'*, ferrocytochrome *c'*-CO complex, and ferrocytochrome *c'*-NO complex to characterize molecular perturbations induced by ligand binding. All attempts to study the formation of the ferrocytochrome *c'*-NO

FIG 7. Sedimentation equilibrium analysis of ferricytochrome *c'* (A) and ferrocytochrome *c'*-CO complex (B). Rotor speed was 25,000 rpm for 20 hours prior to data collection. The inset for each figure shows the examination of the residuals after data points are fitted to the model of a single ideal solute. The random distribution indicates the presence of one ideal solute species and the lack of protein aggregates.

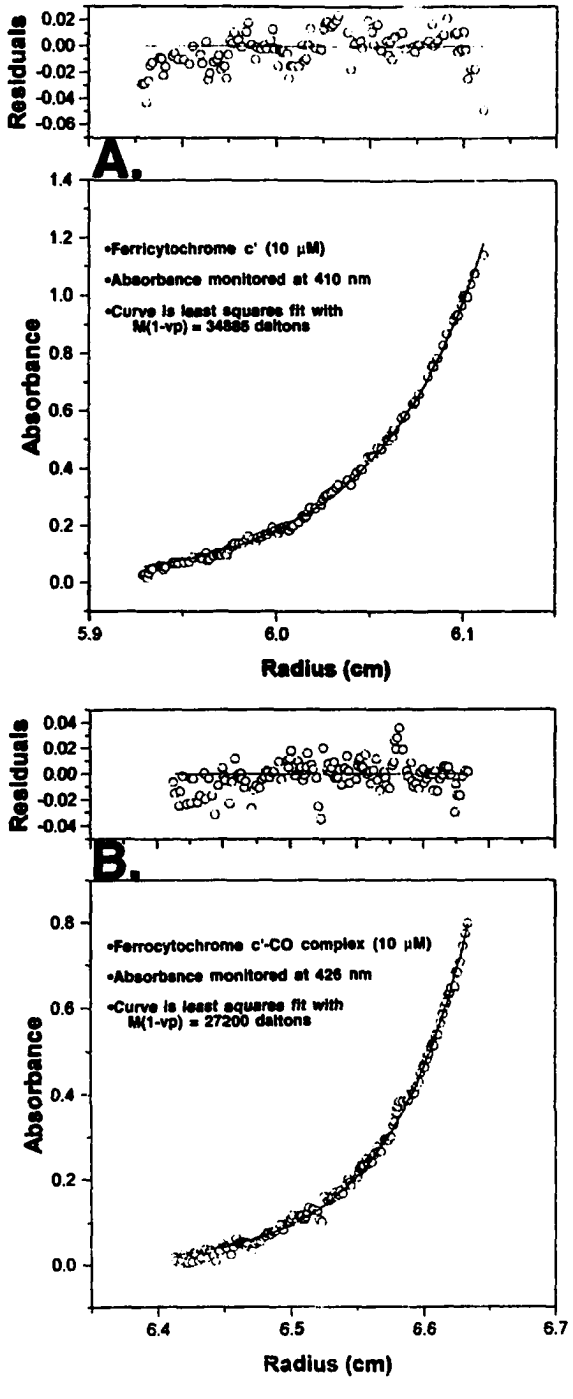
Residuals
0.02
0.00
-0.02
-0.04
-0.06
A.
1.4
1.2
1.0
0.8
0.6
0.4
0.2
0.0
Absorbance
•Ferricytochrome c' (10 μM)
•Absorbance monitored at 410 nm
•Curve is least squares fit with
M(1-vp) = 34886 daltons
5.9
6.0
6.1
Radius (cm)
Residuals
0.04
0.02
0.00
-0.02
-0.04
B.
0.8
0.6
0.4
0.2
0.0
Absorbance
•Ferrocytochrome c'-CO complex (10 μM)
•Absorbance monitored at 426 nm
•Curve is least squares fit with
M(1-vp) = 27200 daltons
6.4
6.5
6.6
6.7
Radius (cm)

complex resulted in abnormally high sedimentation values which were consistent with NO-mediated protein aggregation. Typical sedimentation and diffusion coefficients for experiments with ferrocytochrome *c'* - NO complex were $2.23 \cdot 10^{-12}$ sec and $1.00 \cdot 10^{-5}$ $cm^2 \cdot sec^{-1}$, respectively. Therefore, further sedimentation experiments with nitric oxide ligation were not performed. The coefficients for sedimentation equilibrium and velocity experiments with ferrocytochrome *c'* did not differ (<0.5%) significantly from the ferricytochrome *c'* coefficients (data not shown). However, addition of carbon monoxide to the ferrocytochrome *c'* induced structural changes in cytochrome *c'* which were inconsistent with the dissociation of dimers. The molecular masses for ferricytochrome and ferrocytochrome-CO were calculated from sedimentation velocity data. Using the partial specific volume of cytochrome *c'* derived from the amino acid analysis, the molecular masses for ferricytochrome and ferrocytochrome-CO differed from their predicted masses by (+)7.2% and (-)16.1%, respectively. The difference between the masses for ferricytochrome and ferrocytochrome-CO (7,685 Da) was only 45.6% of the subunit mass predicted by mass spectroscopy. Therefore, the sedimentation data suggest that the differences between ferricytochrome and CO-ferrocytochrome resulted from conformational changes associated with partial specific volume rather than mass differences due to dimer dissociation (Fig 7). Table 3 shows the values for the estimated partial specific volume for ferricytochrome *c'* and CO-ferrocytochrome *c'* complex according to sedimentation velocity, sedimentation equilibrium, and mass spectroscopy data. The geometrical shape of ferricytochrome and CO-ferrocytochrome *c'* have been assigned based on the prolate ellipsoid model using the values for the estimated

FIG. 8. Electron paramagnetic resonance spectrum of *M. capsulatus* Bath cytochrome *c'*- cytochrome. P-460 complex in 10 mM Tris-HCl (pH 8.2) at 8° K (trace A). EPR spectrum immediately following the aerobic addition of 3 mM hydroxylamine-HCl (trace B) and following aeration of the sample for 1 minute following the addition of hydroxylamine-HCl (trace C). Instrumental conditions were as follows: modulation frequency 100 kHz, modulation amplitude 4 G, microwave frequency 9.422 GHz, time constant 100 ms, microwave power 2.02 mW. Temperature was maintained at 8°K during spectral acquisition.

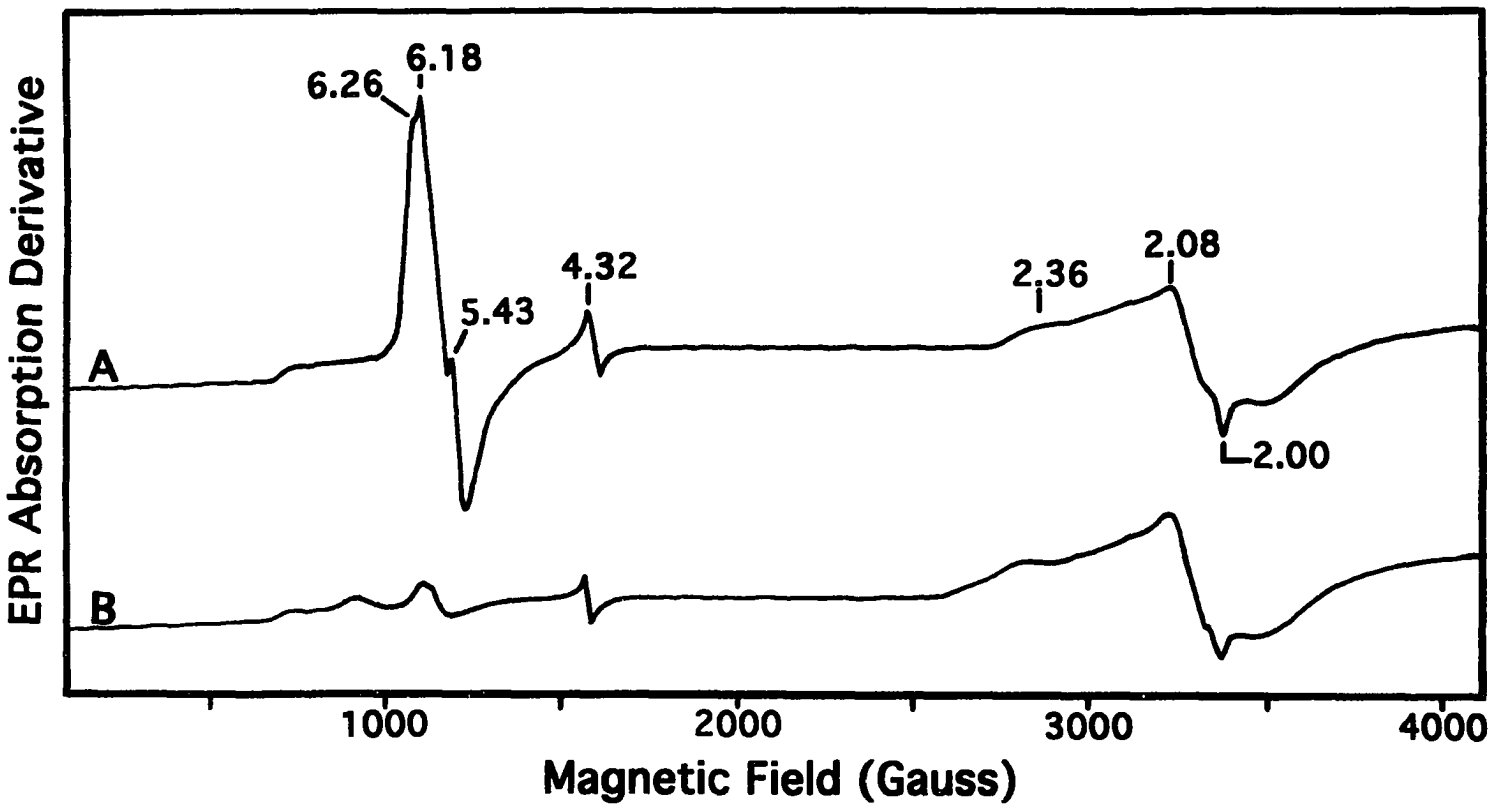
EPR Absorption Derivative
6.26
6.18
4.32
5.43
2.36
2.08
2.00
A
B
1000
2000
3000
4000
Magnetic Field (Gauss)

partial specific volumes (Table 3). The geometrical shape predicted through the corrected sedimentation data shows that the ferricytochrome undergoes approximately a 2-fold decrease in the axial ratio parameter with the ligation of carbon monoxide. The corrected molecular masses based on the estimated partial specific volume for ferricytochorme *c'* and ferrocytochrome *c'* plus CO were 30,899 and 28,977 Da, respectively.

Enzymatic reduction of cytochrome *c'*

During the purification of cytochrome P-460, a major blue-shift in the soret maxima (463 nm in cell free extracts to 450 nm in the final sample) was accompanied by the obligatory dependence for the artificial electron acceptor, phenazine methosulfate, to support turnover of hydroxylamine [1]. The spectral and enzymatic changes in purified fractions of cytochrome P-460 was accompanied by the removal of cytochrome *c'* and two non-heme proteins with molecular masses of 61,200 and 26,000 Da from the active hydroxylamine oxidizing complex [1] Cytochrome *c'* was hypothesized to function in an electron transfer role.

The effect of reduction by hydroxylamine on active preparations of cytochrome P-460/cytochrome *c'* complex is shown in Figure 8. Prior to reduction with 2 mM hydroxylamine-HCl, the EPR spectrum indicates the presence of three high spin signals at g = 6.27, 6.17, 5.43, and 2.00 with signal intensities which are consistent with a complex containing approximately equimolar levels cytochrome *c'* and cytochrome P-460. Following the addition of 2 mM hydroxylamine-HCl to the active hydroxylamine oxidizing complex, EPR signals associated with ferric cytochrome P-460 and ferric cytochrome *c'* are absent due to formation of the

ferrous (S=0 or S = 2) heme species. This is the first demonstration of reduction of cytochrome *c'* in the presence of hydroxylamine.

DISCUSSION

With growth of *M. capsulatus* Bath on nitrate as a nitrogen source, cytochrome *c'* co-purified with the hydroxylamine oxidizing enzyme, cytochrome P-460. EPR spectra shown here of hydroxylamine-reduced cytochrome *c'* - cytochrome P-460 complex demonstrate that both heme centers are reduced in the presence of hydroxylamine. Since cytochrome *c'* is not directly reduced by hydroxylamine, cytochrome *c'* can function as an electron acceptor to cytochrome P-460 in the oxidation of hydroxylamine. The physical and functional association between cytochrome *c'* and cytochrome P-460, suggests that cytochrome *c'* functions in dissimilatory nitrogen metabolism in *M. capsulatus* Bath.

The redox-potential for cytochrome *c'* of *M. capsulatus* Bath (E_{m7} = -205 mV) was found to differ greatly from previously characterized eubacterial cytochromes *c'* (E_{m7} = -10 to 202 mV) [7, 9]. Determination of the redox-potentials for the cytochromes involved in the electron transfer pathway from cytochrome P-460 (E_{m7} = -300 to -380 mV; Zahn et al., unpublished results) to cytochrome c_{555} (E_{m7} = +175 to 195 mV) has provided additional evidence for the role of cytochrome *c'* (E_{m7} = -202 mV) as a mediator between hydroxylamine oxidation and reduction of cytochrome c_{555} [1, 22]. In light of the high cellular concentration, hydroxylamine dependent reduction in cell free fractions [1], and the favorable redox-potential, cytochrome c_{555} is also a likely candidate for the *in vivo* electron acceptor to cytochrome *c'*.

Table 3. Sedimentation coefficients for *M. capsulatus* Bath ferrocytochrome *c'* and ferrocytochrome *c'* plus CO.

Property	Ferrocytochrome *c'*	Ferrocytochrome *c'* - CO
$M_{calculated}$[1] (Da)	32,372	32,428
$M_{observed}$[2] (Da)	34,885 ±1 50	27,200 ± 1,020
Sedimentation coefficient (S^*_{20})[3] (seconds)	$2.952 \cdot 10^{-13}$	$2.771 \cdot 10^{-13}$
Diffusion coefficient (D_{20})[3] ($cm^2 \cdot sec^{-1}$)	$8.006 \cdot 10^{-7}$	$8.631 \cdot 10^{-7}$
Partial Specific $Volume_{calculated}$ ($mg \cdot g^{-1}$)[4]	0.728	0.728
Partial Specific $Volume_{estimated}$ ($mg \cdot g^{-1}$)[5]	0.709	0.730
Buoyant molecular weight[1,2] (M(1-vp))	9418.95	7344
Maximum Hydration (g H_2O/g Dimeric cytochrome *c'*)[4]	0.268	0.268
Frictional Coefficient (f)[6]	$3.191 \cdot 10^{16}$	$2.650 \cdot 10^{16}$
Frictional Coefficient for a Spherical Particle (f_o)[7]	$2.354 \cdot 10^{16}$	$2.328 \cdot 10^{16}$
f/f_o	1.356	1.139
Prolate model axial ratio (a/b)	7	3.5

[1]The calculated molecular mass was based on the subunit molecular mass of cytochrome *c'* as determined by mass spectroscopy. The calculated mass of the *M. capsulatus* Bath ferrocytochrome c' plus carbon monoxide was based on the binding of 1 mole of CO per subunit of cytochrome c' and assumes the cytochrome was in a dimeric state.

[2]Calculated from the buoyant molecular weight which was estimated from sedimentation equilibration experiments using *M. capsulatus* Bath cytochrome *c'* at a concentration of 10.50 µM (0.17 mg/ml) and 6.18 µM (0.10 mg/ml).

[3]Based on sedimentation velocity experiments using *M. capsulatus* Bath cytochrome *c'* at a concentration of 10.50 µM (0.17 mg/ml).

[4]Calculated from amino acid analysis (Laue, et al.,1992).

[5]Based on values from 1, 2, and 3.

[6]Frictional constant formula from Svedberg and Pedersen (1940): f=M(1-Vp)/s.

[7]Frictional constant formula for a compact, unhydrated sphere at 20° C from Svedberg and Pedersen (1940): $f_o=2.44 \cdot 10^{18}[[(s \cdot V)/D(1-Vp)]^{1/3}]$.

FIG. 9. Major biological transformation pathways of nitrogen compounds and their oxidation states.

BIOTRANSFORMATION OF NITROGEN

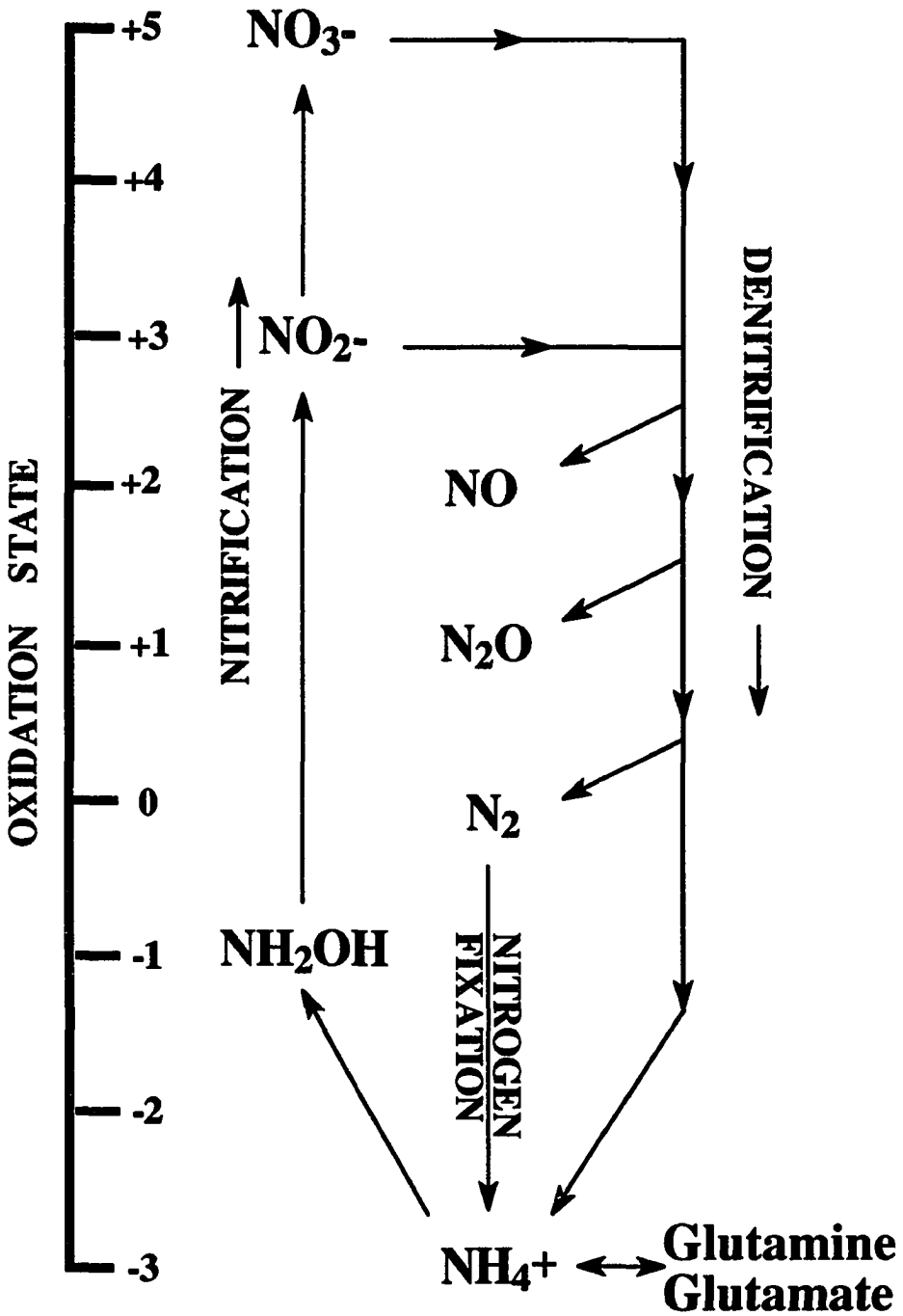

Several physical properties of *M. capsulatus* Bath cytochrome *c'* including absorption and EPR spectra, amino acid composition, and dimeric quaternary structure were found to be similar to other eubacterial cytochromes *c'*. However, the *M. capsulatus* Bath cytochrome showed major differences in molecular mass, ligand binding properties and redox potential as compared with cytochromes *c'* from other eubacterial sources. Based on amino acid composition, cytochrome *c'* from *M. capsulatus* Bath was estimated to consist of a polypeptide chain length of 152 amino acid residues. The estimated polypeptide chain length estimation was supported by the comparison of the amino acid composition-derived minimum molecular mass calculation (16,204 Da) and the molecular mass predicted by mass spectroscopy (16,136 Da). The subunit (16,186 Da) and dimeric (34,885 Da) molecular mass of *M. capsulatus* Bath cytochrome *c'* also differ significantly from subunit (12,000 ± 2000 Da) and dimeric (27,000 ± 3,000 Da) molecular masses of previously characterized cytochromes *c'* [11].

The complex ligand binding properties induced by ligation of nitric oxide to cytochrome *c'* as well as the increased concentration of cytochrome *c'* in cells cultured in AMS media, suggests that cytochrome *c'* may function in a secondary role of protection against the toxic effects of nitric oxide generated in the oxidation of hydroxylamine or reduction of nitrite (Fig. 9). Cells or cell free extracts of *Nitrosomonas europeae* have been shown to produce nitrous and nitric oxides under microaerophilic conditions [28 - 33]. Evidence for the production of N_2O and NO from NH_4^+, or NH_2OH oxidation has been proposed [30, 34], as well as for a reductive pathway via HNO_2 reduction [30, 35, 36]. Production of nitrous oxide by

Methylosinus trichosporium OB3b during ammonia oxidation under microaerophilic conditions has also been observed [37]. The similarity in ammonia oxidation by nitrifying and methanotrophs [1] suggests that the mechanism of nitric oxide production may also be similar. Although the formation of nitric oxide has been shown to occur in nitrifying bacteria, the specific or nonspecific mechanism(s) for the removal of the toxic intermediate has not been shown. If nitric oxide is formed during hydroxylamine oxidation by cytochrome P-460, the binding of NO to ferrocytochrome *c'* may reduce this toxic intermediate to nitrous oxide. The conformational changes associated with ligand binding may serve an important function in either the release of the NO-bound ferrocytochrome from the hydroxylamine oxidizing complex or release of the reduced ligand.

ACKNOWLEDGMENTS

We thank B.L. Hoyle (ISU) for her evaluation of the manuscript and useful suggestions. We also thank J. Nott (ISU) for amino acid analysis, and amino acid sequencing, the ISU protein facility for use of the mass spectrometer and analytical ultracentrifuge, and H.M Starr (ISU) for metal analysis.

This work was supported by grants from Iowa State University Office of Biotechnology (ADS), National Science Foundation MCB-9316906 (ABH) and Iowa State University Professional Advancement Grant (JAZ).

REFERENCES

1. Zahn, J.A., Duncan C. & DiSpirito, A.A. (1994) Oxidation of hydroxylamine by cytochrome P-460 of the obligate methylotroph *Methylococcus capsulatus* Bath. *J. Bacteriol. 176*, 5879 - 5887.

2. Colby, J., Stirling, D.I. & Dalton H. (1977) The soluble methane monooxygenase from *Methylococcus capsulatus* Bath: its ability to oxygenate *n*-alkanes, *n*-alkenes, ethers, and alcyclic, aromatic and heterocyclic compounds. *Biochem. J. 165*, 35 - 402.

3. Dalton, H. (1977) Ammonia Oxidation by the methane oxidizing bacterium *Methylococcus capsulatus* strain Bath. *Arch. Microbiol. 114*, 273-279.

4. Schmidt, T.M. & DiSpirito, A.A. (1990) Spectral characterization of *c*-type cytochromes purified from *Beggiatoa alba. Arch. Microbiol. 154*, 453 - 458.

5. Maltempo, M. M. & Moss, T. H. (1976) The spin 3/2 state and quantum spin mixtures in haem proteins. *Quart. Rev. Biophys. 9*,181 - 215.

6. Meyer, T.E. & Kamen, M.D. (1982) New perspectives on *c*-type cytochromes. *Adv. Prot. Chem. 35*, 105 - 212.

7. Gilmour, R., Goodhew, C. F. & Pettigrew, G. W. (1991) Cytochrome *c'* from *Paracoccus dinitrificans. Biochim. Biophys. Ac ta 1059*, 233-238.

8. Monkara, F., Bingham, S.J., Kadir, H. A., McEwan, A. G. , Thomson, A. J., Thurgood, A. G. P. & Moore, G. R. (1992) Spectroscopic studies of *Rhodobacter capsulatus* cytochrome *c'* in the isolated state and in intact cells. *Biochim. Biophys. Acta 1100*, 184 - 188.

9. Wood, P.M. (1984) Bacterial proteins with CO-binding *b* or *c*-type heam functions and absorption spectroscopy. *Biochim. Biophys. Acta 768*, 293 - 317.

10. Doyle, M. L., Weber, P. C. & Gill, S. J. (1985) Carbon monoxide binding to *Rhodospirillum molischianum* ferrocytochrome *c'*. *Biochemistry 24*, 1987 - 1991.

11. Montie, M., Kassner, R. J., Terrence, T. E., Meyer, E. & Cusanovich, M. A. (1990) Kinetics of cyanide binding to *Chromatium vinosum* ferricytochrome *c'*. *Biochemistry 29,* 1932 - 1936.

12. Ren, Z., Meyer, T. & McRee, D. E. (1993) Atomic structure of a cytochrome *c'* with an unusual ligand-controlled dimer dissociation at 1.8Å resolution. *J. Mol. Biol. 234*, 433 - 445.

13. Zahn, J.A. & DiSpirito, A.A. (1996) The membrane-associated methane monooxygenase from *Methylococcus capsulatus* Bath. *J. Bacteriol. 178*, 1018 - 1029.

14. Laemmli U.K. (1970) Cleavage of structural proteins during the assembly of the head of bacteriophage T4. *Nature (London) 227*, 680 - 685.

15. McDonnel A., & Staehelin, L.A. (1981) Detection of cytochrome *f.* a *c*-class cytochrome, with diaminobenzidine in polyacrylamide gels. *Anal. Biochem. 117*, 40 - 44.

16. Laue, T. M., Shah, B. D., Ridgeway, T. M. & Pelletier S. L. (1992) Computer-aided Interpretation of Analytical Sedimentation Data for Proteins in *Analytical Ultracentrifugation in Biochemistry and Polymer Science*, S. E. Harding, A. J. Rowe, and J. C Horton, eds., Redwood Press, England.

17. Lowry, O.H., Rosebrough, N.J., Farr, A.L., & Randall, R.J. (1951) Protein measurement with the Folin phenol reagent. *J. Biol. Chem. 193*, 265 - 275.

18. DiSpirito, A.A. (1990) Soluble cytochromes *c* from *Methylomonas* A4. *Meth. Enzymol. 188*, 289 -297.

19. Fuhrhop, J.-H. (1975) *Laboratory methods in porphyrin and metalloporphyrin research*. Elsevier Scientific Publishers, New York.

20. Collins, M.J., Arciero, D.M., & Hooper, A.B. (1993) Optical spectropotentiometric resolution of hemes of hydroxylamine oxidoreductase. *J. Biol. Chem. 268*, 14655 - 14662

21. Ambler, R.P., Dalton, H., Meyer, T.E., Bartsch, R.G. & Kamen, M.D. (1986) The amino acid sequence of cytochrome *c*-555 from the methane-oxidizing bacterium *Methylococcus capsulatus. Biochem. J. 233*, 333 - 337.

22. Svedberg, T. & Pedersen, K. O. (1940) *The Ultracentrifuge.* Oxford Press. London.

23. Ambler, R.P., Bartsch, R.G., Daniel, M. , Kamen, M. D., McLellan, L., Meyer, T.E. & van Beeumen, J. (1981) Amino acid sequences of bacterial cytochromes *c'* and *c*-556. *Proc. Natl. Acad. Sci. USA. 7*, 6854 - 6857.

24. Kassner, R.J. (1970) Ligand binding properties of cytochrome *c'*. *Biochim. Biophys. Acta 1058*, 8 - 12.

25. Suzuki, S., Nakahara, A., Yoshimura, T., Iwasaki, H., Shidara, S. & Matsubara, T. (1988) Spectral properties of carbon monoxide or cyanide complexes of cytochrome *c'* from denitrifying bacteria. *Inorg. Chim. Acta 153*, 227 - 233.

26. Emptage, M.H., Zimmermann, R., Que, L., Jr., Münck, E., Hamilton, W.D., and Orme-Johnson, W.H. (1977) Mössbauer studies of cytochrome *c'* from *Rhodospirillum rubrum. Biochim. Biophys. Acta 495*, 12 - 23.

27. Doyle, M. L., & Gill, J. (1986) Ligand-controlled dissociation of *Chromatium vinosum* cytochrome *c'*. *Biochemistry 25*, 2509 - 2516.

28. Goreau, T.J., Kaplan, W.A., Wofsy, S.C., McElroy, M.B., Valois, F.W. & Watson, S.W. (1980) Production of NO_2^- and N_2O by nitrifying bacteria at reduced concentrations of oxygen. *Appl. Environ. Microbiol. 40*, 526 - 532.

29. Hooper, A.B. (1968) A nitrite-reducing enzyme from *Nitrosomonas europaea.* Preliminary characterization with hydroxylamine as electron donor. *Biochim. Biophys. Acta 162*, 49 - 65.

30. Hooper, A.B., Arciero, D.M., DiSpirito, A.A., Fuchs, J., Johnson, M., LaQuier, F., Mundfrom, G. & McTavish, H. (1990) Production of nitrite and N_2O by ammonia-oxidizing nitrifiers. in. *Nitrogen Fixation: Achievements and Objectives.* Gresshoff, Roth, Stacey and Newton (eds). Chapman and Hall, NY.

31. Poth, M. (1986) Dinitogen production from nitrite by a *Nitrosomonas* isolate. *Appl. Environ. Microbiol. 52*, 957 - 959.

32. Poth, M., & Focht, D.D. (1985) ^{15}N kinetic analysis of N_2O production by *Nitrosomonas europaea* and examination of nitrifier denitrification. *Appl. Environ. Microbiol. 49*, 1134 - 1141.

33. Richie, G.A.F., & Nicholas, D.J.D. (1972) Identification of the sources of nitrous oxide produced by oxidative and reductive processes in *Nitrosomonas europaea. Biochem. J. 126*, 1181 - 1191.

34. Hollocher, T.C., M.E. Tate and D.J.D. Nicholas. 1981. Oxidation of ammonia by *Nitrosomonas europaea.* Definitive ^{18}O-tracer evidence that hydroxylamine formation involves a monooxygenase. J. Biol. Chem. 256: 10834 - 10836.

35. DiSpirito, A.A., Taaffe, L.R., Lipscomb, J.D. & Hooper, A.A. (1985) A "blue" copper oxidase from *Nitrosomonas europaea*. *Biochim. Biophys. Acta 827*, 320 - 326.

36. Miller, D.J. & Wood, P.M. (1983) The soluble cytochrome oxidase of *Nitrosomonas europaea*. J. *Gen. Microbiol. 129*, 1645 - 1650.

37. Yoshinari, T. (1985) Nitrite and nitrous oxide production by *Methylosinus trichosporium*. *Can. J. Microbiol. 31*, 139 - 144.

CHAPTER 6. GENERAL CONCLUSIONS

Summary

The enzymology and microbial physiology of methane and ammonia oxidation by the membrane-associated methane monooxgenase (pMMO) from the obligate methylotroph, *Methylococcus capsulatus* Bath were studied. Conditions leading to the stabilization of the pMMO were defined, and an active preparation of the membrane-associated methane monooxygenase (pMMO) from *M. capsulatus* Bath was isolated by ion exchange and hydrophobic interaction chromatography using dodecyl-β-D-maltoside as the detergent. The active preparation consisted of three major polypeptides with molecular masses of 47,000 and 27,000, and 25,000 Da and contained 2.5 iron and 14.5 copper atoms per mole of enzyme. The 27,000 Da polypeptide was identified as the acetylene binding protein by enzymatic labeling with ^{14}C-acetylene. Using duroquinol as a reductant, the specific activity of purified enzyme was 9.6 ± 2.4 nmol propylene oxidized • min.$^{-1}$ • mg protein^{-1}. Additionally, a novel siderphore-like copper-binding cofactor, which was found to be associated with the pMMO, is described. Immunoblot analysis of the membrane fraction from Type I and Type II methanotrophs and of the nitrifying bacterium, *Nitrosomonas europaea*, with antibodies against the pMMO from *M. capsulatus* (Bath) has confirmed the highly conserved nature of the pMMO and ammonia monooxygenase polypeptides.

Studies on the nitrification pathway in *M. capsulatus* Bath have yielded two, previously uncharacterized enzymes that function in the nitrification/denitrification

process. The first enzyme, cytochrome P-460, is responsible for the oxidation of hydroxylamine to nitrite. Absorption spectra in cell free extracts, electron paramagnetic resonance spectra, molecular weight, covalent attachment of heme group to polypeptide, and enzymatic activities suggest that the enzyme is similar to cytochrome P-460 from the nitrifying bacterium, *Nitrosomonas europaea.*

The second enzyme, cytochrome *c'*, had native and subunit molecular masses of 34,855 and 16,186 Da, respectively. The value for the midpoint potential, ($E_{m\ 7.0}$, - 205 mV) of cytochrome *c'* from *M. capsulatus* Bath was well below the range of values reported for other cytochromes *c'*. Enzymatic and redox potential data support the possibility that cytochrome c' can function as an electron shuttle between cytochrome P-460 and cytochrome *c*-555.

Molecular structure and function of the pMMO: Points of future consideration

The pMMO has been shown to consist of three polypeptides with apparent molecular masses of 47,000, 27,000, and 25,000 Da. The 27,000 Da polypeptide has been shown to be the acetylene-binding protein and, by analogy to the sMMO enzyme, is presumed to contain the active site of the enzyme. Active preparations of pMMO contain 2 to 4 moles of iron, present mainly in the ferrous state, and 12 to 16 moles of copper, which can be classified into three distinct forms.

The first form of copper (Form A) appears to comprise of at least one-quarter of the total copper ions associated with the pMMO. EPR spectroscopy experiments on various purification fractions of pMMO suggest that form A is loosely associated with the enzyme and may be completely removed by harsh purification methods which also inactivate the enzyme. A comparison of the EPR spectra before and

after the removal of form A copper from the enzyme shows 1) a decrease in the intensity of the $g_{\perp}$ signal near g = 2.05 after removal of form A copper and, 2) an increase in the intensity of the copper hyperfine region associated with a type 2 copper signal also following removal of form A copper. Based on these observations, the chemical nature of form A copper is designated as loosely associated or un-coordinated copper. The second form of copper (Form B) is present in the enzyme at 2 to 4 moles of copper per mole of enzyme. Form B copper is tightly coordinated to the pMMO polypeptides and it exhibits EPR parameters consistent with other type 2 copper-containing enzymes. The existence of a third form of copper in the pMMO (form C) is proposed based on major inconsistencies between the concentration estimates of pMMO-copper by elemental analysis and by EPR spectroscopy. These experiments have shown that approximately one-half of the copper present in the purified, active pMMO is EPR-silent, and apparently diamagnetic in chemical nature. The possible roles and location of these metal centers within the pMMO polypeptides are currently unknown.

Figure 1 shows the current molecular model for the pMMO from *M. capsulatus* Bath. The electron transport pathway from the site of NADH + H^+ oxidation to the site of methane oxidation is thought to consist of three major components: 1) NADH:ubiquinone oxidoreducase, 2) a plastoquinol analog of unspecified side chain length, and the 3) pMMO complex. The three-component electron transport chain hypothesis is based on the observation that NADH+H^+ serves as an electron donor to the pMMO before detergent solublization of the

FIG. 1. Biochemical model for the pMMO methane-oxidizing system in *M. capsulatus* Bath. Vectorial proton pumping is shown for the plastoquinol analog (X indicates sidechains on plastoquinol of undetermined length).

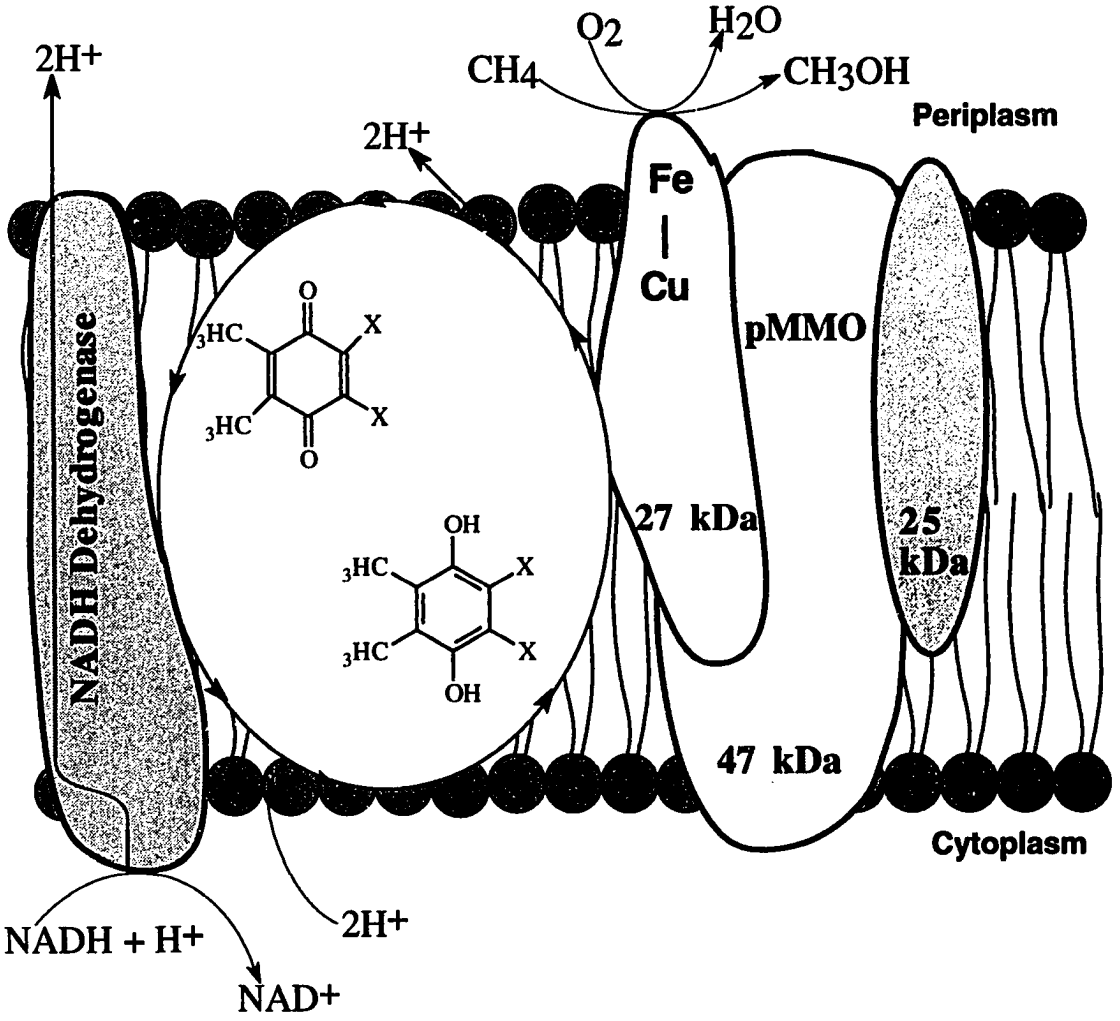
2H+
O2
H2O
CH4
CH3OH
Periplasm
2H+
Fe
Cu
pMMO
NADH Dehydrogenase
27 kDa
25 kDa
47 kDa
Cytoplasm
NADH + H+
NAD+
2H+

membrane fraction, but is not a suitable reductant for the pMMO following solublization. Currently, a membrane-associated NADH:ubiquinone oxidoreductase capable of plastoquinone reduction has not been identified in this organism, nor is there any evidence for additional polypeptide components (such as polypeptides of a membrane-associated NADH:ubiquinone oxidoreducase) other than the pMMO polypeptides, which are induced at switch-over. Alternatively, the oxidation of $NADH+H^+$ (redox potential = -340 mV) could be coupled directly to the reduction of a plastoquinone analog (redox potential ≈ 30 to 200 mV) which in turn, could serve as a pMMO reductant. This theory is equally plausible, since electron transport by this method would also be susceptible to detergent solublization. Future studies must focus on the characterization and validation of these proposed electron transfer components.

An important consideration in the bioenergetics of methane oxidation by the pMMO is the determination of the sidedness of the methane oxidation reaction in respect to the cell membrane. The sMMO is thought to be localized in the cell cytoplasm based on the fact that the enzyme utilizes $NADH+H^+$ as a reductant; a compound generated in the cytoplasm by formate and formaldehyde dehydrogenases and is generally restricted to the cytoplasmic compartment in prokaryotes. The monooxygenase reaction catalyzed by the sMMO utilizes two protons from the cytoplasmic compartment in the oxidation of methane to methanol. Therefore, the cellular location of this reaction is expected to contribute to the chemiosmotic proton gradient necessary for all life forms. Unfortunately, predictions based on electron donor specificity are not helpful in predicting the cellular location

of the pMMO-catalyzed methane oxidation reaction. From a bioenergetic standpoint, it would seem logical that the pMMO-catalyzed methane oxidation reaction should also take place on the cytoplasmic surface of the cell membrane. However, since plastoquniol and quinol analogs serve as suitable reductants for the pMMO, a periplasmic location for the reaction could also derive protons from the cytoplasm through quinol or plastoquinol-mediated vectorial proton pumping (Fig. 1). A periplasmic sidedness of the pMMO reaction site would also be most efficient for the subsequent methanol dehydrogenase reaction, since the methanol dehydrogenase has been localized in the cell periplasm. Current methods for the cellular localization of polypeptides (cytochemical, histocytochemical, and mechanical) are useful in determining cellular location of soluble or peripheral membrane proteins but, are generally unsuitable for integral membrane polypeptides which by definition, face both cellular compartments. Future attempts to determine the sidedness of the enzyme reaction site may likely employ low-energy radiolabeled suicide substrates (i.e., ^{3}H-acetylene) to label the pMMO active site for radiohistocytochemistry experiments.

A Physiological model for methane and ammonia oxidation in *M. capsulatus* Bath

The compilation of published and unpublished data, some of which is presented in this dissertation, has allowed for the synthesis of a cellular and biochemical model for methane (Fig. 2A) and ammonia (Fig. 2B) oxidation in *M. capsulatus* Bath cells expressing the pMMO. This model is expected to serve as

FIG. 2. Models for the oxidation of methane (A) and ammonia (B) in *M. capsulatus* Bath. Abbreviations: QH_2 and Q, quinol and quinone, respectively; MDH, methanol dehydrogenase; CCP *c*-556, cytochrome *c*-556 peroxidase; cyt., cytochrome; FDH, formate dehydrogenase; FalDH, formaldehyde dehydrogenase; and Nitrite red., nitrite reductase. Question marks represent hypothesized components or processes. The bold arrows represent biotransformation reactions and the "thin" arrows represent electron transfer events.

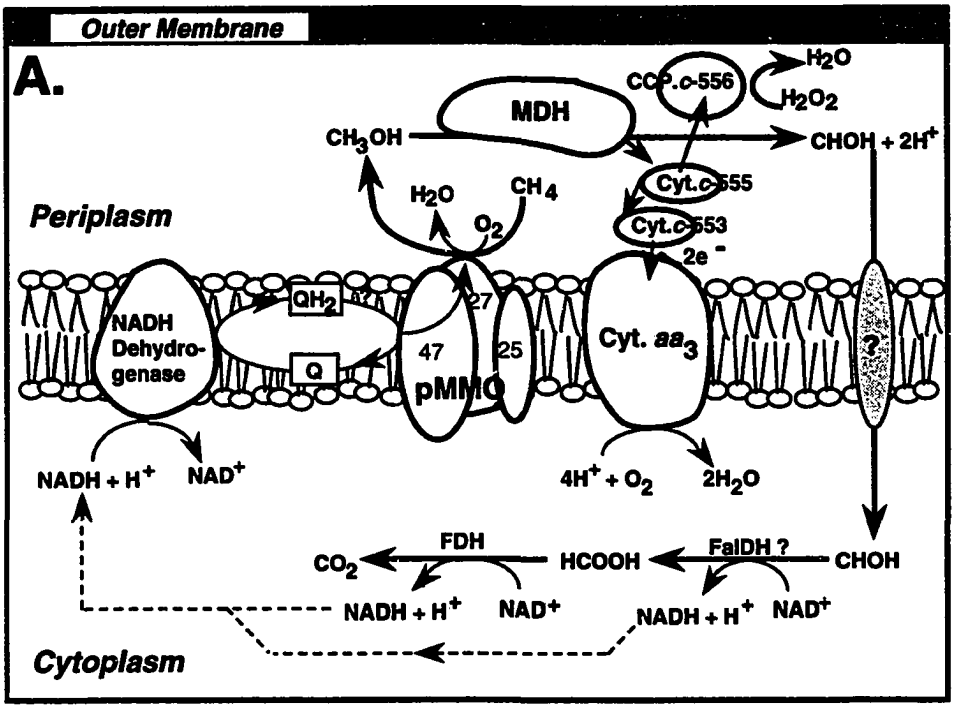
Outer Membrane
A.
CCP.c-556
H_2O
H_2O_2
MDH
CH_3OH
CHOH + $2H^+$
Cyt.c-555
H_2O
CH_4
O_2
Periplasm
Cyt.c-553
2e⁻
QH_2
Q
NADH Dehydro-genase
47
27
25
pMMO
Cyt. aa_3
?
$NADH + H^+$
NAD^+
$4H^+ + O_2$
$2H_2O$
FDH
FalDH ?
CO_2
HCOOH
CHOH
$NADH + H^+$
NAD^+
$NADH + H^+$
NAD^+
Cytoplasm

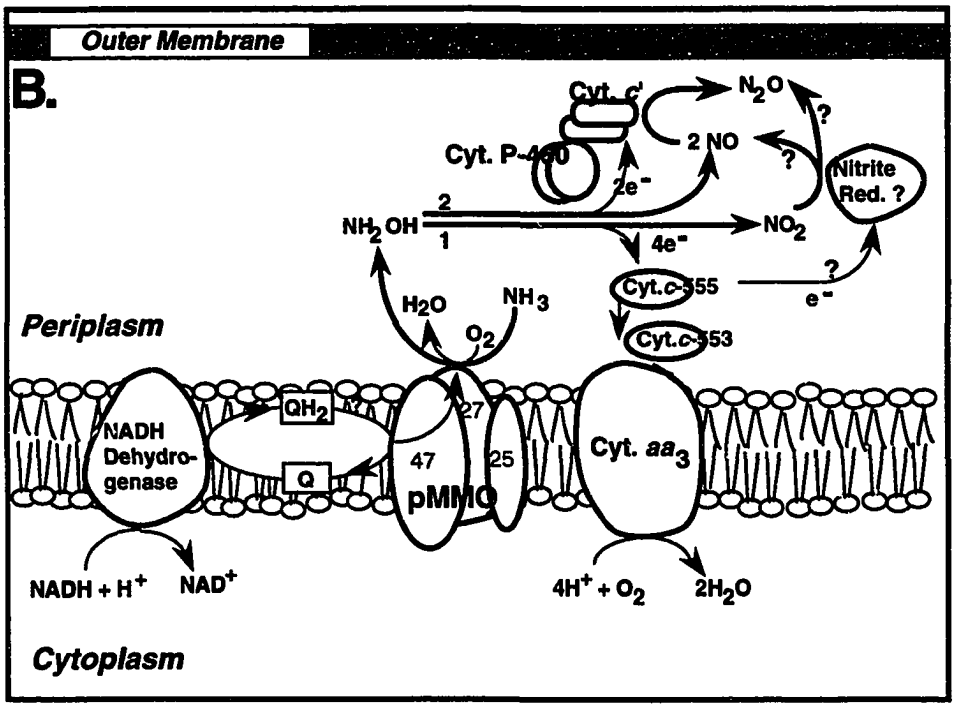
Outer Membrane
B.
Cyt. c'
N_2O
?
2 NO
?
Cyt. P-460
2e⁻
Nitrite Red. ?
2
NH_2OH
1
NO_2
4e⁻
?
e⁻
Cyt.c-555
H_2O
NH_3
O_2
Periplasm
Cyt.c-553
QH_2
Q
NADH Dehydro-genase
47
27
25
pMMO
Cyt. aa_3
$NADH + H^+$
NAD^+
$4H^+ + O_2$
$2H_2O$
Cytoplasm

basis for future experiments addressing methane and ammonia oxidation in *M. capsulatus* Bath.